18

STABLE ISOTOPES OF THE THERMAL SPRINGS OF THE CAPE FOLD BELT

Roger Diamond

Submitted as fulfillment for the degree of
Master of Science.

Department of Geological Sciences
University of Cape Town

February 1997

ABSTRACT

The Cape Fold Belt is a 250Ma orogenic belt comprised of rocks of the Cape Supergroup, an Ordovician to Devonian sedimentary sequence. The mountainous areas, which reach over 2000m, are composed of the faulted and highly jointed quartzites and sandstones of the Table Mountain Group, which acts as the main deep aquifer. It is from the secondary porosity of this aquifer that over ten thermal springs issue forth, ranging in temperature from ~27°C to 64°C.

Samples of the integrated total monthly rainfall were taken for several months at each of four stations around the Cape Fold Belt. Values ranged from $\delta^{18}O = -8.3‰$ and $\delta D = -37‰$ to 1.2‰ and 7‰, respectively. Integrated recharge values based on a full year of observation at UCT, Cape Town, are $\delta^{18}O = -3.7‰$ and $\delta D = -10‰$. Eleven thermal springs were sampled in 1995, four of which were sampled once a month for several months, over the same period that the rain was being sampled. The average discharge values for the four springs sampled monthly are, for $\delta^{18}O$ and δD respectively, at Malmesbury −3.9‰, −18‰; at Citrusdal −4.9‰, −20‰; at Brandvlei −5.6‰, −30‰ and at Calitzdorp −7.3‰, −40‰. A meteoric water line for the Cape Mediterranean climate area was calculated by the general form of a structural regression, using the monthly data weighted by rainfall amount. It has the equation $\delta D = 7.38\delta^{18}O + 18.6$. Using the same calculation technique, but not weighting the data, the data for the thermal springs yield a water line with the equation $\delta D = 8.32\delta^{18}O + 16.5$. The difference in gradient suggests that the springs are recharged from a colder and isotopically more fractionated weather system, such as during a previous colder climate regime, or at high altitude.

There is no evidence for isotope exchange between the groundwater and host rocks; rather, the shift of the spring water line to less negative $\delta^{18}O$ values suggests evaporation prior to recharge. Oxygen and hydrogen isotope ratios from the discharged spring water are clearly more negative than those expected for rain falling at the spring, which can be explained by recharge at much higher altitudes. The springs are therefore believed to be recharged high on mountains in the near vicinity. A continental effect was observed in the spring data, with respect to the distance from the west coast, which is the direction from which weather systems approach. Most of the thermal springs of the Cape Fold Belt seem to be recharged at high altitude in nearby mountains, whereafter the water is heated by geothermal gradient upon reaching depths of two to three kilometres via the secondary porosity of the Peninsula Formation, finally reaching the surface by means of various faults, which allow passage through the impermeable Cedarberg Formation.

Isotopically light carbon is released at some springs in the form of CO_2 and CH_4 (total carbon $\delta^{13}C \approx -21‰$). These gases could come from near surface bog environments, however, at Malmesbury, where H_2S is also released, a possible geological source is indicated for the CO_2 and the CH_4.

CONTENTS

" I shall not here amuse myself in proposing or supporting any hypothesis on the cause of hot springs; but shall confess myself very much at a loss in attempting to account for the great subterranean operations of Nature, whose dark recesses in the centre of our globe are not less out of the pale of observation, than the wide space beyond the starry system. "

William Burchell, 1811,

Travels in the Interior of Southern Africa, Volume 1, Page 70, 1822.

1 INTRODUCTION

This chapter contains introductory sections on the developments of isotope science and the basic laws of isotope behaviour and isotope hydrology, including various meteoric effects and meteoric water lines. This study of hot springs is then introduced with a brief historical perspective, mention of previous work and then an outline of the aims of this dissertation.

1.1 ISOTOPES

1.1.1 HISTORICAL BACKGROUND

The discovery of radioactivity by Henri Becquerel and Marie Curie in the 1890's triggered research into atomic scale physics and chemistry. The resulting discoveries were many and included the conclusion by Frederick Soddy that there must exist, for certain elements, different species with different atomic masses. These species were called isotopes, sourced from the ancient Greek for `the same' (iso) `place' (topo), referring to the fact that these isotopes occupied the same place on the periodic table.

The existence of isotopes was verified in 1913 by JJ Thomson, when he recorded the atomic masses of 20 and 22 for the element neon. What he used to determine the numbers was then called a `positive-ray' apparatus. This apparatus was modified by FW Aston, who confirmed Thomson's findings, as well as finding a third isotope of neon (^{21}Ne). Aston called his improved device a mass spectrograph and he went on to document 212 of the 287 naturally occurring isotopes. Alfred Nier continued to improve the mass spectrograph with a whole group of others and after World War II, the mass spectrometer started to become a tool for the earth sciences.

Isotopes can be classified as either radioactive or non-radioactive. Non-radioactive isotopes are all stable, however, the word stable is reserved for isotopes that are non-radiogenic as well as non-radioactive; radiogenic isotopes being the daughters of radioactive parents. Stable, as the word is used in the earth sciences, therefore applies to those isotopes which have a fixed abundance.

In the 1930's stable isotopes became a new focus when Harold Urey predicted that, if hydrogen had isotopes, they should have different vapour pressures. Subsequent experimentation proved the existence of ^{2}H, which Urey called deuterium (D), because of its atomic mass being very nearly double that of ^{1}H. Deuterium was discovered in 1932, as was the positron and the neutron, the latter of which provided the explanation for the existence of isotopes.

After World War II, Urey also suggested that oxygen isotopes should fractionate and that the degree of fractionation would be dependant upon temperature. Following this, he developed a

palaeothermometer for the oceans, which makes use of the temperature dependence of the isotope fractionation of oxygen during precipitation of skeletal aragonite. Stable isotope studies have since spread into all realms of earth science and are now fundamental to our understanding of natural processes.

For more on the development of isotope science, see Faure (1986), Valley et al (1986) or Urey (1947).

1.1.2 HYDROGEN AND OXYGEN ISOTOPES

What is arguably the most crucial substance on the planet Earth, water, is remarkably simple in chemical composition. Water is composed of hydrogen and oxygen, and has the chemical formula H_2O. Hydrogen (by mass) constitutes 74% of the solar system, but only 0.14% of the Earth's crust, whereas oxygen (also by mass) makes up only 0.87% of the solar system, but constitutes 45-50% of the Earth's crust (Emiliani, 1987). Both hydrogen and oxygen have isotopes, as detailed below.

Hydrogen has 3 isotopes, two of which are stable:

^{1}H	99.984%	(or just H) - light
^{2}H	0.016%	(or D for deuterium) - heavy
^{3}H	~$5x10^{-6}$%	(or T for tritium) - a cosmogenic, radioactive species with a half life of 12.7 years.

Oxygen also has 3 isotopes, all of which are stable:

^{16}O	99.76%	light
^{17}O	0.04%	
^{18}O	0.20%	heavy.

With the above in mind, nearly all water molecules are either the light and common $H_2{}^{16}O$ (99.747%) or one of the heavy and rare trio of $H_2{}^{17}O$, $H_2{}^{18}O$ and $HD^{16}O$. These four molecules make up approximately all of the natural water on earth, with all the other possible species accounting for less than 1ppm.

1.1.3 BEHAVIOUR

Isotopic species of an element behave similarly during chemical reactions, as do isotopic species of molecules. During physical processes, however, due to the mass differences, the various species will fractionate. Isotopic fractionation is now known to occur in three general ways: these isotope effects are known as equilibrium, kinetic and physical.

1. Equilibrium fractionation is the exchange of isotopes of an element between different substances that contain that element.
2. Kinetic fractionation is the differential distribution of isotopes during unidirectional chemical reactions.
3. Physical fractionation is the separation of isotopes during physical processes such as evaporation, condensation, melting, freezing, sublimation and diffusion.

The extent to which isotopes fractionate between two phases is expressed as the fractionation factor, α, and is given by:

$$\alpha = \frac{R_A}{R_B}$$

where R_A and R_B are the isotopic ratios of an element in two phases, A and B.

Fractionation is inversely proportional to temperature; this is shown by the following relationship:

$$\ln \alpha = \frac{k}{T^2}$$

where ***T*** is temperature in Kelvin and ***k*** is a constant, specific to the pair of phases between which fractionation is occurring.

The vapour pressure of a substance is inversely proportional to its atomic mass: the lighter species of an element or a molecule will evaporate (and diffuse) more easily, while heavier species will condense preferentially. Evaporation produces a vapour enriched in the lighter species relative to the source liquid while the remaining liquid will be progressively enriched in the heavier species as evaporation proceeds.

1.1.4 MEASUREMENT

The isotope ratio of two isotopes of an element in a sample, as measured in a mass spectrometer, is expressed as a deviation from the ratio in a standard. In the case of water, the international standard is a sample of sea water, called Standard Mean Ocean Water (SMOW) (Craig, 1961a, b). The deviation of the sample from the standard, δD or $\delta^{18}O$, is indicated in units of thousandths, or per mil (‰).

For hydrogen:

$$\delta D = \frac{\left(\frac{D}{H}\right)_{sample} - \left(\frac{D}{H}\right)_{SMOW}}{\left(\frac{D}{H}\right)_{SMOW}} \times 1000.$$

For oxygen:

$$\delta^{18}O = \frac{\left(\frac{^{18}O}{^{16}O}\right)_{sample} - \left(\frac{^{18}O}{^{16}O}\right)_{SMOW}}{\left(\frac{^{18}O}{^{16}O}\right)_{SMOW}} \times 1000.$$

A negative δ value means that the sample is enriched in the light isotope and depleted in the heavy isotope relative to the standard, whereas a positive δ value indicates the opposite enrichment and depletion.

1.2 ISOTOPE HYDROLOGY

1.2.1 ISOTOPE FRACTIONATION DURING THE WATER CYCLE

Instead of describing the global water cycle, this section deals briefly with the isotopic encoding of water that occurs, as water moves through the biosphere.

The major global reservoir of water is the oceans. They contain over 99% of all water in or above the crust. Most water that separates from the oceans to add to another reservoir must first evaporate from the surface of the ocean. During this process, the vapour formed is depleted in ^{18}O and D. For this water vapour in the atmosphere to add to another reservoir, condensation or sublimation to water or ice, respectively, must occur. The water droplets, or ice crystals, are enriched in ^{18}O and D relative to the remaining vapour and as precipitation proceeds, the $\delta^{18}O$ and δDvalue of the atmospheric water (total of all phases) will decrease. The isotopic values of precipitation can be attributed to the following effects.

1.2.1.1 TEMPERATURE EFFECT

The most important influence on the final isotopic ratios of precipitated water is temperature (Dansgaard, 1964). The main factor is the temperature of condensation within the cloud, with the temperature of evaporation where the vapour body formed, being subordinate (Dansgaard, 1964). The result is that lower temperatures yield isotopically lighter precipitation values (Dansgaard, 1964).

1.2.1.2 AMOUNT EFFECT

Within a climatic area, heavy rains are associated with lighter isotopic values. The first rain that falls has the heaviest isotopic composition and thereafter the composition will become progressively lighter. This is the amount effect (Gat, 1971). Furthermore, for any one rain event, the more rain that falls, the more saturated the air below the cloud base becomes, and the amount of evaporative enrichment of falling rain drops is less, resulting in lighter isotopic values of later rain.

1.2.1.3 ALTITUDE EFFECT

At higher elevations within a geographic area, the isotopic values of precipitation will tend to be more negative (eg. Siegenthaler & Oeschger, 1980). There are several reasons that could contribute to this effect. Higher altitudes experience lower temperatures and therefore the condensation temperature will be lower. Lower temperatures also mean that the relative humidity will be higher and this, along with the fact that the cloud base will be closer to or at, ground level and the lower temperature, means that less evaporation will occur from falling raindrops. Also, the increasing relative humidity with altitude will most likely trigger rain and thereby a loss of heavy isotopes.

1.2.1.4 CONTINENTAL EFFECT

The greater the distance from the oceans, which is the main source of water vapour, the lighter the isotope values will be for any precipitation (eg. Sonntag et al, 1979, in Mazor, 1991). This correlation can be strengthened by increasing altitude with distance from the sea, but the essence of the continental effect is that of progressive rainout. Rainout of heavy isotopes will occur as a weather system moves inland and therefore the subsequent precipitation will be isotopically lighter.

1.2.1.5 RESERVOIR EFFECT

Genesis of weather systems over different water bodies can result in inherited isotopic differences. Water masses can develop isotope differences through local and regional inputs or outputs, such as from rivers or glaciers and ice, or from evaporation. Ocean currents or upwelling systems can also bring isotopically different water into an area.

1.2.2 METEORIC WATER LINES

Craig (1961a) published the results of about 400 river, lake and rainwater samples and found that their stable isotope values fell along the line, $\delta D = 8\delta^{18}O + 10$. This line is a good meteoric water line for the continental northern hemisphere, however, subsequent investigators have found that meteoric water lines vary quite a lot around the world. Shallower gradients have been found, especially for the tropical

regions, oceanic areas and the southern hemisphere in general (Dansgaard, 1964). In Brazil, Salati et al (1980, in Mazor, 1991) found the meteoric water line to be $\delta D = 6.4\delta^{18}O + 5.5$; similarly, Dansgaard (1964) reported $\delta D = 4.6\delta^{18}O + 1.6$ for most tropical islands, using unweighted monthly means. Using weighted means, the gradient is close to 3.5.

Upon descent of rain, evaporation occurs quickly and therefore under non-equilibirium conditions; kinetic effects such as varying diffusion rates of the isotopic molecules of water play a role. The result is that the enrichment is ^{18}O and D is along lines of $\Delta\delta D/\Delta\delta^{18}O < 8$, so the gradient of meteoric water lines in warmer and drier regions, is flatter than the meteoric water line (Ehhalt et al, 1963).

The local meteoric water line is an important feature for interpreting geohydrological and many other types of studies; e.g. palaeoecology, archaeology. The results of this dissertation provide a firm basis for aspects of research within these other disciplines, in the Western Cape region.

1.2.2.1 DEUTERIUM EXCESS

The deuterium excess parameter, or `d`, is calculated as $d = \delta D - 8\delta^{18}O$ for the measured $\delta^{18}O$ and δD values of a water sample (Dansgaard, 1964). It defines the excess D relative to the global meteroic water line calculated by Craig (1961a). Values of d tend to fluctuate seasonally, greater values in winter reflecting lower humidities in the source region, and vica versa for summer (e.g. Merlivat & Jouzel, 1979).

1.2.3 GROUNDWATER STUDIES

By comparing isotope data of meteoric and groundwater, some insights into the origin and history of groundwater can be gained. If the isotope values are similar, then recent meteoric water is indicated. If the isotope values differ, a number of processes could have occurred: evaporation prior to recharge; mixing with palaeowaters (eg. Issar, 1983) or pure palaeowater, which was recharged during a different climate; exchange with host rocks (chiefly affecting oxygen ratios); recharge at altitude (eg. Mazor & Verhagen, 1983) or significantly far away to invoke a continental (orographic) effect.

1.3 INTRODUCTION TO THIS STUDY

1.3.1 HISTORICAL BACKGROUND

Although the area of the Cape Fold Belt as a whole has a pleasant Mediterranean climate and receives a moderate rainfall, the distribution of rain and heat is seasonal and spatial, with the summer being particularly dry and hot and the valleys being even drier and hotter than the surrounding mountains. This climatic contrast led to the close association of settlements with water. A permanent

and reliable supply of potable water from springs bore an attraction that was irresistible. Furthermore, the heated nature of the hot spring water meant that it could provide for functions other than drinking and irrigation.

As far back as the beginning of the 18th century, the springs of Brandvlei, Citrusdal and certainly others (Malmesbury, Goudini) were known to the Cape Colony, and during the century bathing facilities were erected at Brandvlei, Citrusdal and at Zwartberg (Caledon) (Burchell, 1822). Reading Burchell's account and other information provided by The Baths (Citrusdal), it is apparent that the bathing facilities go through phases of renewal and disuse. At present, most of the hot springs in the Cape are under management as a commercial venture, however, Malmesbury and Toowerwater are both in disuse. The Malmesbury spring is too cool, being only 34°C, and has an odour problem, giving off poisonous and unpleasant smelling H_2S. Toowerwater has closed down as the operators went bankrupt.

In the past, manganese mining took place at the extensive, but patchy and low grade mineralization at Warmwaterberg.

1.3.2 SCIENTIFIC INVESTIGATIONS

The earliest concerted scientific investigations into the springs appear to be those of M.M. Rindl, a Professor of Chemistry at Grey University College, Bloemfontein. He published a series of supplements in the South African Journal of Science, from 1917 to 1934, all entitled 'The Medicinal Springs of South Africa', in which he analysed the dissolved mineral content and the gases emitted, of many of the thermal springs of South Africa, including most of those in the Cape Fold Belt. Kent (1949) published a fairly comprehensive article which also dealt with the dissolved mineral matter in the spring waters.

The first isotopic investigation was done by Mazor and Verhagen (1983) on samples collected in 1971 and 1972. They conducted the full range of analyses: dissolved ions, oxygen and hydrogen isotopes, radiocarbon, tritium and dissolved noble gases. The work is commendable on the basis of the analyses done and their interpretation based on the results, however, the weakness lies in the fact that they took mostly single samples from each spring. Gat (1971) takes cognisance of the natural noise in stable isotope data derived from groundwater; this noise results from meteorologic variability and the complexity of the hydrologic setting. "Because of this noise one should refrain from attempts to overinterpret isotope data." (Gat, 1971).

Subsequent isotopic data has been acquired by the Department of Water Affairs and Forestry, but it remains unpublished; some of it is reported here, along with the data from Mazor and Verhagen (1983).

1.3.3 AIMS OF THIS STUDY

This project is the first undertaken at UCT in isotope hydrology; it was made possible by the acquisition of a Finnigan MAT 252 mass spectrometer which is able to analyse for hydrogen and deuterium, as well as oxygen isotope ratios. Hot springs were the original focus of this project, but it soon became apparent that basic meteorological isotopic constraints were needed and so the project broadened to include collection of precipitation.

The collection of precipitation in this study has resulted in a considerable database of meteoric stable isotope data which can be used in many applications, especially hydrological. This removes the need to acquire such data, although it would still have merit, from the International Atomic Energy Agency in Vienna, whose data is expensive for South African researchers. Since the inception of this project, the IAEA data has become available on the internet on the World Wide Web at http://www.iaea.or.at/.

The reasons for focusing on the thermal springs are as follows:

- there are a manageable number of them, as compared to cold springs,
- they are easy to locate, being the focus of commercial attention,
- the range in temperatures provides a comparitive parameter between springs,
- circulation is clearly deep and therefore borehole investigations are unlikely to ever have penetrated the horizons which are involved in the groundwater circulation of these springs; isotope techniques provide a remote method of investigating processes at depth as well as during and prior to recharge.

The aims of this project are to use stable isotope ratios and observed geological and physical paramaters to provide some constraints on the recharge area and elucidate the subsequent flow path and reservoir size through deep aquifers, thereby also providing a check on the geothermal gradient. The possibility of isotope exchange with aquifer rocks is also discussed and the source of gases, mainly CO_2, is speculated upon.

2 REGIONAL BACKGROUND

In order to place the Cape thermal springs studied into a context and to provide a background against which the results of this project can be interpreted, this chapter summarises the more relevant features of the geology, climate and hydrology of the Cape Fold Belt.

2.1 GEOLOGY

2.1.1 STRATIGRAPHY

The geology of the Western Cape is dominated by the Palaeozoic Cape Supergroup of which the resistant sandstones and quartzites of the Table Mountain Group are the most prominent. Stratigraphically below the Cape Supergroup is a basement consisting of the low grade metamorphic Malmesbury and Kango Groups and the plutons of the Cape Granite Suite. The Table Mountain Group is the basal group in the Cape Supergroup, above which lie the shale and sandstone formations of the Bokkeveld and Witteberg Groups. The Cape Supergroup is overlain by the varied sedimentary succession of the Karoo Supergroup. Cretaceous deposits are present mainly in the southern intermontane and coastal plain basins, as well as offshore. Superficial sediments also occur, particularly in the lowlands.

2.1.1.1 MALMESBURY AND KANGO GROUPS

The Malmesbury Group is a poorly exposed and poorly understood late Precambrian group of mainly pelitic rocks, which were metamorphosed during the Pan-African Saldanian Orogeny and somewhat again during the Cape Orogeny. The Malmesbury Group is divided into 3 terranes on the grounds of lithological and structural changes that occur across narrow zones of tectonic dislocation (Hartnady et al, 1974). The stratigraphy within each of these terranes is highly varied and little systematic difference exists between the terranes. All are dominated by highly metamorphosed shale and phyllite with the less abundant arenitic rocks varying from metagreywacke to sericitic quartzite and conglomerates. This variety is bolstered by the presence of limestone, dolomite and metavolcanics.

The Kango Group is an analogue to the Malmesbury Group, occurring east of Ladismith, and consists of the lower Goegamma Subgroup of predominantly fine clastic sediments and limestone and the upper Kansa Subgroup of medium to very coarse clastic sediments (Theron et al, 1991b). Metamorphism is similar to the Malmesbury Group.

2.1.1.2 CAPE GRANITE SUITE

The Cape Granite Suite is divided into 3 batholiths, one of which is in the Western Cape. This batholith comprises up to 18 major intrusive phases grouped into 8 plutons (Scheepers, 1995).

The Cape Granite Suite intruded into the Malmesbury Group from 600-520Ma and younger (Schoch, 1976; Schoch & Burger, 1976; Scheepers, 1995). Generally speaking, older, S-type granites occur in the Tygerberg Terrane, whereas I-types are found in the other two terranes. Minor, younger, A-type granites are also found. The S-types are metaluminous to slightly peraluminous; the I-types are monzogranites, alkali-feldspar granites and granites.

2.1.1.3 CAPE SUPERGROUP

2.1.1.3.1 Table Mountain Group

The lowermost formation of the Table Mountain Group varies from the Piekerniersкloof Formation in the northern areas of the Cape Fold Belt to the Graafwater Formation in the south-eastern areas. In some areas the Graafwater Formation thins out and leaves the Peninsula Formation as the base of the Cape Supergroup.

The Piekerniersкloof Formation is predominantly conglomeratic in contrast to the Graafwater Formation which is a purplish to reddish sandstone, siltstone and mudstone. The Peninsula Formation is a very thick sequence of mainly planar bedded, light grey, coarse-grained sandstone to quartzite with minor siltstone and vein quartz pebble horizons. The thin Pakhuis Formation is a mixed unit consisting of very fine to very coarse sediments with glacial features. The Cedarberg Formation is also thin and predominantly a shale/siltstone unit. Lastly, the Nardouw Subgroup is very similar to the Peninsula Formation, being mainly constituted by cross-bedded arenites (Broquet, 1992).

The great thickness and well cemented character of the Table Mountain Group sandstones and quartzites results in this group being the chief component of the high and dramatic relief areas of the Cape Fold Belt.

2.1.1.3.2 Bokkeveld Group

The Bokkeveld Group is a series of pelitic and arenitic formations, which, due to the thickness of the pelitic units, forms subdued hogsback type landscapes (Gresse & Theron, 1992).

2.1.1.3.3 Witteberg Group

The Witteberg Group is a more arenaceous set of pelite and arenite formations than the Bokkeveld Group, and is more micaceous. The sandy formations are also more mature and tend to be thicker resulting in the Witteberg Group forming moderately mountainous country (Gresse & Theron, 1992).

2.1.1.4 KAROO SUPERGROUP

The upwards continuation of the Cape Supergroup sedimentation becomes known as the Karoo Supergroup upon the initiation of the tillite of the Dwyka Group. Above the Dwyka tillite lies the Ecca Group which is a mixed package of offshore to onshore facies within various formations.

The Beaufort Group fluvial sediments border on the Cape Fold Belt and the higher groups within the Karoo Supergroup are totally beyond the extent of the Cape Fold Belt (Gresse & Theron, 1992).

2.1.1.5 MESOZOIC DEPOSITS

Of the onshore deposits, several basins along the east-west striking axis of the southern arm of the Cape Fold Belt contain sediments. These deposits are primarily coarse conglomerates with coarse sandstones and some finer horizons (Theron et al, 1991b).

2.1.1.6 CENOZOIC DEPOSITS

In places along the coast, calcareous dunes and beach sand deposits occur. Ferricrete and silcrete occur, sometimes found capping low, flat hilltops. Scree, alluvial fans and gravel deposits are abundant, especially near the main river courses, such as the Berg, Breede and Olifants. These unconsolidated or semi-consolidated coarse deposits can reach several tens of metres in thickness (Gresse & Theron, 1992).

2.1.2 STRUCTURE AND METAMORPHISM

2.1.2.1 SALDANIAN OROGENY

Multiphase deformation is associated with the Kango and Malmesbury Groups during Pan-African times. All orders of structures are present and almost all of these have been reactivated during the Cape Orogeny and during the breakup of Gondwana from the Jurassic to the Cretaceous (Gresse et al, 1992). The two major tectonic boundaries that divide the Malmesbury Group into 3 terranes are near vertical, mylonitised or cataclastic zones. Not only have these zones clearly been reactivated as stated above, but they are along strike with other major fault lines that are in the Table Mountain Group only. Seeps and springs occur along these two major dislocation zones.

Metamorphism during the Saldanian reached greenschist facies conditions (Hoal, 1978). Since this time, the Malmesbury has not had any primary permeability (between grains) and even the secondary permeability (through fractures) is limited due to the dominance of clay rich formations which prevent interconnectivity between fractures.

2.1.2.2 CAPE OROGENY

Deformation has been dated in 4 episodes from 278-230Ma (Hälbich, 1992). Structures include all magnitudes of folds, faults and fractures. Some of the regional faults are still active.

The Cape Supergroup only possesses secondary permeability due to cementation of primary porosity during orogeny. This secondary permeability occurs along faults, joints, bedding planes and duplex ramps. The Table Mountain Group is highly duplexed in some areas. All of the above fractures may be cemented shut by silicification and/or the precipitation of manganese and iron mineral mixtures at low temperatures. Faults can be very narrow, discrete zones with some brecciation or wider cataclasite zones of a few metres.

Orientations of fault and fracture systems are the same within the two major aquifer units of the Table Mountain Group, the Peninsula Formation and the Nardouw Subgroup. The major orientation is NW-SE; E-W fractures are closely spaced; NE-SW fractures are widely spaced, often manifest as master joints (Umvoto, 1995b).

Metamorphic conditions reached greenschist facies grade (Diamond, 1994), in which much of the sandstone in the Table Mountain Group recrystallized to quartzite and some fractures were sealed by cementation.

2.2 CLIMATE

The Western Cape is the small portion of South Africa which experiences a Mediterranean climate. Northward this climate regime grades into semi-desert and to the east, the climate becomes less seasonal and tends towards subtropical on the coast.

The essence of a Mediterranean climate is cold, wet winters and warm, dry summers. This pattern is complicated by the presence of a cold Benguela ocean current and upwelling system to the west and a warm Agulhas ocean current and shallow coastal waters to the south and east. The South Atlantic High Pressure anticyclone also complicates matters by bringing strong summer winds from the south-east, which, having passed over some warm water, are mositure laden and often cause summer rain, especially along the southernmost line of mountains. Furthermore, the generally mountainous nature of the Cape Fold Belt results in the entire region having sharp changes in climate; ie. local microclimates.

Of concern for this project is the fact that the high relief areas (which is not related to the absolute altitude) receive more rain. High altitude areas will simply be colder. In effect, the continental,

altitude and amount effects, as discussed in Chapter 1, will be influenced strongly by the positions of mountains.

Rainfall is highly variable and ranges from low summertime monthly means of 10-20mm in the valleys and on the coastal plains and ±50mm in the mountains, to winter monthly means of 40-100mm and over 200mm, respectively (data from South African Weather Bureau).

Temperatures vary from winter mean minimum daily temperatures of ≤5°C in the inland valleys and ±10°C on the coastal plains, to ≥30°C and ±25°C for the summer mean maximum daily temperature, respectively (data from South African Weather Bureau).

2.3 HYDROLOGY

2.3.1 SURFACE WATER

The Cape Fold Belt area has a very seasonal runoff, with most rain falling from May to September. Human activities have reduced this by drawing off much of the winter flow into dams for agricultural and domestic supplies, especially over the summer period. The Cape has no large rivers. A few natural shallow lakes existed (eg. Voëlvlei, Brandvlei), but these are now some of the many large dams for urban supply. The present situation is that of moderated seasonal flow in the rivers and lots of standing water all year round.

2.3.2 GROUNDWATER

2.3.2.1 UNCONSOLIDATED AQUIFERS

These aquifers are sporadically located around the Cape, with most being on the coastal plains (sand aquifers) and in talus slopes and alluvium of the inland valleys (Theron et al, 1991a). Their flow is seasonal in that some have varying water tables (Maclear, 1995) while others appear to dry up in summer (Umvoto, 1995a).

2.3.2.2 CONSOLIDATED AQUIFERS

The non-igneous basement rocks of the Cape are predominantly argillaceous and have also had their primary porosity and permeability reduced by deformation and metamorphism. Granites possess no primary porosity. The Cape Supergroup is composed of argillaceous layers, which are impermeable, and sandstones which have mostly been recrystallized to quartzite, which is also impermeable, or have simply been compacted to the extent that they are impermeable (Kotze, 1995). Movement of groundwater in the Cape only occurs as a function of secondary permeability along fractures and bedding planes (Umvoto, 1995a and b). Seeing as most rain falls on the mountains, joints and fractures within the Table Mountain Group are therefore the main features responsible for the distribution of groundwater flow in the Cape.

2.3.2.2.1 Cold springs and seeps

Numerous springs and seeps occur throughout the Cape Fold Belt. Cold springs often occur at the contact between the Peninsula and Cedarberg Formations, especially in the presence of a major linear structure (Kotze, 1995; Umvoto, 1995a).

2.4 THERMAL SPRINGS

All groundwater which sinks to any appreciable depth will be heated by the ground. A purely arbitrary temperature of 6°C above average annual surface temperature is given in Mazor (1991) as that which divides cold springs from thermal springs. With annual average temperatures between 15°C and 20°C for towns in the Cape valleys and coastal plains, any water discharging at or above 20°C to 25°C can be said to have circulated to depths of at least a few hundred metres.

Various classifications also exist in order to group springs into classes by temperature (eg. Kent, 1949), however, they have no geological significance in the Cape. This is because there is a full gradation of springs from cold (<20°C) to very hot, which is represented by Brandvlei, the hottest spring in the country at 64°C. This temperature coincides very nicely with Mazor (1991, page 52) who says that "Warm springs with temperatures up to 65°C are common in tectonically bisected terrains, where groundwater can circulate to appreciable depths." This can be taken to indicate that temperatures above 65°C are restricted to tectonically active (volcanic) areas. Two examples of springs intermediate between cold and hot are Witzenberg and Rietfontein, which are not commonly regarded as `hot springs'.

Table 2.1 contains some basic information about the thermal springs of the Cape. The data is derived from many sources and in the case where various sources reported the same parameter, the sources all agreed.

Figure 2.1 is a map of the Cape Fold Belt area, with the springs and rainfall stations marked on it. Major faults and the outcrop area of the Table Mountain Group are also indicated.

SPRING	T	flow	altitude	West Coast distance	geological environment # ⇒ Fe,Mn,Si mineralization
Brandvlei *Brandvlei Prison*	64°C	126l.s^{-1}	220m	90km	TMG-Bokkeveld Group contact + regional fault in TMG
Caledon *The Overberger*	53°C	10l.s^{-1}	360m	100km	TMG-Bokkeveld Group contact + regional fault in TMG #
Calitzdorp *Calitzdorp Spa*	52°C		200m	310km	TMG-Bokkeveld Group contact + TMG-Uitenhage Group unconformity
Citrusdal *The Baths*	43°C	30l.s^{-1}	250m	80km	fault in Nardouw Subgroup of TMG
Goudini *Goudini Spa*	39°C	3l.s^{-1}	290m	80km	regional fault in TMG (Peninsula Formation/Nardouw Subgroup faulted together)
Malmesbury	34°C	±4l.s^{-1}	120m	40km	on fault in Malmesbury Pluton of Cape Granite Suite
Montagu *Avalon Springs*	45°C		280m	155km	TMG-Bokkeveld Group contact + near regional fault in TMG
Rietfontein	~27°C	±2l.s^{-1}	700m	260km	Dwyka Group-Prince Albert Formation contact
Toowerwater	49°C		800m	455km	regional fault in TMG (Peninsula Formation/Enon Formation faulted together) #
Warmwaterberg *Warmwaterberg*	44°C	±5l.s^{-1}	500m	225km	near top of Nardouw Subgroup + regional fault in TMG #
Witzenberg	~28°C	±1l.s^{-1}	800m	105km	in Peninsula Formation

Table 2.1: Some basic information about thermal springs in the Cape Fold Belt. The distance from the West Coast was measured by taking a straight line with an E-W orientaion. TMG = Table Mountain Group. A '±' indicates that the flow rate was estimated by observation. A '~' indicates that the temperatures were estimated on one occasion.

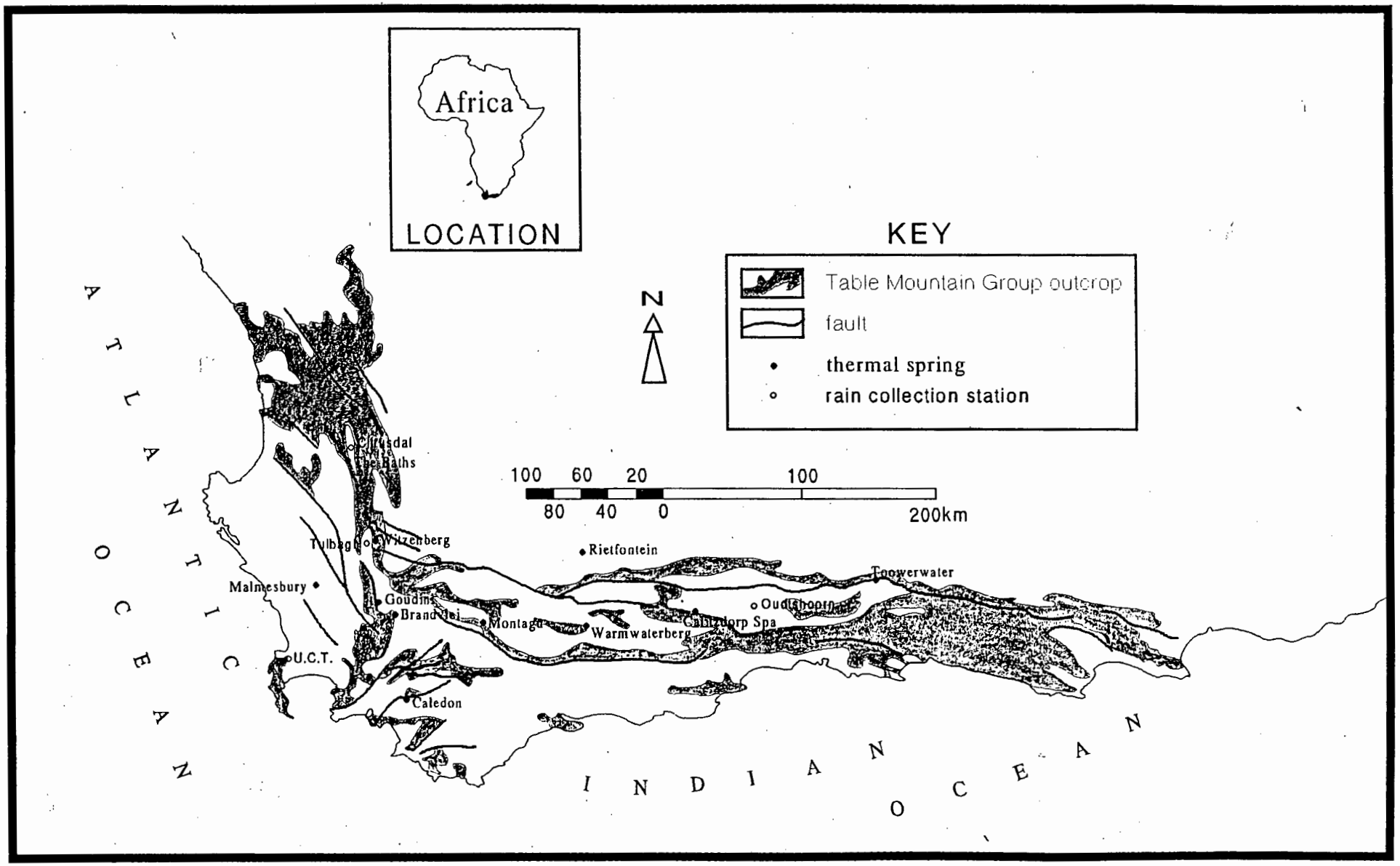

Figure 2.1: A map of the Cape Fold Belt area with thermal springs and rain collection stations (after Hammerbeck and Allcock, 1985).

3 METHODS

In this chapter, the sampling, preparation, analysis and raw data treatment of samples is presented. Statistical or other treatment of the data is presented in the appropriate sections in the Results (Chapter 4).

3.1 SAMPLE COLLECTION

3.1.1 ROCKS

Rocks from the Malmesbury Group, the Table Mountain Group and the Bokkeveld Group were collected, from surface exposures, either natural outcrops or roadcuts. Effort was taken to obtain the least weathered sample from a locality, however, there were some outcrops which were weathered throughout. Each sample weighed about 1kg.

3.1.2 RAIN WATER

Rain water was collected in four locations around the Cape for a period of several months: Cape Town (UCT), Citrusdal, Oudtshoorn and Tulbagh. Some basic information about these four stations is given in *Table 3.1*. Rain was allowed to collect in a rain gauge and after each rain event or series of showers, the contents of the gauge would be emptied into a larger container which was kept sealed. At the end of each month, two sample bottles (Haynes and Matthews plastic 100ml flat medical type) were filled with the contents of the large container and stored in a cool, dark place. This method ensured that an integrated sample of the month's rain was retained.

STATION	ALTITUDE	TEMPERATURE	n	RAINFALL	n
UCT	120m	16.7°C	29	1200mm	25
Citrusdal	190m	19.7°C*	9	365mm	23
Tulbagh	180m	17.2°C	8	477mm	116
Oudtshoorn	320m	18.1°C	13	247mm	55

Table 3.1: Basic details for the rain collection stations. n = number of years of observation. Temperature and rainfall are both mean annual figures. The short periods for some of the temperature data are not critical, as temperature is not subject to fluctuations as drastic as rainfall. This data has also not been used further in this project. * ⇒ station at Clanwilliam Dam, 50km north of Citrusdal. (Data from the South African Weather Bureau.)

3.1.3 SPRING WATER

Water was collected at monthly intervals at 4 of the thermal springs: Brandvlei, Calitzdorp Spa, Citrusdal (The Baths) and Malmesbury. Two sample bottles were filled with water which was collected from as close to the source as possible in order to minimize fractionation by evaporation. Samples

were kept in cool dark places.

3.1.4 SPRING GAS

Gas bubbling up through the source pools at Brandvlei, Calitzdorp and Malmesbury was collected in November 1995. A plastic bottle with the bottom cut off was attached to an evacuated glass vessel shut off to the system with a valve. The whole apparatus was lowered into the pools and the hot water was allowed to displace all the atmosphere in the system, barring a few millilitres in the mouth of the vacuum vessel. 'Fishing' for bubbles then commenced and they were allowed to accumulate in the plastic bottle and displace the spring water. Once sufficient gas had been trapped, the valve to the vacuum vessel was opened to allow the collected gas into the vessel. Obviously this gas would be saturated with H_2O and also, a small amount of air was included in the sample, however, the H_2O was removed during sample preparation and the contamination from atmospheric CO_2 is insignificant.

3.2 SAMPLE PREPARATION

3.2.1 SILICATES

Highly weathered rinds were sawn or broken off samples which were then scrubbed clean of surface dirt, dried, jaw-crushed and then milled for about 100 seconds to a fine powder.

3.2.1.1 OXYGEN

These whole rock powders were reacted with ClF_3 at 550°C overnight according to the methods outlined in Borthwick & Harmon (1982) and Vennemann & Smith (1990). The quartz standard NBS-28 was duplicated with each run of 8 samples.

3.2.1.2 HYDROGEN

Samples were dried at 110°C for 24 hours prior to analysis. Structural water was driven off by heating with a propane/O_2 torch to ~1400°C. The water was collected in tubes containing Zn shavings (supplied by Finnigan Mat), according to the method described in Vennemann & O'Neil (1993). The glass tubes containing Zn and H_2O were heated at 450°C for 30 minutes just prior to analysis, in order to reduce the H_2O to H_2 (and ZnO).

3.2.2 WATER

3.2.2.1 OXYGEN

For the original description of this method, see Socki et al (1992). A 7ml vacutainer test tube was placed onto the vacuum line (*Figure 3.1*) via a hypodermic needle and then evacuated. Approximately 0.5atm of CO_2 was loaded into the vacutainer from a cylinder of medical grade CO_2. The vacutainer was removed from the line and injected with ±2ml of sample water. The vacutainer was then fixed to

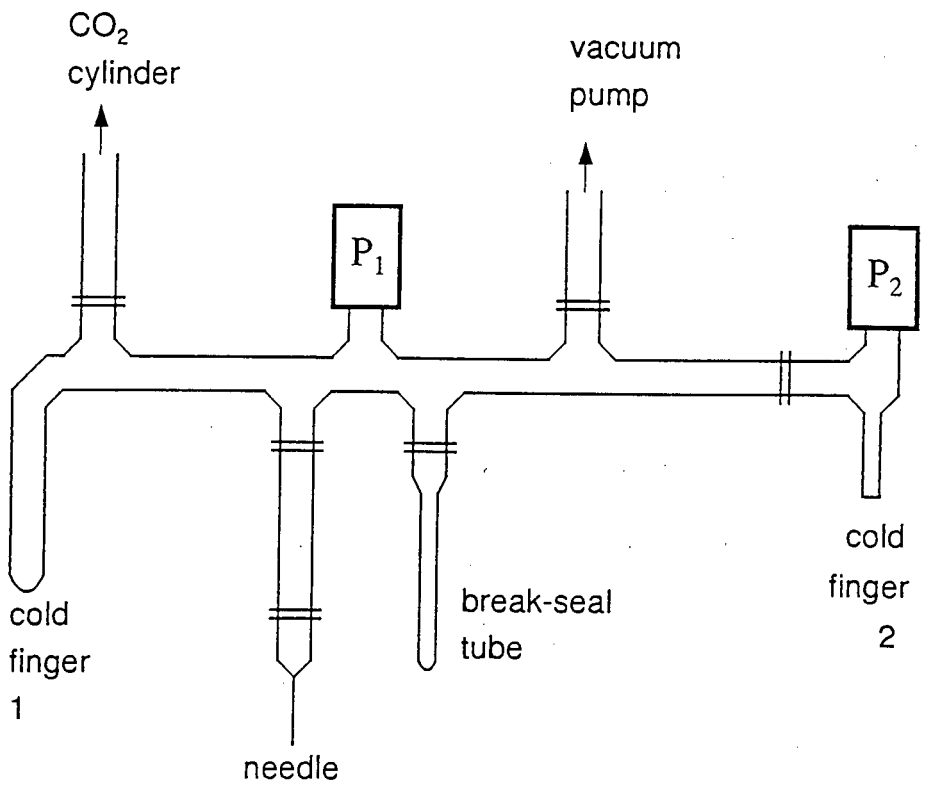

Figure 3.1: The sample preparation line for analysis of the oxygen isotopes of water. CO_2 is let into the system, in order to eventually be captured in the break-seal tube, before being released into a mass spectrometer for determination of the $\delta^{18}O$ of the water sample. $\mathbf{P_1}$ is a Pirani pressure gauge and $\mathbf{P_2}$ is a pressure transducer. || indicates a valve across the line.

an automatic shaker and submerged in a 25°C bath for at least 1.5 hours.

The vacutainer was placed onto the line with the hypodermic needle just piercing the rubber seal and not the contents, and the line evacuated. A small portion of the line was closed off and the vacutainer was pushed over the mouth of the needle, allowing an aliqout of the vacutainer gas contents to enter the closed off portion of the line. Within 4 to 5 seconds, the vacutainer must be closed to the line to prevent excess water vapour getting into the line and degassing CO_2, or producing kinetic fractionation of the CO_2. This aliqout method gives exactly the same results as the freezing method originally advocated by Socki et al (1993).

The aliquot was allowed into the line and frozen into a cold finger with liquid nitrogen. The non-condensibles were then pumped out. The liquid nitrogen was removed from the cold finger and immediately replaced with a slush of nearly frozen isopropyl alcohol. The CO_2 was allowed to warm up and expand into the line, only to be frozen into a second cold finger attached to a pressure transducer. The second cold finger was shut off from the line and heated to room temperature in order to measure the voltage which can be used to calculate the quantity of CO_2 and hence the yield. The yield was required to estimate whether or not there had been any leakage of CO_2 from the vacutainer. Assuming approximately the same amount of CO_2 had been let into the vacutainer, the yields should all be similar. The second cold finger was opened to the line and liquid nitrogen was placed around a break-seal tube in order to freeze out the CO_2. The break-seal tube was then shut off from the line and sealed with an oxygen-propane torch.

3.2.2.2 HYDROGEN

Two methods were employed. Both gave identical results. Break-seal tubes were loaded with 5 or 6 grains of zinc, weighing about 10mg, and left to dry in a 100°C oven. The ratio of zinc to water is as recommended by the suppliers of the zinc, Finnigan Mat.

3.2.2.2.1 Micropipette method

A break-seal tube was then placed onto the vacuum line (*Figure 3.2*) and evacuated. 1μl of sample water was micropipetted into a short glass tube which was placed onto the line and immediately immersed in liquid nitrogen. Once the water had frozen, the short glass tube was evacuated. The liquid nitrogen was then removed and placed over the break-seal tube while the short glass tube was heated with a hot air gun. Any non-condensibles were then pumped out and the break-seal tube was shut off from the line and burnt off with an oxygen-propane torch.

3.2.2.2.2 Capillary tube method

A 2μl capillary tube had its tip lowered into the sample water which rose into the tube. The tube was

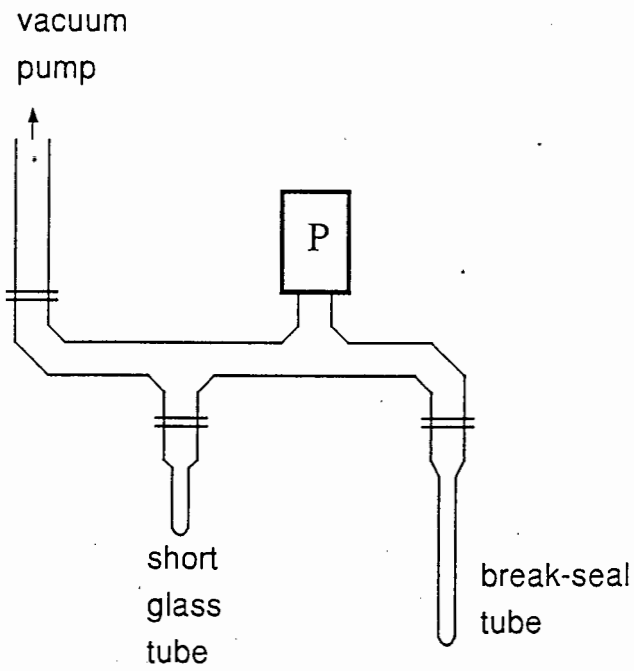

Figure 3.2: The sample preparation line for the analysis of the D/H ratio in water. This line is really just a part of the one shown in *Figure 3.3*. $H_2O(l)$ is the input and output substance. **P** is a Pirani pressure gauge and ‖ indicates a valve.

carefully wiped dry on the outside and dropped to the bottom of a break-seal tube (with Zn loaded in) which was immediately placed onto the vacuum line (*Figure 3.2*) and immersed in liquid nitrogen. The water was allowed to freeze after which the line was evacuated and the break-seal tube burnt off with an oxygen-propane torch.

For both methods, just prior to analysis, the break-seal tube was put in a furnace at 450°C for 30 minutes in order to reduce the H_2O to H_2.

3.2.3 SPRING GAS

The preparation procedure described below enables the analysis of the total C in a CH_4 and CO_2 mixture, such as the gas that was collected from the springs.

The sample vessel was placed onto the line (*Figure 3.3*). The sample was then let into the line and the CO_2 and H_2O were frozen into the 1st U-tube with liquid nitrogen. The line was opened to a furnace containing CuO at 650°C for CH_4 to react to CO_2 which was indicated when the pressure dropped back to a vacuum, as the CO_2 froze out. The furnace was then closed to the line and U-tube 1 was opened to U-tube 2. The liquid nitrogen on the 1st U-tube was removed and immediately replaced with a slush of nearly frozen isopropyl alcohol while the liquid nitrogen was placed onto the second U-tube. Once the CO_2 had frozen into the 2nd U-tube, the 1st U-tube was shut off from the line. The liquid nitrogen was removed from U-tube 2 and immediately replaced with a slush of nearly frozen isopropyl alcohol while the liquid nitrogen was placed around the break-seal tube. Once the CO_2 had frozen into the break-seal tube, the non-condensibles were evacuated and then the break-seal tube was shut off from the line and burnt off with an oxygen-propane torch.

3.3 SAMPLE ANALYSIS

All isotope ratios were measured using a Finnigan MAT 252 mass spectrometer, housed in the Archaeology Department at UCT.

3.3.1 SILICATES

Oxygen isotope ratios of the whole rock were measured in the form of CO_2 with the working standard, NBS-28, having a $\delta^{18}O$ value of 9.64‰ on the SMOW scale (Coplen et al, 1988). Hydrogen isotopes of some whole rocks were measured as H_2. The working standard used is CTMP (Cape Town Millipore Water) which has δD of -9‰ on the SMOW scale.

3.3.2 WATER

Oxygen isotope ratios of water were measured in the form of CO_2. The working standard, CTMP has a $\delta^{18}O$ value of -2.85‰ on the SMOW scale, as measured at Geochron Labs (C. Harris, pers. comm,

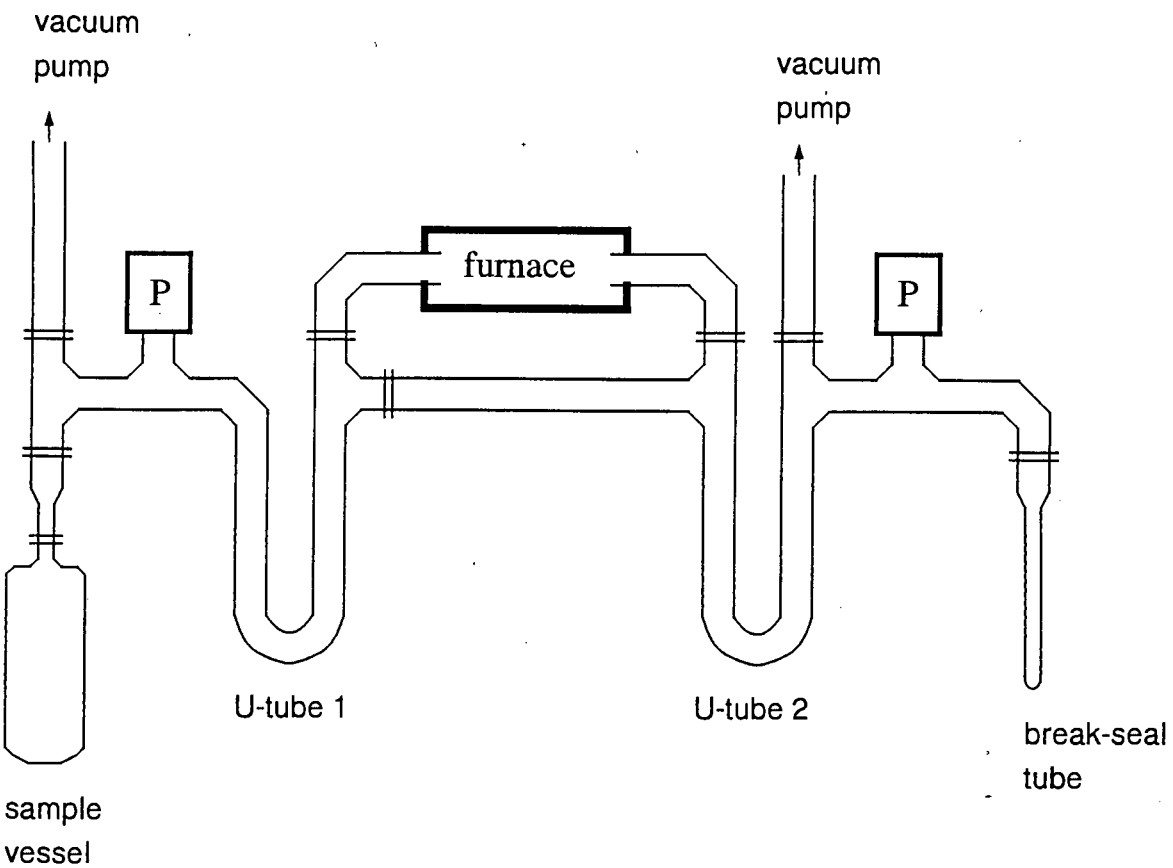

Figure 3.3: The sample preparation line for the spring gas. The furnace is of the miffle type and both pressure gauges are of the Pirani type (**P**). || shows the position of a valve in the vacuum line. A gaseous mixture of CO_2 and CH_4 is let into the system, the CH_4 is converted to CO_2, and the CO_2 is collected.

1996). Hydrogen-deuterium ratios in water were measured in the form of H_2 gas. The working standard, CTMP, has a δD value of -9‰ on the SMOW scale, determined as for $\delta^{18}O$ above.

3.3.3 SPRING GAS

The $\delta^{13}C$ of the carbon dioxide and methane in the gas was measured in the form of CO_2. The working standard is Nama Group marble with a $\delta^{13}C$ value of 1.57‰ on the PDB scale. The Nama marble was calibrated against NBS-19, which has a $\delta^{13}C$ value of 1.95‰ on the PDB scale.

3.4 DATA TREATMENT

Data needs to be reported relative to internationally recognized values, such that values from different studies may be compared. Standard Mean Ocean Water (SMOW) is used as the standard relative to which all $\delta^{18}O$ and δD values are reported. As there is some debate in stable isotope circles about the desirability of replacing SMOW with V-SMOW (Vienna-SMOW) (Chris Harris, personal communication), it has been decided to report data relative to SMOW in this work. The correction procedures used here are such that SMOW is exactly equivalent to the V-SMOW of Coplen (1988).

The raw isotope ratios obtained from the mass spectrometer were converted to values relative to SMOW according to the equations of Coplen (1988). Samples of V-SMOW and SLAP (Standard Light Antarctic Precipitation) were analyzed to determine the degree of raw data compression required. The internal water standard, CTMP (Cape Town Millipore Water), was calibrated against V-SMOW and SLAP (and independently analyzed) and used to correct for drift in the reference gases in the mass spectrometer.

Hydrogen and oxygen were corrected using the same methods, except that oxygen underwent an additional initial correction for equilibration betweeen H_2O and CO_2 at 25°C. The fractionation factor was assumed to be 1.0412 (Coplen, 1988).

The average deviation from the mean of duplicate runs of CTMP over the course of this research is 0.9‰ for hydrogen (n=14) and 0.13‰ for oxygen (n=7). The corresponding 2σ values are 1.1‰ and 0.18‰, respectively. These error bars are displayed in all the appropriate graphs in Chapter 4.

4 RESULTS

The bulk of this chapter presents new stable isotope data acquired for this project. Oxygen and hydrogen isotope ratios were measured in rocks, rain water, thermal spring water and gas discharged at three of these springs. The other significant type of data is meteorological, the most important of which is monthly rainfall figures. The data that has been gathered on rain, spring water, gas and rocks, will be dealt with in that order.

4.1 RAIN

4.1.1 RAINFALL DATA

The four rain stations at which rainfall was collected for isotope analysis were at UCT, Tulbagh, Citrusdal and Oudtshoorn (see *Figure 2.1*). The first three fall within the Mediterranean climate classification, whereas Oudtshoorn is semi-arid with an even, all year round rainfall. Some basic information on each station is listed in *Table 3.1.*

Total annual rainfall for 1995 tended to be well above average throughout the Cape; Cape Town was an exception, receiving roughly average, which, for the UCT area is 1100mm. The mean excess rainfall that stations received is around 17%. Graphs illustrating 1995 (and 1996 for UCT) versus average rainfall at the four stations are shown in *Figures 4.1 - 4.4* (data from South African Weather Bureau).

Rainfall in 1995 was quite erratic and tended to differ be large amounts from the monthly means for at least two months at each station. For the Cape Mediterranean area, the rainfall in July was above normal; October and December were both well above normal because of a family of cold fronts in late October and some convective rain (including thunderstorms) during late December; February was drier than usual; April was particularly dry due to the late onset of winter; September was also well below average, because of a reduced supply of frontal depressions. The area of the Little Karoo, which includes Calitzdorp and Oudtshoorn, experienced some of the same fluctuations from the normal, in 1995. Specifically, November and December were well above average, while January, April and September were all somewhat low.

4.1.2 STABLE ISOTOPES

Table 4.1 and *4.2* contain all the stable isotope data recorded for rain, hail and snow. In *Figures 4.5 - 4.8* the isotope ratios are plotted against time and it can be seen that $\delta^{18}O$ and δD covary. This is a known and expected result for meteoric water (Craig, 1961; Dansgaard, 1964). The most noticeable thing about these data is the remarkably good interstation correlation that exists for δD

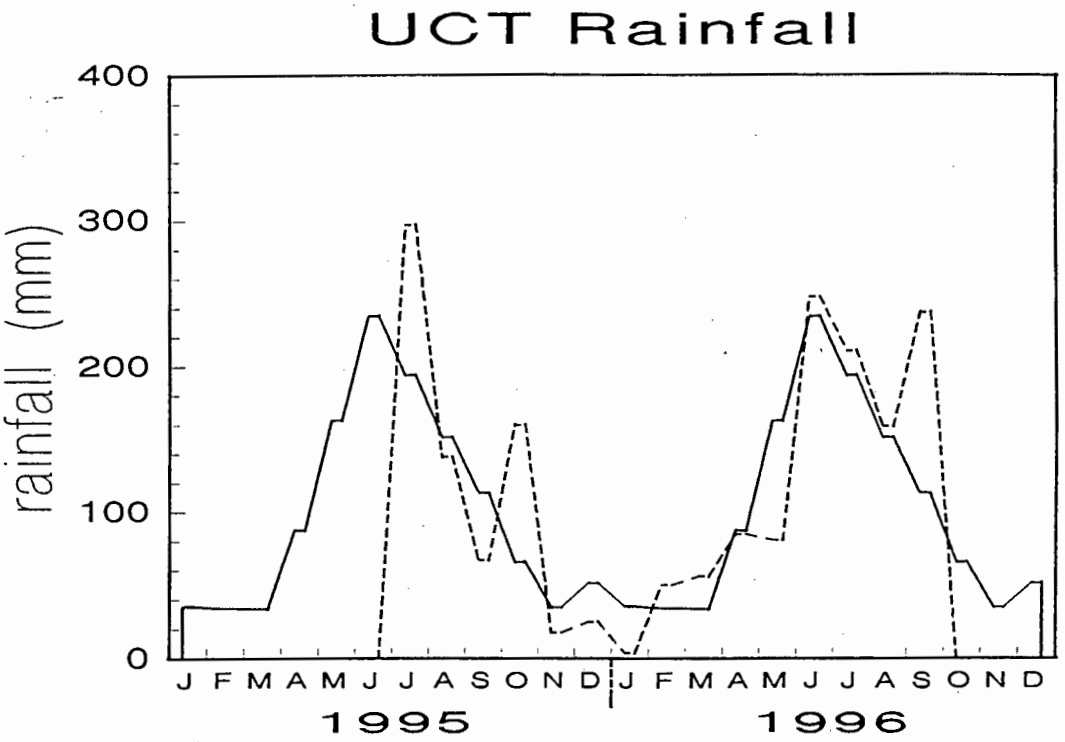

Figure 4.1: Monthly rainfall totals for July 1995 until September 1996 at UCT (dashed line) compared with the monthly averages (n = 25 years) as recorded at Groote Schuur (solid line) in the near vicinity.

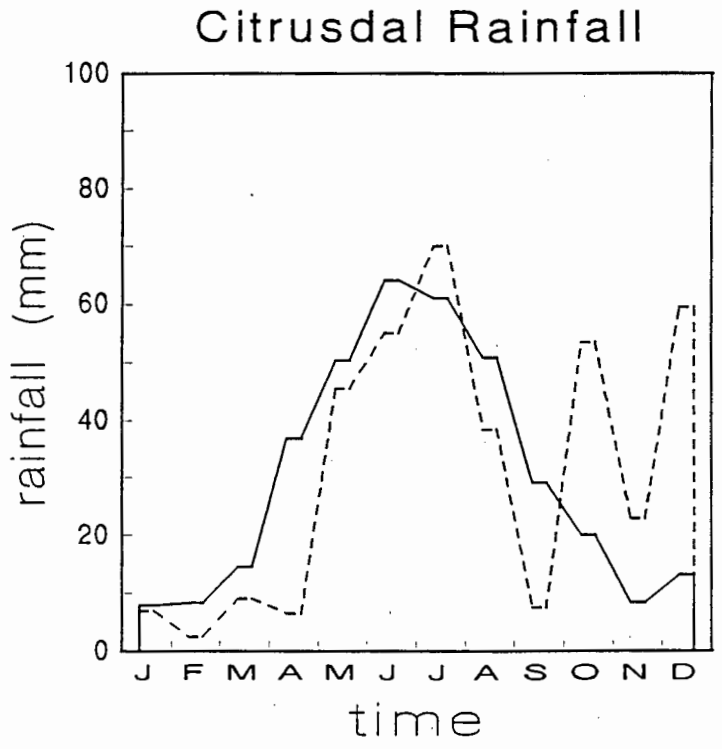

Figure 4.2: Monthly rainfall totals recorded in 1995 at Citrusdal (dashed line) compared to monthly means (n = 24 years) (solid line).

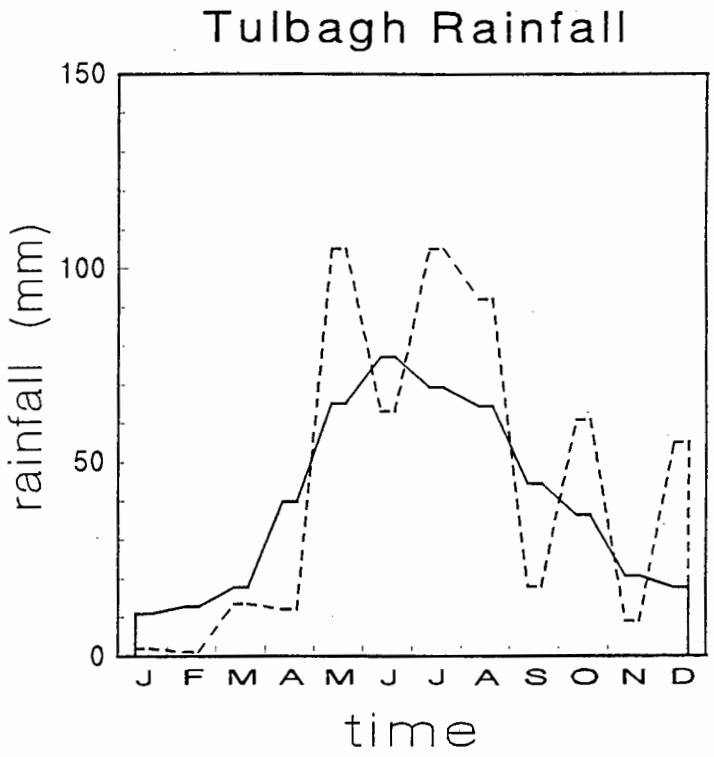

Figure 4.3: Monthly rainfall totals recorded at Tulbagh in 1995 (dashed line) shown against the monthly means (n = 116 years) (solid line).

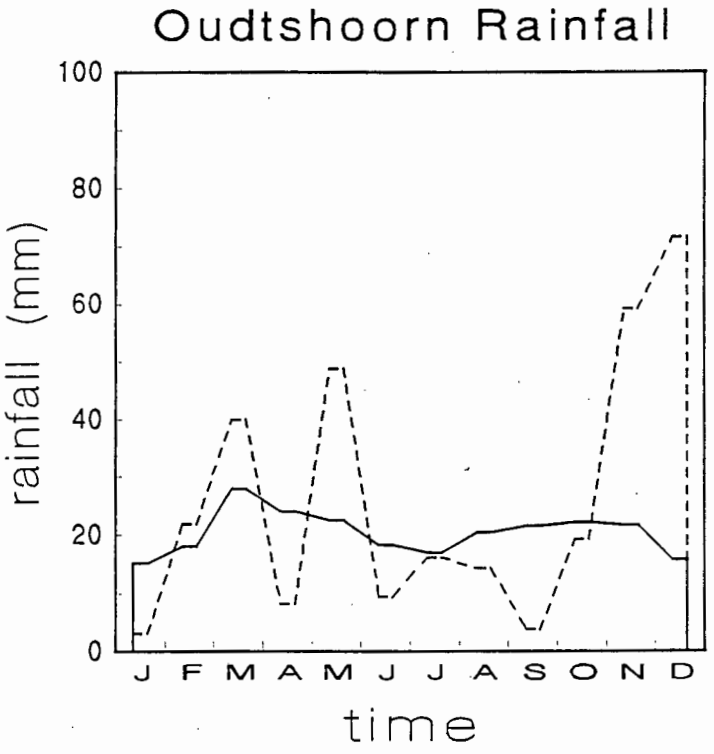

Figure 4.4: Monthly rainfall totals recorded for Oudtshoorn in 1995 (dashed line) as against monthly averages (n = 55 years) (solid line).

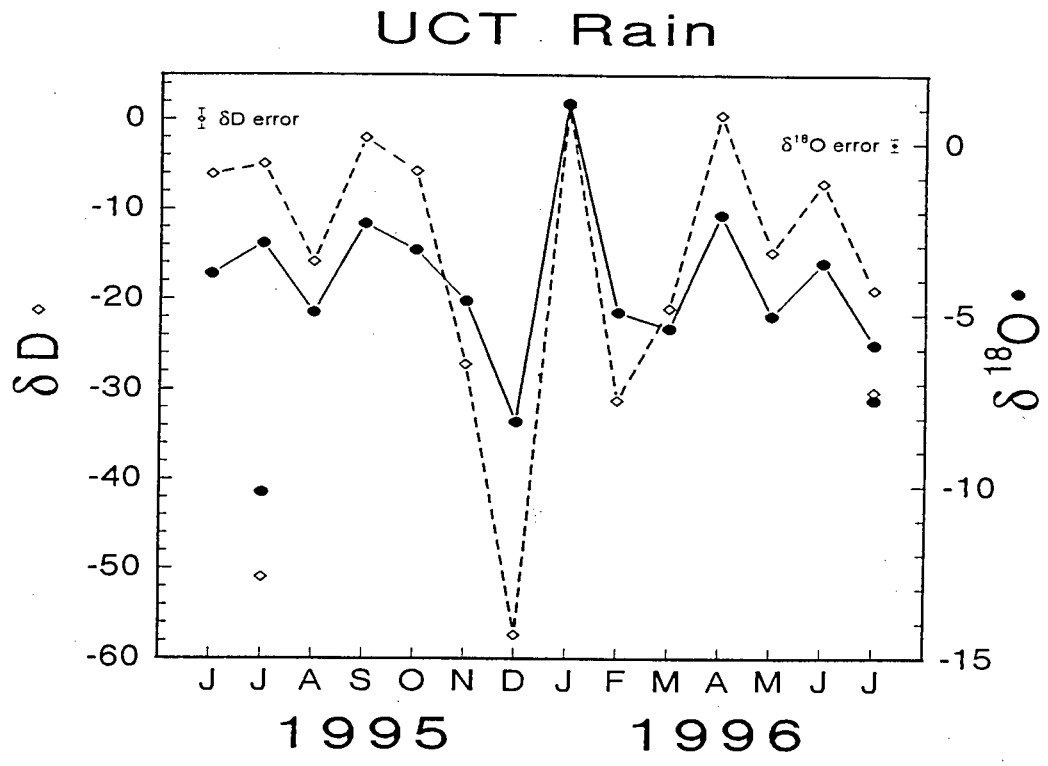

Figure 4.5: Integrated monthly totals of $\delta^{18}O$ (●) and δD (◇) for rain water collected on the Geological Sciences roof at UCT, plotted against time. The two hail samples are shown as separate pairs of values for July 1995 and 1996. Error bars are $\pm 2\sigma$.

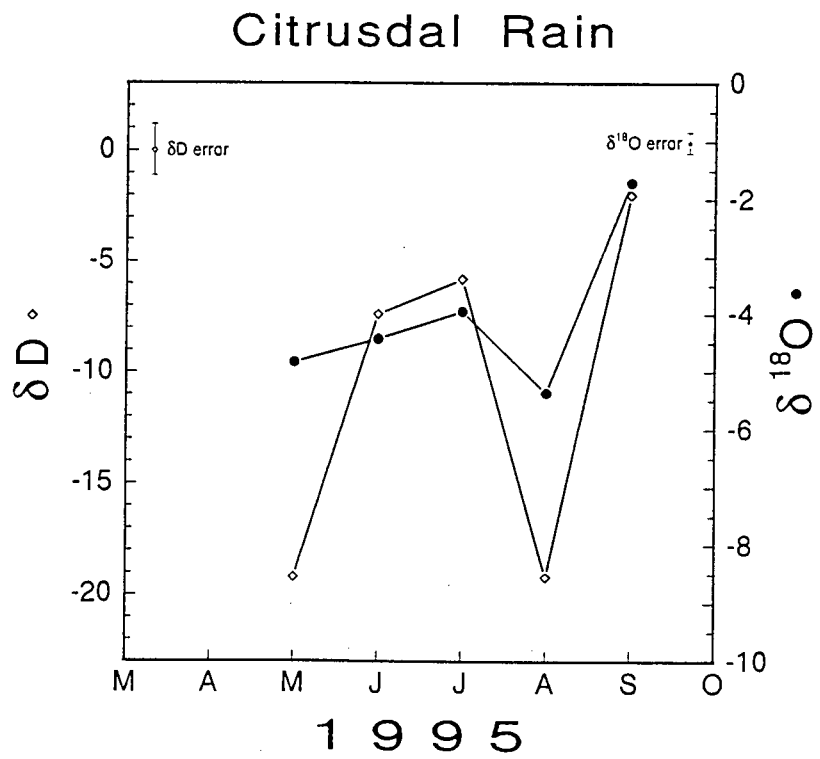

Figure 4.6: Monthly values for $\delta^{18}O$ (●) and δD (◇) for rain water collected in Citrusdal, plotted against time. Error bars are $\pm 2\sigma$.

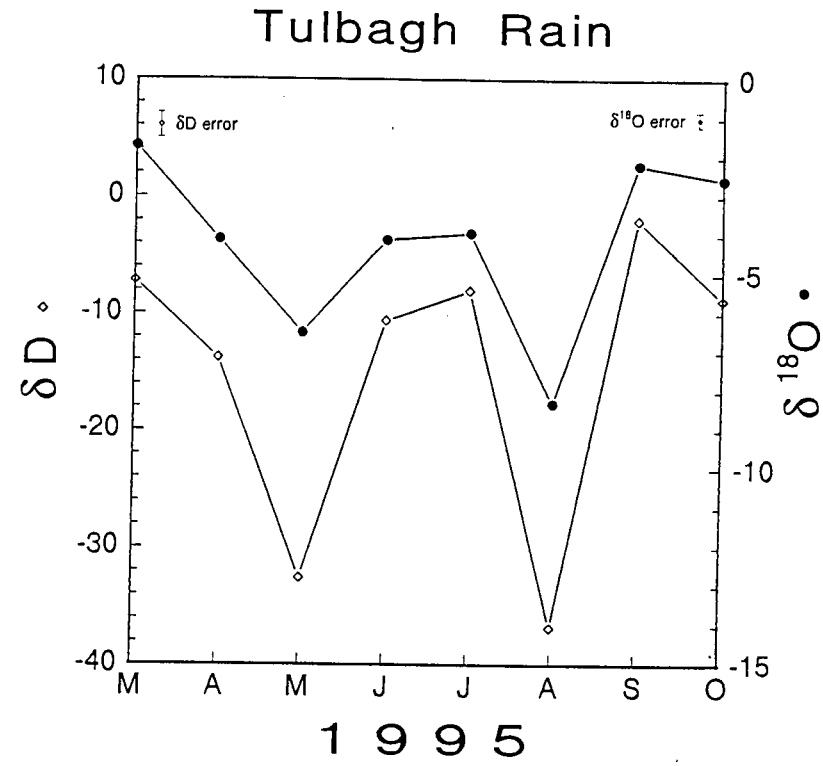

Figure 4.7: Total monthly values for $\delta^{18}O$ (●) and δD (◇) for rain that fell in Tulbagh, against time. Error bars are $\pm 2\sigma$.

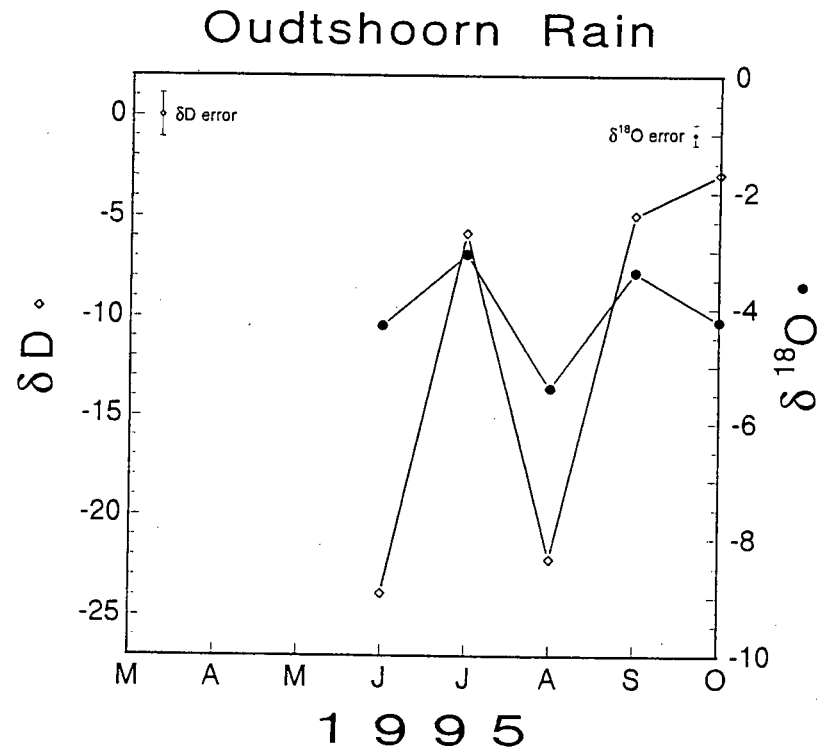

Figure 4.8: Integrated monthly values for $\delta^{18}O$ (●) and δD (◇) for rain from Oudtshoorn in 1995. Error bars are $\pm 2\sigma$.

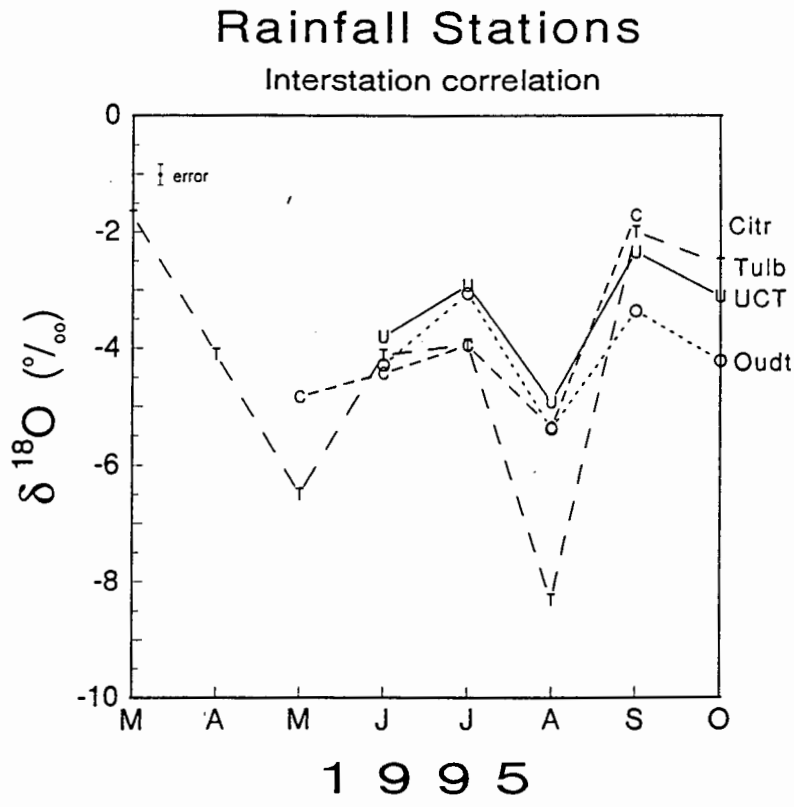

Figure 4.9: $\delta^{18}O$ of the integrated monthly rainfall from the four stations, against time, to illustrate the interstation correlation. UCT = U, Citrusdal = C, Tulbagh = T, Oudtshoorn = O. Error bar is $\pm 2\sigma$.

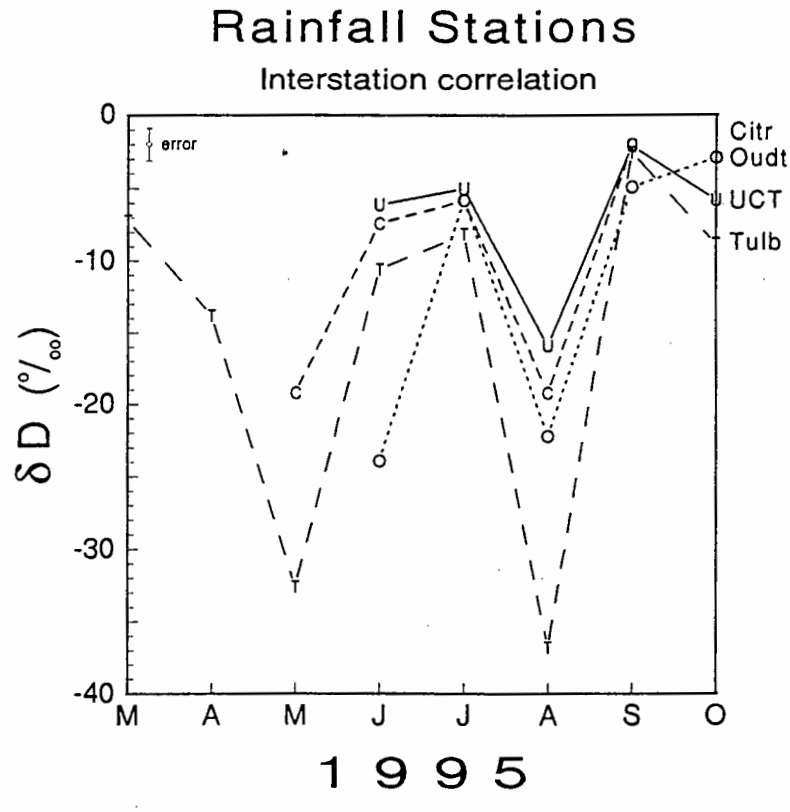

Figure 4.10: δD of the monthly rainfall plotted against time, to illustrate the interstation correlation. UCT = U, Citrusdal = C, Tulbagh = T, Oudtshoorn = O. Error bar is $\pm 2\sigma$.

and for $\delta^{18}O$. This can be seen in *Figures 4.9 and 4.10* and is attributable to the fact that the weather systems that cause rain and operate in winter, affect the entire area under study.

DATE		RAIN COLLECTION STATION							
		UCT		Citrusdal		Oudtshoorn		Tulbagh	
		$\delta^{18}O$	δD	$\delta^{18}O$	δD	$\delta^{18}O$	δD	$\delta^{18}O$	δD
	Mar							-1.7	-7
	Apr							-4.1	-14
	May			-4.8	-19			-6.5	-33
1	Jun	-3.8	-6	-4.4	-7	-4.3	-24	-4.1	-11
9	Jul	-2.9	-5	-4.0	-6	-3.0	-6	-3.9	-8
9	Aug	-4.9	-16	-5.4	-19	-5.4	-22	-8.3	-37
5	Sep	-2.4	-2	-1.7	-2	-3.4	-5	-2.2	-2
	Oct	-3.1	-6			-4.2	-4	-2.6	-9
	Nov	-4.6	-25						
	Dec	-8.1	-57						
	Jan	1.2	7						
	Feb	-4.9	-31						
1	Mar	-5.4	-21						
9	Apr	-2.1	1						
9	May	-5.0	-15						
6	Jun	-3.5	-7						
	Jul	-5.9	-19						
mean		-3.9	-14	-4.1	-11	-4.1	-12	-4.2	-15
std. dev.		2.16	16.1	1.41	7.9	0.91	10.0	2.24	12.7

Table 4.1: All the isotopic data for rain, with means and sample standard deviations for each locality.

The overall range in isotope ratios is not particularly large. This is because the stations all fall within one climatic region, their siting all being in valleys and below 300m and the fact that each sample is an integrated monthly value. This latter factor, which is probably the most significant, moderates freak values such as those created by a hail storm. Values are also known to change significantly during one rain event (eg. Midgley & Scott, 1994). The drier a particular month, the more variable that month's isotopic values will be. This is because a smaller amount of rain is

likely to have been sourced in fewer rain events and therefore can contain isotopic values far off the mean, as can be seen in *Figure 4.5.* The lightest and heaviest values are all displayed in *Table 4.3.*

SAMPLE	DATE	$\delta^{18}O$	δD
UCT hail	July 1995	-10.2	-51
UCT hail + rain	July 1996	-7.5	-30
Ceres snow	July 1996	-10.5	-58
Waaihoek snow	August 1996	-6.6	-30

Table 4.2: Light isotope ratios obtained by sampling hail and snow. The July 1996 hail sample was diluted with rain that fell in the same shower; hence the heavier value than for the pure hail sample.

		$\delta^{18}O$	δD
LIGHTEST	FREAK SAMPLE: Ceres Snow, 3/7/96	-10.5	-58
	MONTHLY SAMPLE: Tulbagh, August 1995, 92mm	-8.3	-37
HEAVIEST	MONTHLY SAMPLE: UCT, January 1996, 4mm	+1.2	+7

Table 4.3: The isotopic extremes found for this project.

For reasons outlined in section 1.2, snow and midsummer (January) rainfall, are likely bearers of light and heavy isotope values, respectively. Tulbagh's August 1995 rain is the lightest monthly value of samples taken. Tulbagh's isotope values are generally lower than those of the other stations, the only real exception being a couple of the Oudtshoorn points, especially September 1995, as can be seen in *Figures 4.9 & 4.10.* Oudtshoorn lies much further from the weather source than the other areas and so may receive very isotopically light rainfall, because of the continental effect, but its arid climate will often result in great enrichment by evaporation as rain falls to the ground and hence the erratic occurrence of the lighter values. Oudtshoorn also lies outside the Mediterranean climate area of the Cape, however, in winter it still recieves rain from frontal depressions which sweep the entire Cape.

Another noticeable feature of the rain isotope values is the large difference in $\delta^{18}O$ and δD values between months. Despite the overall small range in values, consecutive monthly values do differ considerably. This has to be accounted for by the weather. Factors such as the temperature and amount effects, which vary as new frontal depressions pass over, will play a role. It is beyond the scope of this project to provide certain reasons for these monthly fluctuations. The aim of the meteorological aspect of this project is to gain an idea of the integrated input the stable isotopes of water into the ground. Detailed sampling of each frontal depression, over the months, would be

required; a future study into this could be of merit.

4.1.3 METEORIC WATER LINE

A meteoric water line has been calculated for the Cape Mediterranean climatic region. All the precipitation that was collected has been plotted in Figure 4.11. This data includes two points for hail and rain mixtures of two separate showers and two points for snow. The Pearson's r, correlation coefficient is 0.92 for all this data.

Various statistical methods can be employed in order to calculate a best fit line or regression line to bivariate data. Five different equations have been obtained by using different calculation techniques. All five lines of these equations have been plotted on *Figure 4.12* along with all the data points for analysed rainfall (the snow and hail points have been omitted as they are temporally discrete samples and may be unrepresentative of the rain event or weather system as a whole). The details of the calculation of the equations for the five lines is presented in the Appendix.

Firstly, a classical regression line was calculated using CoPlot (scientific graphical software from CoHort). This regresses y on x producing a line which minimizes the distances in the y direction of the points from the line and is suitable for data with no error in x. For isotope data both axes are subject to error, however, the error in the x axis data ($\delta^{18}O$) is ten-fold less than the error in the y axis data (δD), so this method is in fact quite applicable. Not only does this technique generate 2s confidence limits in the gradient and the y-intercept, but it is also very easy to do. The equation obtained is $\delta D = 6.05\delta^{18}O + 10.8$ (equation **1** on the graph). The 2σ confidence limits on these values are ±1.3 and ±5.75, respectively.

The reduced major axis (RMA) technique yields a line that minimizes the triangular areas between the points and the line. This technique is applicable for data with errors on both axes, although, with a ten-fold difference in the size of the errors between the axes, this technique is not perfect. The equation for a RMA regression is $\delta D = 6.96\delta^{18}O + 14.6$ (equation **2**).

The third technique involves the use of the general equation for structural regressions, which has a variable, λ, that is the ratio of the random error variances of y over x (Rock, 1988). For oxygen and hydrogen isotope studies, λ is approximately 10. The equation obtained in this way is $\delta D = 7.69\delta^{18}O + 17.5$ (**4**).

A variable is attached to all the pairs of isotope values and that is the amount of rainfall that occurred during each month. By using this amount as a weighting factor, one can rework the last two techniques and obtain different equations for the weighted data. A weighted RMA regression

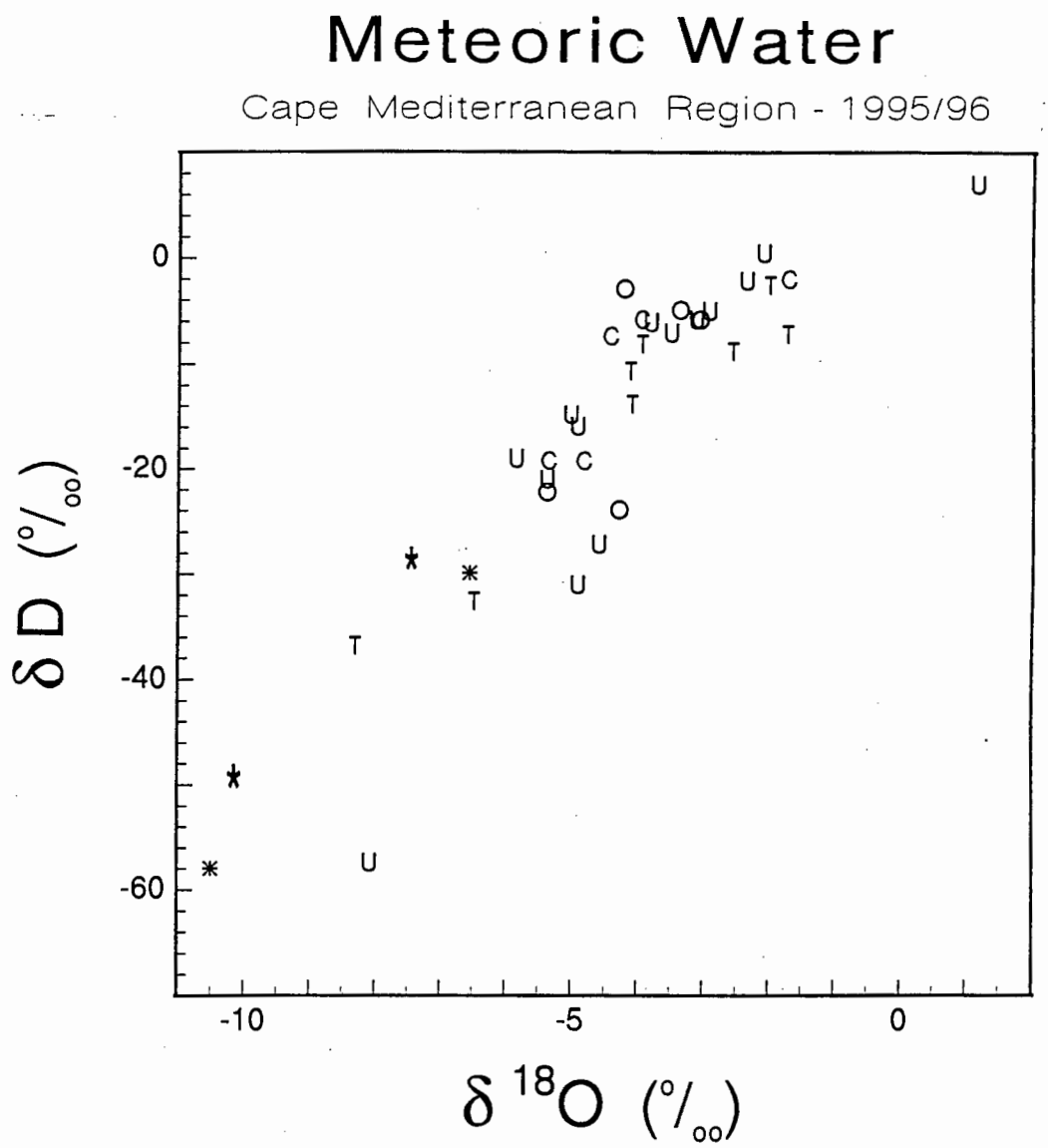

Figure 4.11: δD plotted against δ^{18}O for every sample of rainwater collected at the four stations and the two snow localities. This data has an excellent positive correlation (r = 0.92) and the best fit line through this sort of data is known as a meteoric water line (Craig, 1961b). C = Citrusdal, O = Oudtshoorn, T = Tulbagh and U = UCT. The two hail points are labeled as ⁎ and the two snow points as *.

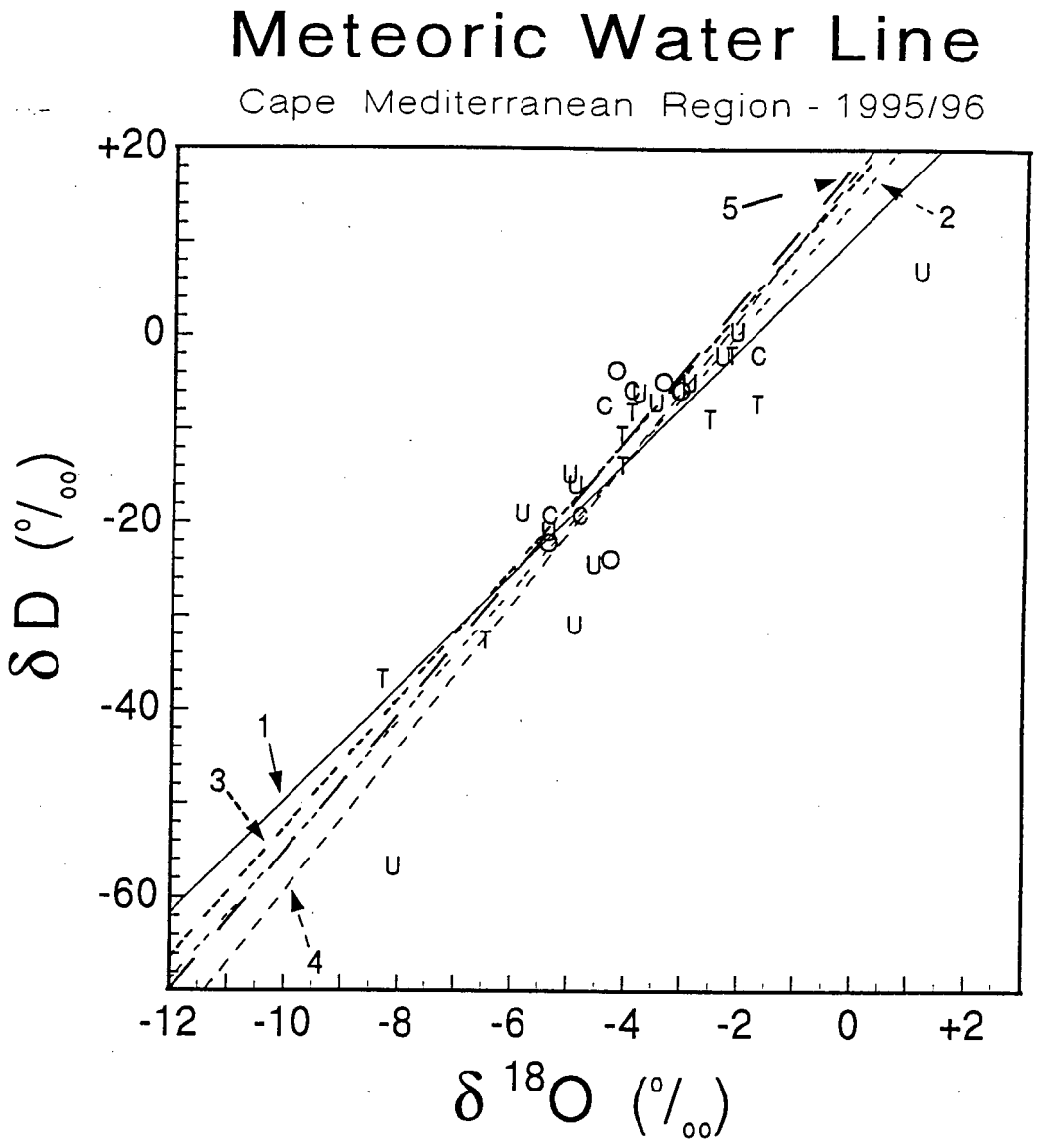

Figure 4.12: δD versus δ^{18}O for the monthly rainfall samples only. The five equations are explained more fully in the text (4.1.3) and in the Appendix. **1** is a classical regression calculated by computer software: $\delta D = 6.05\delta^{18}O + 10.8$. **2** is a reduced major axis (RMA) regression: $\delta D = 6.96\delta^{18}O + 14.6$. **3** is a weighted RMA: $\delta D = 6.93\delta^{18}O + 16.7$. **4** is a general form of a structural regression: $\delta D = 7.69\delta^{18}O + 17.5$. **5** is a weighted structural regression: $\delta D = 7.38\delta^{18}O + 18.6$. C = Citrusdal, O = Oudtshoorn, T = Tulbagh and U = UCT.

has the equation $\delta D = 6.93\delta^{18}O + 16.7$ (**3**) and the weighted $\lambda = 10$ structural regression equation is $\delta D = 7.38\delta^{18}O + 18.6$ (**5**).

Five points fall marginally away from the linear cluster of the MWL. These five can be inferred to have undergone evaporation in excess of that usually experienced by rain in this area. Four of the points are for November 1995 to February 1996 at UCT. Precipitation during summer can easily experience increased amounts of evaporation during descent to the ground, as a result of a high cloud base and low humidity, and in the rain gauge.

Interestingly, November, and December particularly, have more negative values than one would expect, if similar weather systems are causing the rain in summer as in winter. An explanation for both, but better suited to December, exists: in summer, the frontal systems become more anabatic (convective, with greater vertical extent) and so rain is likely to form at higher altitude where conditions are colder (Preston-Whyte & Tyson, 1988). So, some of the rain in December 1995 is likely to have been melted hail.

The fifth outlier value is for June 1995 in Oudtshoorn. The eastern Little Karoo often experiences markedly different weather from the Western Cape. In June 1995 only 9.5mm fell. This small amount of water can easily have its isotopic signature changed by evaporation, as a small amount of rain falling through relatively dry air will be prone to high degrees of evaporation.

Figures 4.11 and 4.12 show that the data from the four stations generally overlap. This suggests that a single meteoric water line is applicable for hydrological applications in the Cape Fold Belt area.

It should be noted that the weather and climate at all four stations differs in respect of rainfall, temperature, wind, etcetera, yet this does not affect the MWL on which the data falls. On occasion, the amount effect yielded isotopically light rainfall and hence it seems that the weather is responsible for determining whereabout on the meteoric water line the data falls and also, on occasion, for shifting a point to an outlier position below the line, by evaporation.

4.1.4 INTEGRATED RECHARGE VALUES

Integrated rainfall values are useful as they are a simple approximation to the mean isotopic ratios of rain that falls in a certain area. As such they are the input value for many hydrological studies and important for the study of springs. It is assumed that the integrated rainfall value is a good approximation to the integrated recharge value.

Integrated recharge values are calculated by multiplying the $\delta^{18}O$ and δD values recorded for each month, by the fraction of rainfall that fell in that month, the fraction being calculated as a fraction of all the months collected, which is a full year only in the case of the UCT station. The calculation of the integrated recharge values at UCT is shown in *Table 4.4*.

At UCT, for the period June 1995 to July 1996, all the rain was collected and so more than a full year's values are recorded. By taking different full years (ie. June to May, July to June and so on) or by taking more than a year and dividing each month's rainfall by the total, a 12 point moving average can be obtained. These moving averages are, however, all very similar, being only slightly more than the analytical error of ±0.2‰ for $\delta^{18}O$ and ±2‰ for δD. The integrated rainfall values for UCT, as calculated over the period June 1995 to May 1996, are $\delta^{18}O$ = -3.7‰ and δD = -10‰.

DATE	RAINFALL	RAINFALL FRACTION	$\delta^{18}O$	δD	$\delta^{18}O \times$ fraction	$\delta D \times$ fraction
June `95	120mm	0.1095	-3.81	-6.1	-0.417	-0.668
July `95	297mm	0.2710	-2.92	-5.0	-0.791	-1.355
Aug `95	138mm	0.1259	-4.92	-15.9	-0.619	-2.002
Sept `95	67mm	0.0611	-2.35	-2.1	-0.144	-0.128
Oct `95	160mm	0.1460	-3.12	-5.8	-0.455	-0.847
Nov `95	18mm	0.0164	-4.59	-24.5	-0.075	-0.402
Dec `95	20mm	0.0182	-8.09	-56.7	-0.148	-1.035
Jan `96	4mm	0.0037	1.17	7.0	0.004	0.026
Feb `96	50mm	0.0456	-4.91	-31.0	-0.224	-1.414
March `96	56mm	0.0511	-5.38	-21.0	-0.275	-1.073
April `96	85mm	0.0776	-2.09	0.5	-0.162	0.039
May `96	81mm	0.0739	-5.02	-14.8	-0.371	-1.094
sum	1096mm	1	N/A	N/A	-3.7‰	-10‰

Table 4.4: An example of the calculation of integrated recharge values, for the 12 month period June 1995 to May 1996, at UCT. Rainfall figures are those recorded at the collection station for the rainwater.

At Tulbagh, the rainfall was collected from March 1995 until October 1995 (inclusive). These months in 1995 accounted for 88% of the year's rainfall, while these months account for 87% of the rainfall in an average year. Furthermore, the precipitation during the dry months of November to April will have very little effect on the groundwater, as most of it will be intercepted by plants or fall on dry soil or rocks and get re-evaporated, or if it seeps into the soil, will be taken up and

transpired by plants. The integrated recharge values for the eight months in 1995 at Tulbagh are $\delta^{18}O$ = -5.1‰ and δD = -20‰.

It is not possible to calculate proper or reliable integrated rainfall values for Oudtshoorn, as over the five months of rainfall collection only a small percentage of the average annual rainfall fell. (A weighted average for the data that was obtained yields $\delta^{18}O$ = -4.1‰ and δD = -11.6‰.) At Citrusdal, the months over which rain was collected account for 70% of the annual rainfall in an average year, however, in 1995, these months only accounted for 57% of the annual rainfall. None the less, the best estimate recharge values, using the available data, are $\delta^{18}O$ = -4.4‰ and δD = -11‰, using the May to September (inclusive) 1995 rainfall values.

4.2 STABLE ISOTOPE DATA FOR THERMAL SPRINGS

Water samples from the thermal springs are not integrated samples of the outflow; they were taken at discrete moments. The isotope values for all the samples of spring water collected are given in *Table 4.5*.

The data for each spring is presented in *Figures 4.13 - 4.16*. The Pearson's r co-efficient for each of the 4 springs with long records is 0.16 for Brandvlei, 0.41 for Calitzdorp, 0.30 for Citrusdal and 0.29 for Malmesbury. Positive correlations such as these indicate the slightest of trends which is probably random and due to the low number of points (n = 7 for Calitzdorp and 8 for the others). This correlation is not very strong, not as strong as for the rain data. The conclusion here is that the springs discharge water with isotope values that vary unsystematically around some mean. There are no trends in the discharged isotope values.

When the data from all four springs is viewed in the comparative plots of *Figures 4.17 and 4.18*, it is clear that neither $\delta^{18}O$ nor δD between the different springs are correlated. There is no correlation between isotope ratios and spring water temperature, altitude or flow rate. There is however, a correlation between continentality (distance from sea) and isotope ratios, which will be discussed further in Chapter 5.

4.2.1 SPRING WATER LINE

All the $\delta^{18}O$ and δD values from samples of spring water that were collected have been plotted in *Figure 4.19*. A good positive correlation exists (r = 0.802) between $\delta^{18}O$ and δD when all the spring values are plotted together: each of the four springs which were sampled over a period of time, when plotted alone on a δD against $\delta^{18}O$ graph, have no linear correlation - only when they are plotted together do they form a line, each spring alone simply clusters around some average.

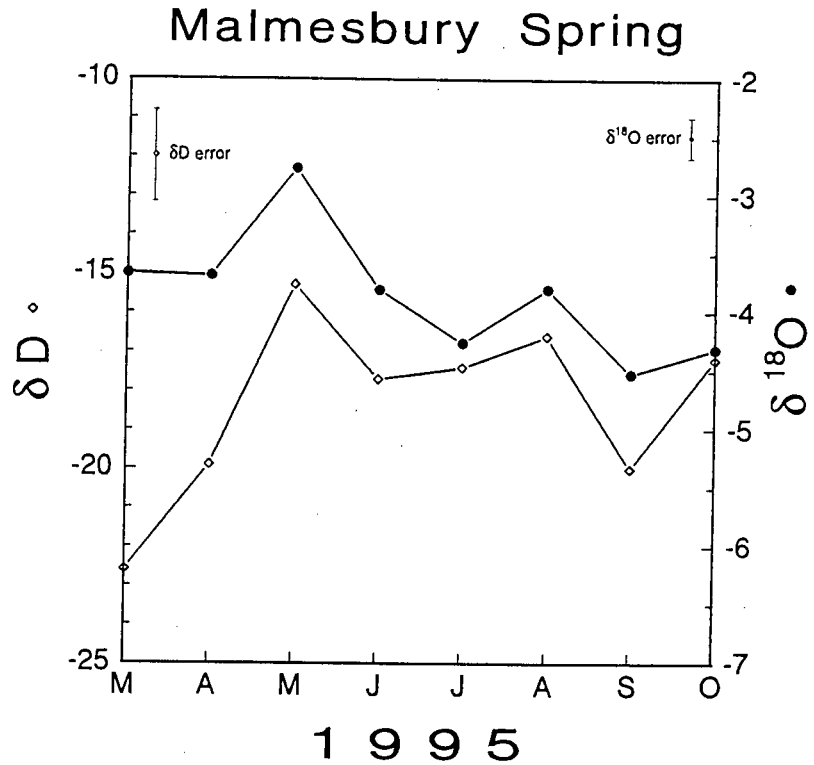

Figure 4.13: $\delta^{18}O$ (●) and δD (◇) plotted against time, of samples taken at monthly intervals, from the Malmesbury Spring in the middle of the town of Malmesbury. Error bars are $\pm 2\sigma$.

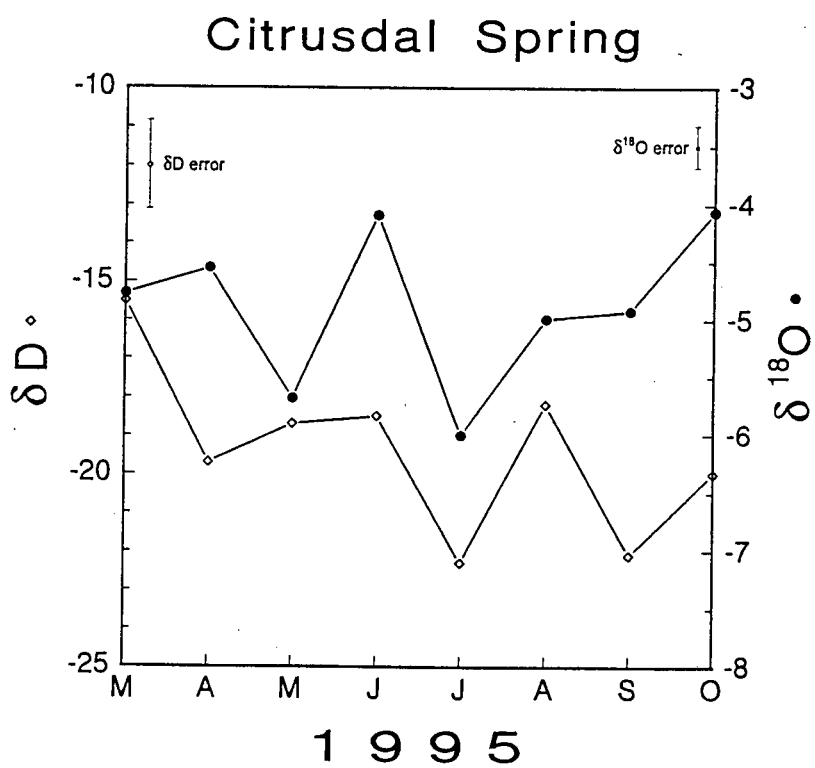

Figure 4.14: $\delta^{18}O$ (●) and δD (◇) of monthly samples of spring water from The Baths, south of Citrusdal. Error bars are $\pm 2\sigma$.

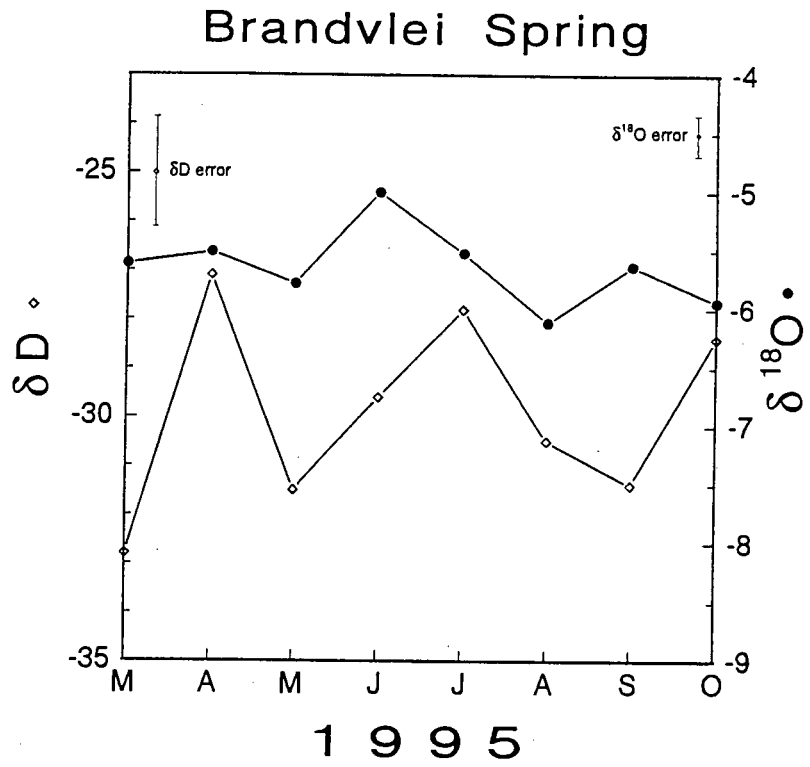

Figure 4.15: $\delta^{18}O$ (●) and δD (◇) of samples taken monthly from the Brandvlei Spring in the Brandvlei Prison, south of Worcester. Error bars are $\pm 2\sigma$.

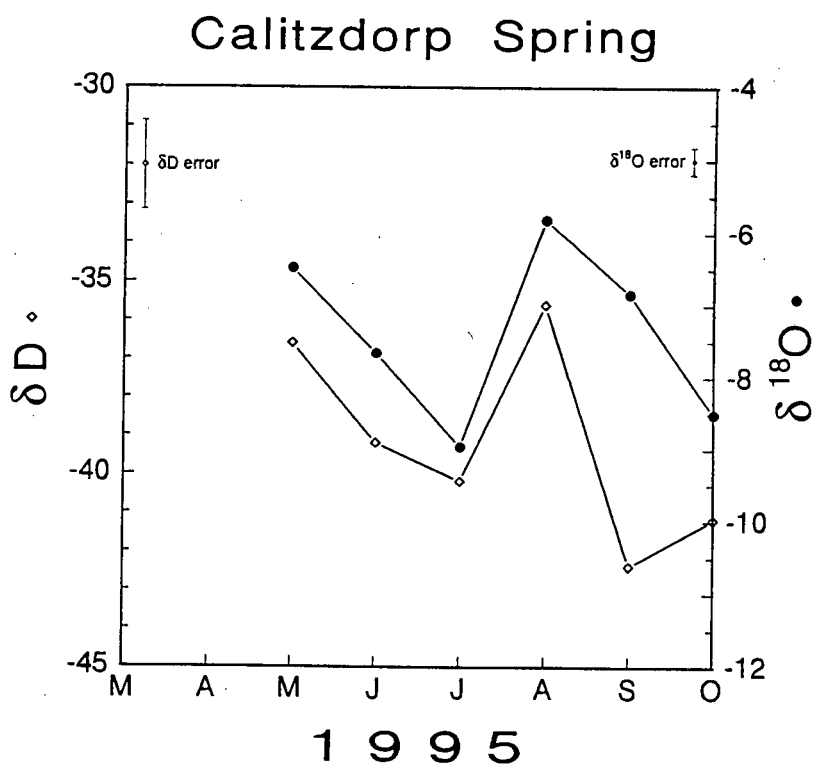

Figure 4.16: $\delta^{18}O$ (●) and δD (◇) of monthly samples of spring water taken from the Calitzdorp Spa, SE of Calitzdorp. Error bars are $\pm 2\sigma$.

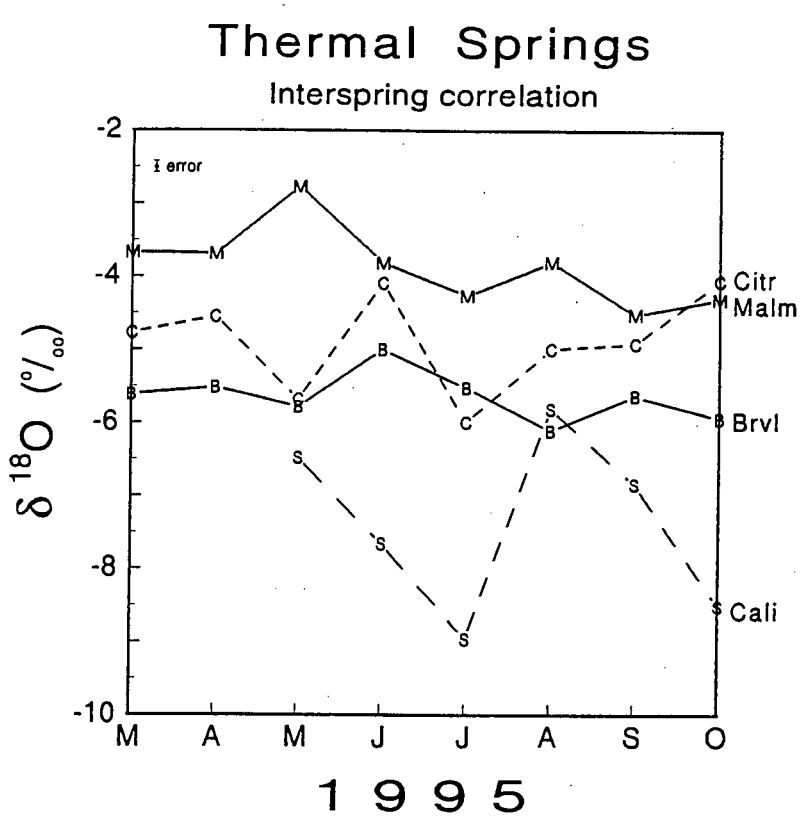

Figure 4.17: $\delta^{18}O$ for all the samples of spring water collected at the four springs, plotted against time. Malmesbury = M, Citrusdal = C, Brandvlei = B and Calitzdorp Spa = S. Error is $\pm 2\sigma$.

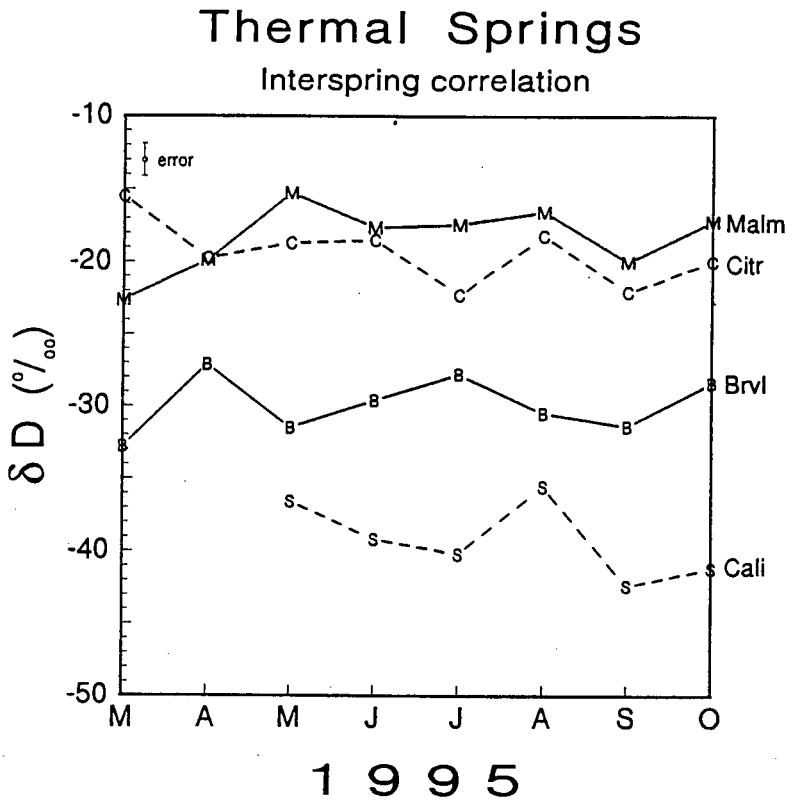

Figure 4.18: δD for the samples of spring water taken at the four springs, against time. Malmesbury = M, Citrusdal = C, Brandvlei = B and Calitzdorp Spa = S. Error is $\pm 2\sigma$.

1995	$\delta^{18}O$	δD	$\delta^{18}O$	δD	$\delta^{18}O$	δD	$\delta^{18}O$	δD
Feb	Montagu		Toowerwater		Warmwaterberg			
	-6.4	-33	-6.9	-41	-7.0	-46		
Mar	Caledon		Goudini		Witzenberg			
	-5.5	-31	-4.4	-26	-5.6	-30		
Apr	Rietfontein							
	-5.2	-42						
SPRING	Brandvlei		Calitzdorp		Citrusdal		Malmesbury	
Feb			-6.9	-44				
Mar	-5.6	-33	-	-	-4.8	-16	-3.7	-23
Apr	-5.5	-27	-	-	-4.6	-22	-3.7	-20
May	-5.8	-32	-6.5	-37	-5.7	-19	-2.8	-15
Jun	-5.0	-30	-7.7	-39	-4.1	-19	-3.8	-18
Jul	-5.5	-28	-9.0	-40	-6.0	-22	-4.3	-18
Aug	-6.1	-31	-5.8	-36	-5.0	-18	-3.8	-17
Sep	-5.6	-31	-6.8	-42	-4.9	-22	-4.5	-20
Oct	-5.9	-28	-8.5	-41	-4.1	-20	-4.3	-17
mean	-5.6	-30	-7.3	-40	-4.9	-20	-3.9	-18
std. dev.	0.33	2.0	1.13	3.0	0.69	2.4	0.54	2.3

Table 4.5: All the stable isotope values from spring water, with means and sample standard deviations for the 4 springs which were sampled on a monthly basis.

As with the rain water, three methods for calculating regression lines have been employed. These three lines were based on only 11 points; 7 for the springs sampled once and the 4 averages for the springs that were sampled over a period of months. The equations for the lines are as follows: using the classical regression available in CoPlot $\delta D = 6.61\delta^{18}O + 5.3$; using the RMA regression $\delta D = 8.23\delta^{18}O + 14.6$ and with the general form of the structural regression with $\lambda = 10$, $\delta D = 9.78\delta^{18}O + 23.4$. These best fit lines (spring water lines) can be further improved by the removal of the point for Rietfontein.

Rietfontein is on the northern extremity of the Cape Fold Belt, being in the southern Great Karoo, and is situated in Karoo rocks (see *Table 2.1*). These are not really criteria to exclude it, whereas its temperature of about 27°C puts in the intermediate category between a hot spring and a cold spring. Its circulation is likely to be shallow with recharge presumably in the near vicinity. The

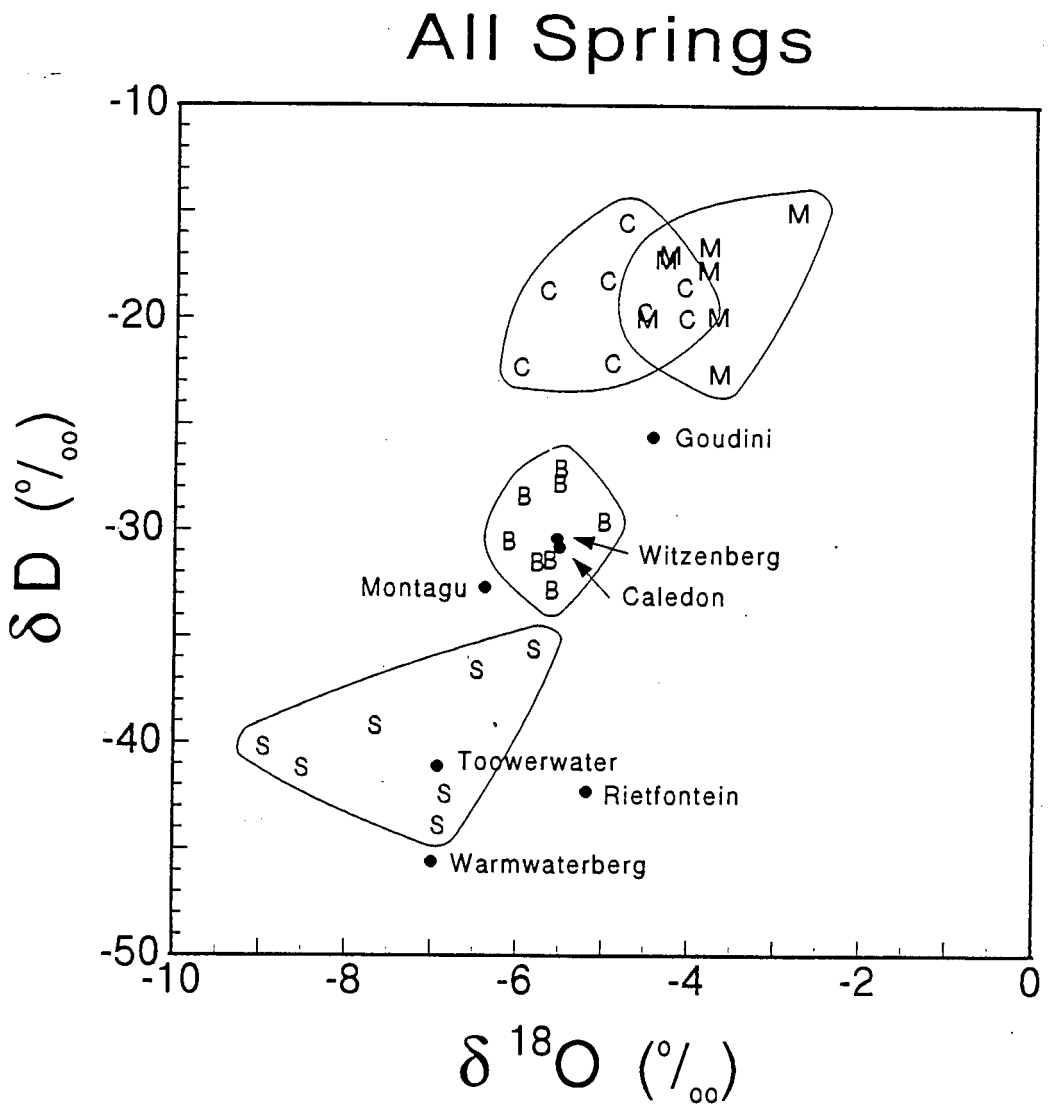

Figure 4.19: δD versus δ^{18}O for all the springs analysed. Lines have been drawn around the data fields for each of the four springs which were sampled monthly. The fact that the variation in each of these four springs is that of a cluster, suggests that analytical and sampling error are the cause of these variations. Malmesbury = M, Citrusdal = C, Brandvlei = B and Calitzdorp Spa = S.

signature it bears is that of an evaporated source, because it lies on a shallow line away from the spring water line; see Chapter 1. This could be due to evaporation of the rainfall, evaporation on the ground surface or at shallow depths. The first of these is very likely because of the dry Karoo air through which much of the precipitation in this area falls. The second and third factors are more likely in a shallow system where the recharging water infiltrates slowly down and moves horizontal distances in shallow environments with evaporation pathways above.

With the exclusion of the data point for Rietfontein, the Pearson's r is radically improved to 0.918. The equations for the regression lines which follow are plotted in *Figure 4.20*: with CoPlot $\delta D = 7.23\delta^{18}O + 10.3$ (2σ confidence limits of ±2.31 and 13.5 respectively); the RMA yields $\delta D = 7.77\delta^{18}O + 13.3$ and the $\lambda = 10$ technique gives $8.32\delta^{18}O + 16.5$.

4.2.2 COMPARISON WITH OTHER DATA

A study by Mazor and Verhagen (1983) includes stable isotope data for six of the thermal springs analysed for this project. The samples were all collected in December 1971 or 1972. A set of samples taken by the South African Government's Department of Water Affairs and Forestry mostly in January 1994 has been analysed for $\delta^{18}O$ (personal communication, Milo Simonic, 1995). The $\delta^{18}O$ and δD values for these two sample sets are shown in *Table 4.6* and are very similar to the values obtained for this project.

	Mazor & Verhagen (1983)			DWAF		this study	
	date	$\delta^{18}O$	δD	date	$\delta^{18}O$	$\delta^{18}O$	δD
Brandvlei	12/71, 12/72	-6.1	-31	1/94	-5.6	-5.6	-30
Caledon	12/71	-6.2	-	1/94	-5.3	-5.5	-31
Calitzdorp		-7.4	-35	1/94	-6.9	-7.3	-40
Citrusdal	12/72	-4.2	-	1/94	-4.8	-4.9	-20
Goudini	12/71, 12/72	-4.8	-21	1/94	-4.5	-4.4	-26
Malmesbury	12/71, 12/72	-4.2	-18		-	-3.9	-18
Montagu	12/71	-7.1	-	1/94	-6.4	-6.4	-33
Toowerwater		-	-	7/94	-6.8	-6.9	-41
Warmwaterberg		-	-	1/94	-6.9	-7.0	-46

Table 4.6: Stable isotope data for Cape thermal springs as measured in two other studies and this study. Comparison amongst the data sets indicates that the spring water does not undergo any large temporal shifts in isotope values in the medium term. (DWAF = Department of Water Affairs and Forestry).

The data from Mazor & Verhagen (1983) is plotted with data from this project in *Figure 5.8* and is

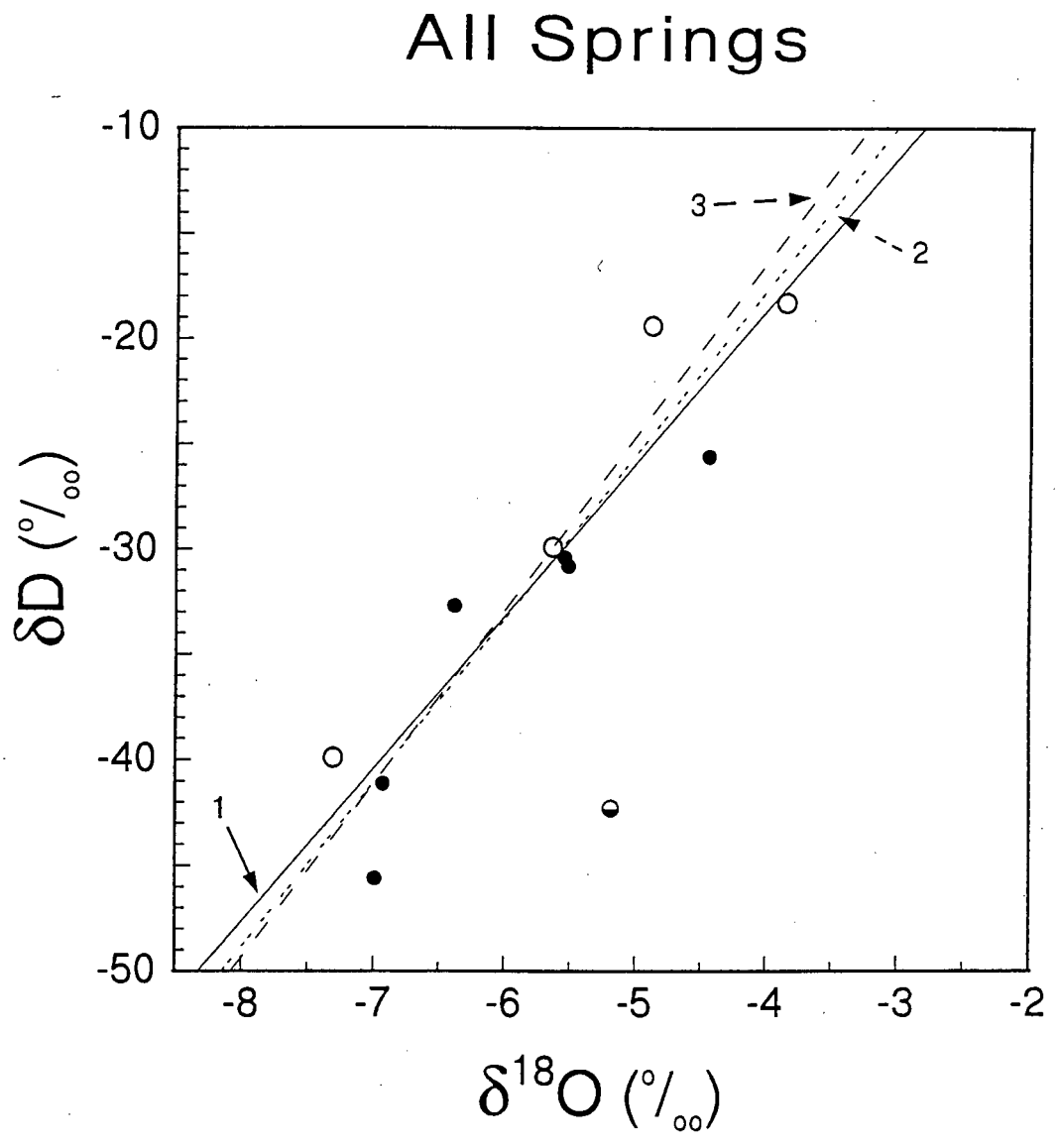

Figure 4.20: δD plotted against δ^{18}O of the averages of the four springs sampled monthly (○) and the springs sampled once off (●), with Rietfontein emphasized as the half filled circle. The three lines drawn are all calculated excluding the point for Rietfontein. **1** is a classical regression line calculated by software where $\delta D = 7.23\delta^{18}O + 10.3$. **2** is the RMA regression line for which $\delta D = 7.77\delta^{18}O + 13.3$. **3** is the structural regression which gives $\delta D = 8.32\delta^{18}O + 16.5$.

discussed in 5.4.5.

4.2.3 GAS DATA

The $\delta^{18}O$ and $\delta^{13}C$ values obtained for samples of gas discharged with the spring water, are shown in *Table 4.7*. The $\delta^{18}O$ values are all very similar as they will have been buffered by the CuO in the furnace (see 3.2.3). Their similarity provides some confirmation of the reliability of the sample preparation.

The gas was collected at all the springs where this was possible, which are the only three springs where the water discharges directly from the ground upwards into a pool above. In all three cases the gas was predominantly CO_2, with the majority of the balance being made up of another C bearing species, most likely CH_4. At Malmesbury, H_2S is also present. In the three cases the quantities of gas bubbling up are approximately proportional to the water discharge, with Brandvlei releasing on the order of a litre or so of gas every second, Calitzdorp significantly less and Malmesbury releasing streams of bubbles of up to only a few millilitres each, every few seconds.

SPRING GAS VALUES		
SPRING	$\delta^{18}O_{SMOW}$	$\delta^{13}C_{PDB}$
Brandvlei	-12.3	-22.7
Calitzdorp	-12.4	-21.5
Malmesbury	-12.1	-23.2

Table 4.7: Stable isotope data for gas discharged with spring water. Two samples of bubbles were collected at each spring and analysed separately, the averages being reported above.

4.3 STABLE ISOTOPE DATA FROM ROCKS

Whole rock oxygen isotope values were obtained for the Malmesbury Group and the 3 groups of the Cape Supergroup. Feldspar oxygen isotope ratios from the Cape Granite Suite have been taken from Harris et al (submitted). Hydrogen isotope data was obtained for some samples of the Malmesbury Group and for a few samples from the Cape Granites (Harris et al, submitted).

4.3.1 MALMESBURY GROUP

The whole rock oxygen isotope data for the Malmesbury Group is displayed in *Table 4.8* and in *Figure 4.21*. The data clusters fairly well around the mean of 13‰ with a standard deviation of 1.83‰. The data includes two values for quartz veins, which are known to generally display slightly higher $\delta^{18}O$ values (eg. Gray et al, 1991). If the one point for the Klipheuwel Formation (marked K in the histogram) is taken out, then the data show a much better grouping with a mean of 12.8‰ and a standard deviation of 1.44‰. This outlier value for the Klipheuwel sample

provides good evidence for the distinction of the Klipheuwel Formation from the Malmesbury Group, which has until now been based only on field data. Samples varied from very fresh at some road cuts, to extremely weathered at some natural outcrops. Based on the data alone, it is impossible to separate out the more or less weathered samples. Five whole rock δD values are also given in *Table 4.8*.

4.3.2 CAPE GRANITE SUITE

A very limited data set from Harris et al (submitted), shown in *Table 4.9* has been taken and plotted in *Figure 4.21*. The pluton selected is the Malmesbury Pluton, which underlies the town of Malmesbury where the thermal spring is sited. The $\delta^{18}O$ values of feldspar only have been plotted for two reasons. Feldspar is the most abundant mineral in the rock, occurring as 60-70% of the modal mineralogy (Scheepers, 1995) and it is also the mineral most likely to exchange with percolating meteoric water (eg. Taylor, 1968). This small data set yields a mean of 9.0‰ and a standard deviation of 0.6‰.

4.3.3 CAPE SUPERGROUP

The samples of the Table Mountain Group were taken from all around the Western Cape; sample numbers and some descriptions are given in *Table 4.10*. The Bokkeveld and Witteberg Group samples came from a more restricted area south of Laingsburg, which is in the middle of the southern arm of the Cape Fold Belt.

Although the number of samples is limited for the Witteberg Group, the Cape Supergroup as a whole has similar $\delta^{18}O$ values, which can be seen plotted in *Figure 4.22*. The individual means ($\delta^{18}O$) and standard deviations (s) are, for the Table Mountain Group $\delta^{18}O = 10.7$, $s = 0.9$, for the Bokkeveld Group $\delta^{18}O = 11.0$, $s = 0.6$ and for the Witteberg Group $\delta^{18}O = 11.1$, $s = 0.6$. The overall mean for the Cape Supergroup is 10.9‰, with $s = 0.8$‰.

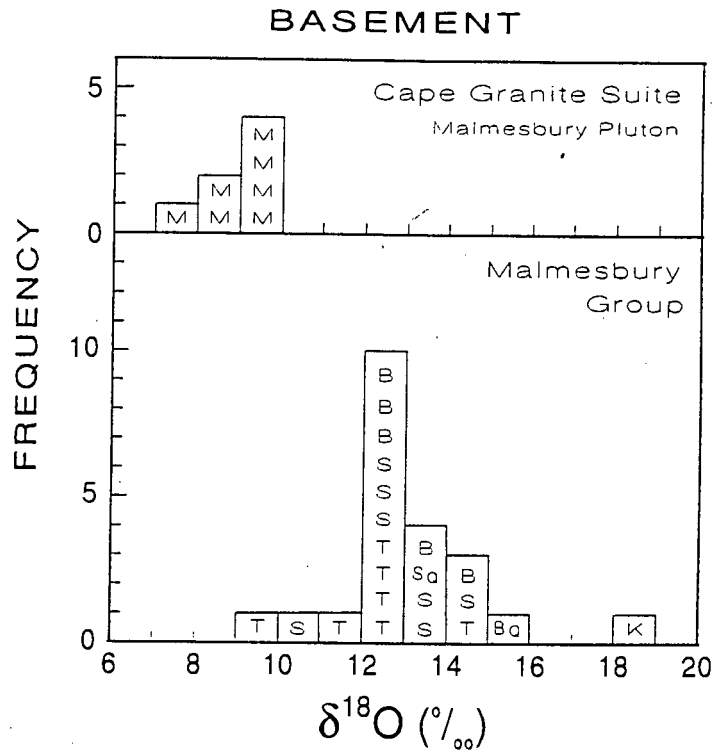

Figure 4.21: Whole rock $\delta^{18}O$ and feldspar $\delta^{18}O$ values for the Malmesbury Group and the Malmesbury Pluton of the Cape Granite Suite. For the Malmesbury Group, T = Tygerberg Terrane, S = Swartland Terrane, B = Boland Terrane, K = Klipheuwel Formation, Q ⇒ quartz vein.

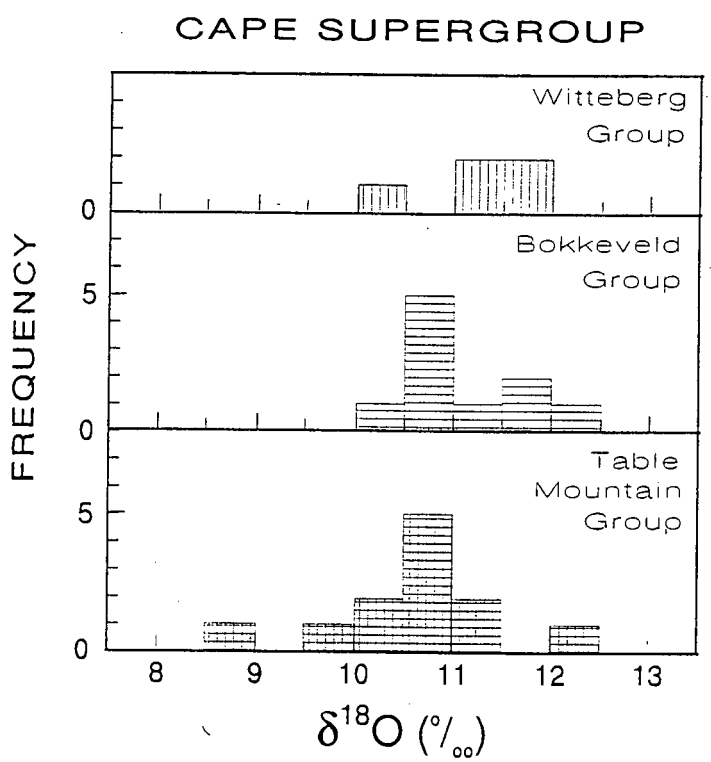

Figure 4.22: Whole rock $\delta^{18}O$ values for the three groups of the Cape Supergroup.

SAMPLE NUMBER	SAMPLE DESCRIPTION	$\delta^{18}O$	δD
Klipheuwel Formation			
MAL06	gritty, feldspathic sandstone	18.3	
Boland Terrane			
MAL11	Klipplaat Fm: micaceous sandstone	14.3	
MAL12	Klipplaat Fm: quartz vein	15.4	
MAL13	Morreesburg Fm: silvery-blue phyllite	12.7	-67
MAL14	Klipplaat Fm: yellowish phyllitic schist	13.7	-74
MAL15	Morreesburg Fm: bluish schist	12.5	-84
MAL16	Morreesburg Fm: bluish schist	12.6	
Swartland Terrane			
MAL01	Porterville Fm: grey-green phyllite	12.0	-47
MAL02	Porterville Fm: bluish quartzite	14.3	
MAL04	Porterville Fm: green shale	10.2	-76
MAL08	Piketberg Fm: light grey greywacke	14.0	
MAL09	Piketberg Fm: maroon micaceous shale	12.4	
MAL10	Piketberg Fm: quartz vein	14.0	
MAL20	Brandwacht Fm: purplish grey shale	13.2	
MAL21	Norree Fm: purple phyllite	12.4	
Tygerberg Terrane			
MAL18	Tygerberg Fm: dark micaceous quartzite	12.9	
M14A	Tygerberg Fm: phyllite	12.0	
M15	Tygerberg Fm: quartzite	12.0	
JT08	Tygerberg Fm: cordierite hornfels	12.3	
JT10	Tygerberg Fm: quartzite	11.6	
JT11	Tygerberg Fm: phyllite	9.6	
CG121	Tygerberg Fm: quartzite	15.0	
mean		13.06	-70
std. dev.		1.83	12.5

Table 4.8: Stable isotope data for the Malmesbury Group. The 2σ analytical error is 0.18‰ for $\delta^{18}O$ and 1.1‰ for δD.

SAMPLE		$\delta^{18}O_{fsp}$	δD
NUMBER	LOCATION		
CG125	Nassau granite	7.8	
CG126	Lammershoek granite	9.4	-54
CG128	Graskop granite	9.8	-47
CG129	Lammershoek granite	9.0	
CG130	Weltevrede quartz porphyry	8.8	
CG131	Slent granite	8.8	
FTCG16	Reetbok microgranite	9.1	
mean		8.96	-50.5
std dev.		0.62	4.9

Table 4.9: Stable isotope data for the Malmesbury Pluton, type Ia (Scheepers, 1995), a pluton of the Cape Granite Suite, which has intruded into the Swartland Terrane of the Malmesbury Group and underlies the town of Malmesbury where the spring discharges.

SAMPLE NUMBER	SAMPLE DESCRIPTION	$\delta^{18}O$
Table Mountain Group		
TMG1	Piekerniersklоof Fm: quartz pebble conglomerate/sandstone	12.4
TMG2	Graafwater Fm: fine grained maroon sandstone	11.8
TMG3	Peninsula Fm: bluish grey sandstone/quartzite	10.2
TMG4	Peninsula Fm: medium grained maroon sandstone	10.2
TMG5	Peninsula/Pakhuis Fm: orange, coarse, pebbly sandstone	10.9
TMG6	Cedarberg Fm: brown, ripple cross-bedded siltstone	10.7
TMG7	Cedarberg Fm: black and maroon fine grained sandstone	9.8
TMG8	Skurweberg Fm: medium to coarse grained sandstone	10.7
W079AB	*	11.2
W079BC	*	10.9
W080A	*	11.2
W129A	*	10.8
WSHSE15	*	8.7
Bokkeveld Group		
W-075B/I	*	12.0
W-104A	*	11.6
W-107A	*	10.7
W1-117	*	11.0
W-SHSE16a	*	12.1
W1-SHSE11	*	10.2
W1-SHSE12	*	10.8
W1-SHSE13	*	10.7
W2-SHSE12	*	10.7
W2-SHSE13	*	10.6
Witteberg Group		
W-028BC	*	10.0
W-043B/II	*	11.5
W-135	*	11.0
W1-SHSE8	*	11.6
W2-SHSE8	*	11.4

Table 4.10: Oxygen isotopes for the Cape Supergroup. The data for samples marked with an asterisk is from S. Egle (personal communication, 1995) for which no sample description was provided. These are all fresh samples derived from the area south of Laingsburg, in the centre of the southern arm of the Cape Fold Belt.

5 DISCUSSION

This chapter attempts to consolidate and interpret all the data acquired in this study. The bulk of the discussion revolves around the likely recharge sites for the springs concentrating on isotope altitude effects, the groundwater flow paths considering mainly the geothermal gradient, the stratigraphy and structure, and the origin of the CO_2 and other gases released at the springs.

5.1 RAINFALL

All climate and weather data and basic statistics were obtained from the South African Weather Bureau, contactable at http://cirrus.sawb.gov.za/.

For each of the months during which rainfall was collected, from March 1995 to July 1996, the amount of rain that fell was usually within one standard deviation of the mean monthly rainfall for that site; at each site, one or two of the months sampled received amounts of rain which only fell inside two standard deviations from the mean. These means and other statistics are based on data from between 24 and 116 years of observation (see *Figures 4.1-4.4*). No amounts received were more than two standard deviations from the mean. The stable isotope ratios for every month recorded should therefore be within the usual range of values for that month.

5.2 STABLE ISOTOPES OF RAIN WATER

The $\delta^{18}O$ and δD ratios observed at the four stations are typical, expected values for a mid-latitude region with a mediterranean climate (eg. Midgley & Scott, 1994, for the Cape; Sharma & Hughes, 1985, for Perth, Western Australia). An interesting result is that Tulbagh has the most negative integrated recharge values. This could be because the town is surrounded by mountains on three sides, with peaks of around 2000m to the north and 1600m to the north-west; the latter is the direction from which the rain clouds approach. These mountains could drive the air masses upwards forcing them to colder heights and hence generating rain that is isotopically more negative. An alternative hypothesis is that these mountains produce a rain out effect, removing some of the initial and isotopically heavy cloud droplets as rain, leaving lighter isotopes to precipitate over the Tulbagh Valley.

5.2.1 METEORIC WATER LINES

The five meteoric water lines shown in *Figure 4.12*, calculated from the rain isotope data in *Table 4.1*, all appear to provide satisfactory fits to the data within the bulk of the range in isotope values observed; ie. from -1‰ to -8‰ for $\delta^{18}O$ and from 0‰ to -40‰ for δD. Selection of one of these lines should therefore be concerned not only with which line appears to provide

the best fit through the data, but also, which method of calculation seems to be the most statistically satisfactory or robust. In other words, which calculation method is not sensitive to outlier values and hence should be able to be employed on a different data set from the Cape and yield a similar equation.

The first stage of this selection is to exclude the three methods in which the data is not weighted by rainfall amount. Any method in which this form of weighting is not employed, is vulnerable to freak values, such as those recorded during summer at UCT. The two remaining lines are very close to each other in *Figure 4.12*, so the selection of the general form of the structural regression, with $\lambda = 10$, is purely on the grounds that it seems to be the more correct way of dealing with data in which both variables depend on each other and in which the random error of each is different. The weighted meteoric water line for the Cape Mediterranean Region, as determined in this study, is: $\delta\mathbf{D = 7.38\delta^{18}O + 18.6}$. This line is plotted on *Figure 5.1* along with all the data used to derive it. A simplified plot is given in *Figure 5.2*, for clarity.

This meteoric water line is quite similar to the line calculated by Craig (1961a), which is known as the global meteoric water line and has the equation $\delta D = 8\delta^{18}O + 10$. The line is also similar to the lines calculated by Bortolami et al (1979, in Mazor, 1991) for the Maritime Alps ($\delta D=7.9\delta^{18}O+13.4$) and by Gat (1971) for the Mediterranean/Middle East area ($\delta D=8\delta^{18}O+22$).

The gradient of all meteoric water lines in which isotope fractionation of the cloud and vapour mass subsequent to condensation has not occurred, is about 8 (Welhan, 1987). The slope of 7.4 found in this study is marginally different and therefore suggests that the vapour masses responsible for precipitation in the Cape, or the precipitation itself, is undergoing evaporation as the weather system moves inland.

The deuterium excess, d, is subject to great variation (Welhan, 1987), which, according to Merlivat & Jouzel (1979), is primarily a function of the humidity over the ocean where the vapour mass forms. Values of d range from -2.6 to 29.6 with the mean being 18.7 and s = 7.4. High and low values are distributed evenly around the four collection stations. This homogeneity is further evidence for the area under study being a single climatic region.

5.2.1.1 ALTITUDE EFFECT

An attempt was made to calculate an altitude effect on Table Mountain, in Cape Town, but this yielded unrealistic results with an altitude effect $-0.74‰.100m^{-1}$ (Diamond and Harris, 1997). An unrealistic result can be expected, because the altitude effect is partly related to progressive rainout as a weather system moves upslope and inland, whereas the situation on

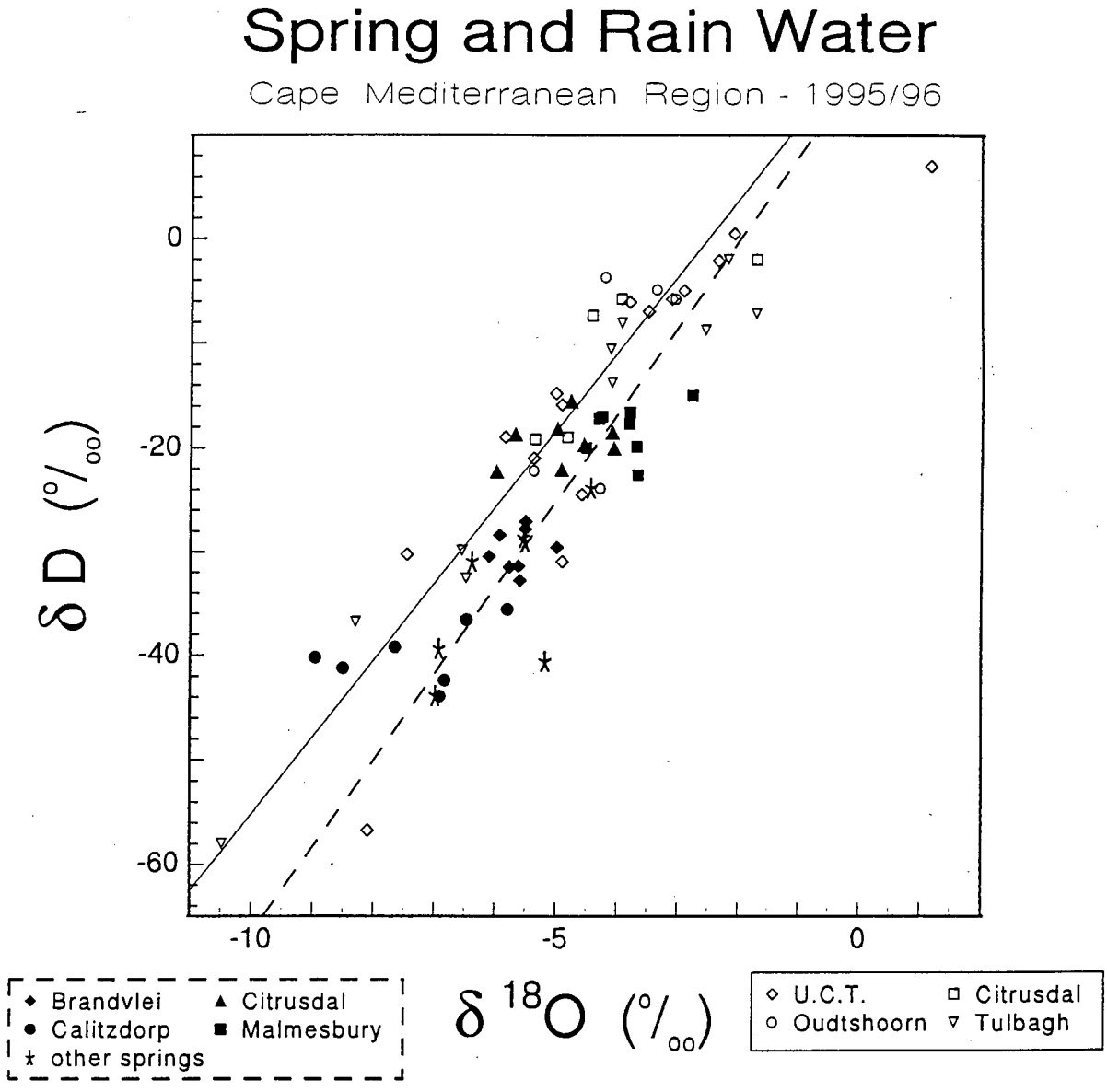

Figure 5.1: A plot of all the stable isotope data of all waters measured for this project. The solid straight line is the 'best' meteoric water line (see 5.2.1) which has the equation $\delta D = 7.38\delta^{18}O + 18.6$, calculated by weighting the data (open symbols) and using a general form for a structural regression. Six of the points plotted here (two snow, two hail and two others) were not used to calculate this line (see 4.1.3). The dashed straight line is the 'best' best fit line (see 5.4.1.1) for the spring data, which is $\delta D = 8.32\delta^{18}O + 16.5$. This equation was calculated as is described in 4.2.1, using averages for the four springs that were sampled on a monthly basis (solid symbols), and the data for all the other springs (stars), except Rietfontein.

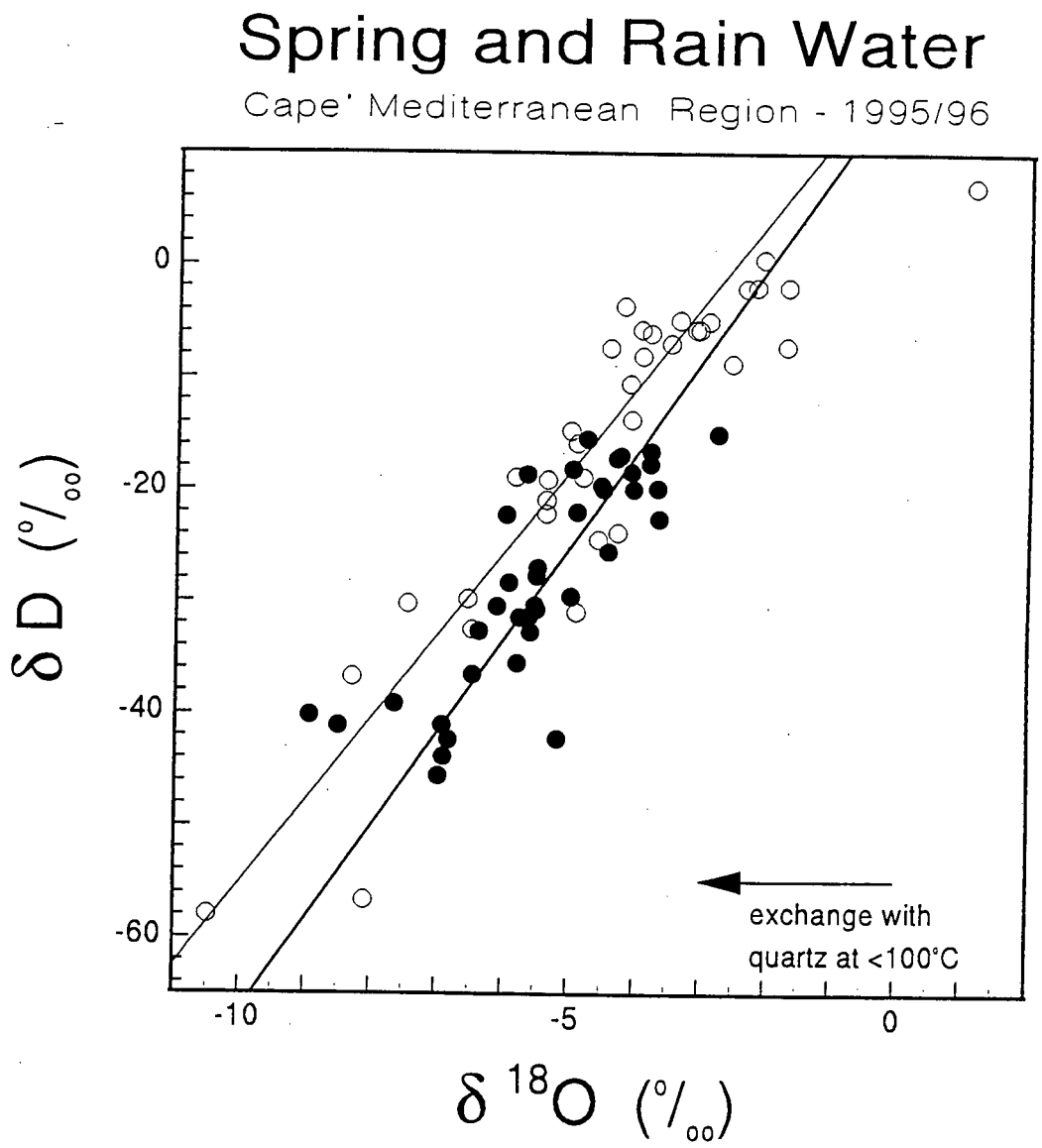

Figure 5.2: A simplified plot of exactly the same data and two functions as in *Figure 5.1*. Filled circles (●) represent spring values and open circles (○) precipitation values. The thicker line runs through the spring data ($\delta D = 8.32\delta^{18}O + 16.5$) and the thinner line runs through the rain data ($\delta D = 7.38\delta^{18}O + 18.6$). The arrow shows the exchange vector for meteoric waters of this study with quartz of $\delta^{18}O = 10\text{-}11‰$ at temperatures below about 100°C. Clearly the shift in spring water $\delta^{18}O$ values is in the wrong direction to be due to exchange at temperatures that can be expected for deeply circulating water in the Cape Fold Belt.

Table Mountain is that of a very sudden change in altitude. Sharp changes in altitude do not yield clear, gradual decreases in $\delta^{18}O$ or δD ratios with increasing altitude, as the scale of turbulence in a weather system is on the order of the size of Table Mountain itself. Lighter isotopes are therefore apparently randomly precipitated over the mountain. This is in agreement with results obtained on Gran Canaria Island, which is a steep volcanic massif rising from the sea, in which the altitude effect was lower than expected (Custodio, 1988).

Due to the lack of an altitude effect determined in this project, some of those reported in the literature have been taken and used here as a guideline for a likely rate of change of $\delta^{18}O$ with increasing altitude. Some examples are:
$-0.18‰.100m^{-1}$ (Zojer & Stichler, 1989) determined in a study in the Pelopónnisos, Greece;
$-0.25‰.100m^{-1}$ (Flora & Longinelli, 1989) for the NE coast of the Adriatic Sea, in Italy;
$-0.32‰.100m^{-1}$ (Midgley & Scott, 1994) on the Jonkershoek Mountains, about 70km east of Cape Town;
$-0.44‰.100m^{-1}$ (Leontiadis et al, 1983) in northern Greece, near Bulgaria. All these altitude gradients are for Mediterranean climate areas, but obviously the local one is the most applicable. A best estimate for the altitude effect based on the above results is $-0.3‰.100m^{-1}$.

5.3 GEOLOGICAL AND PHYSICAL PARAMETERS AT THE SPRINGS

5.3.1 DISCHARGE TEMPERATURE AND VOLUME

The major thermal springs of the Cape Fold Belt, in other words, all those analyzed besides Rietfontien and Witzenberg, plus Baden Baden, which was never analyzed for this project, are known to have constant discharge volumes and temperatures. The constancy of discharge temperature and volume is a generally known fact and was confirmed by discussion with the resort managers at The Baths in Citrusdal, The Calitzdorp Spa (for which measurements go back to the 19th century), Caledon and Goudini and can also be confirmed by examination of old research, such as work by Rindl (1928, 1931 & 1934). A particularly useful observation was made by Burchell (1822) in 1811, when he measured the temperature of the Brandvlei spring: "The thermometer, when plunged into the pond, rose only to 144° [62°C]; but, to the hand, it felt nearly scalding hot,... Where it bubbles up out of the earth, it is, perhaps, a few degrees hotter."

In a region with a seasonal rainfall, such as the Cape, the constant discharge indicates reservoirs which are large relative to the discharge, in order to buffer the seasonal effects - this could be achieved by a long flow path, which could involve deep circulation; the high temperatures (34°C-64°C) corroborate the deep circulation hypothesis.

5.3.2 GROUNDWATER CIRCULATION

Deep groundwater movement in the Cape is either in fractures in the Cape Granite Suite, or in fractures in the Table Mountain Group which has very limited residual primary porosity. The fractures in the Table Mountain Group are either horizontal bedding planes or vertical joints. The joints occur in 3 roughly parallel sets throughout the Cape Fold Belt: NW-SE, NE-SW and E-W. These and the bedding planes provide a network of fractures which is most probably very thorough, through which water can flow. The Table Mountain Group contains two main aquifers separated by the thin but impermeable shales and siltstones of the Cedarberg Formation: the lower aquifer is the Peninsula Formation and the upper one is the Nardouw Subgroup.

Faults punctuate the stratigraphy and are present at nearly all the springs. Thus, it seems that faults are critical in providing breaks through the otherwise impermeable Cedarberg Formation, for heated water to percolate upwards (see *Figures 5.3-5.5*). This environment appears to be similar to that proposed by Goyal & Kassoy (1977, 1980) and Goyal (1978) (in Donaldson, 1982): "the hot fluid flows up a single fault from an extensive basement fracture system in which the heating takes place."

5.3.3 GROUNDWATER HEATING

The geothermal gradient of the Cape Fold Belt area is not known with absolute certainty. A reliable estimate can be made from two sources. The first is from two bore holes drilled into the Karoo Supergroup, just north of the centre of the southern arm of the Cape Fold Belt, which is within about 50km of the spring Rietfontein. The second source is that of observations of regions in the world with similar age and tectonic history.

The two bore holes of interest are reported in Jones (1992). The first bore hole penetrates to 850m below surface, through rocks with an average geothermal gradient of about 18°C.km^{-1}. The second bore hole reaches to 1760m below surface and has a geothermal gradient which is about 21°C.km^{-1} until 1450m and then jumps up to around 27°C.km^{-1} in the deeper section of the hole.

Unfortunately, most of the references in the literature report geothermal gradients as heat flow. These two parameters are related to each other as follows:
surface heat flow or $\mathbf{q = -K\,(dT/dz)}$,
where **T** is temperature and **z** is depth and therefore **dT/dz** is the geothermal gradient, and **K** is the thermal conductivity of the rocks. So, if K is known, then the geothermal gradient can be calculated from q.

Reported values for the heat flow from places of similar geological history to the Cape Fold Belt are listed here now. Vitorello and Pollack (1980) calculated averages of the heat flow for

the eastern United States, the south-eastern Appalachians and eastern Australia, which are, respectively, ±60, ±40 and ±70mW.m^{-2}. Chapman and Furlong (1977), in Pollack's paper of 1982 which expounds on the relationship between heat flow and crustal age, give a value of 61mW.m^{-2} for areas which last underwent a thermal episode (such as orogeny) in the Late Palaeozoic and 73mW.m^{-2} for the Mesozoic. From the above sources only, the Cape Fold Belt is therefore likely to have a heat flow a few units above 60mW.m^{-2}.

Given a particular surface heat flow, the geothermal gradient will be lower if the rock type has a high thermal conductivity. No data could be found on the thermal conductivity of the Cape Supergroup, however, values for the shale/sandstone of the Karoo Supergroup are 2.2±0.6W.m^{-1}.K^{-1} and the Witwatersrand Supergroup quartzites are 6.3±0.8W.m^{-1}.K^{-1} (Jones, 1992, after Jones and Bottomley, 1986). The Table Mountain Group quartzites are well recrystallized, however, they are not as fully recrystallized as those of the Witwatersrand Supergroup and there are also significant clay rich horizons in the Graafwater and Cedarberg Formations. The thermal conductivity of the Table Mountain Group must therefore be lower than the Witwatersrand Supergroup quartzites, but higher than the Karoo rocks measured. An estimate of 4W.m^{-1}.K^{-1} is used here to calculate a likely average geothermal gradient for the Cape Fold Belt.

Using the surface heat flow equation given above, the geothermal gradient ($\delta T/\delta z$) for the Cape Fold Belt is 16°C.km^{-1}, assuming K = 4W.m^{-1}.K^{-1} and q = 64mW.m^{-2}. This calculated geothermal gradient is considerably lower than the measurements derived from the bore holes. Although the bore holes are somewhat removed from exposures of the Cape Supergroup, they are within the zone of structural deformation of the Cape Fold Belt and are close or within the suboutcrop boundary of the Cape Supergroup.

Based on the above information the geothermal gradient of the Cape Fold Belt area can be estimated to be about 20°C.km^{-1}. The geothermal gradient will vary somewhat, as there is up to 2km of altitude difference in the topography.

5.4 STABLE ISOTOPES OF THE SPRING WATERS

5.4.1 SPRING WATER LINE

All the values measured for spring water samples are plotted on *Figure 5.1*, along with the best fit line. The data and the functions are all plotted again in *Figure 5.2* for clarity.

Again, as with the meteoric water line, the best fit line was chosen because it was calculated using the general form of the structural regression; this yields a line with the equation **$dD = 8.32d^{18}O + 16.5$**. This is quite similar to the Cape meteoric water line.

5.4.1.1 DEUTERIUM EXCESS

The d values range from -0.4 to 27, with the mean equal to 15.4 and s = 6.3. This range and mean are very similar to those obtained for the rain water isotopes. The conclusion here is that the humidity over the oceanic source region is the same for the rain and the spring water and therefore it is quite likely that the same weather systems are producing the rain that was analyzed directly and the rain that recharges the springs.

5.4.1.2 GRADIENT

The gradient of a meteoric water line is dependent upon the temperature of the air mass and its precipitation history (Welhan, 1987). The spring water line has a steeper gradient than the Cape meteoric water line, 8.3 compared to 7.4, respectively. If the 2σ errors from the CoPlot generated lines (2.3 for the springs and 1.3 for the rain) are used as a guideline as to the 2σ errors on these lines, then these lines could be closer or the same, if different sample sets were used.

The spring water line is closer to the northern hemisphere lines, such as those of Craig (1961a) and Dansgaard (1964). The latter is $dD = 8.1d^{18}O + 11$ and is specifically for the continental areas (removed from the coast). In contrast, meteoric water lines from warm areas and places near to the sea, tend to have gentler gradients (Ehhalt et al, 1963). The difference in gradient between the meteoric water line and the spring water line indicates that the rain that recharges the springs has had a different precipitation history to that of the rainfall analyzed. The steeper gradient of the spring water line suggests that the air mass producing the rain that recharges the springs is more fractionated and/or precipitates at lower temperatures. Mountain tops could provide such a setting.

5.4.1.3 EVAPORATION

Assuming the difference in equations for the rain and springs is real, displacement of the spring water line to a position below the Cape meteoric water line is evidence for evaporation, isotopic exchange or palaeorecharge. Recharge under any markedly different climatic regime would result in a meteoric water line distinctly different from that established for the present. Therefore, the similarity of the rain and spring lines is evidence against recharge during a glacial event, such as the one prior to the Holocene.

This result suggests that recharge occurs in rain events where evaporation is able to take place, in other words, during gentle rain showers, as opposed to large downpours where the water would infiltrate into the ground without any chance for evaporation. This conclusion is in keeping with the nature of rain in the Cape, which tends to come from stratus clouds in frontal depressions and is of a gentle, soaking nature. Larger showers do occur at the end of the passing of a cold front, however, these are short clearing showers, after each of which the sun

usually comes out and there is most often wind, so evaporation can easily occur (Preston-Whyte & Tyson, 1988).

One puzzling factor is that soils in the Cape generally and in the mountains in particular, are poorly developed and so the evaporation for which there is evidence above, is unlikely to be occurring in the soil horizon prior to recharge. On the other hand, though, there are flat areas within the high mountain landscape in which water collects in bogs in winter and in which evaporation could well occur. These flat areas are perched vleis (very shallow lakes/wetlands) or bogs which have standing water all year round (except for late summer) as they sit above an impermeable layer of quartzite. As such, these perched reservoirs cannot be contributing directly to the recharge of the springs. The winter and spring time overflow, however, may well be able to permeate into fractures and reach great depths.

5.4.2 ISOTOPE EXCHANGE BETWEEN ROCK AND WATER

When water comes into contact with rocks containing oxygen and/or hydrogen, equilibrium isotopic fractionation can occur. In the Table Mountain Group, hydrogen bearing minerals are extremely scarce, so only oxygen fractionation is considered for the springs.

Two equations have been used to calculate the difference in isotope ratios that would exist between quartz/silica and water at equilibrium, at different temperatures. Both sets of data are presented in *Table 5.1*.

T (°C)	$\Delta_{quartz\text{-}water}$ **1**	$\Delta_{quartz\text{-}water}$ **2**
150	4.2‰	16.0‰
100	16.3‰	21.4‰
80	21.2‰	24.2‰
70	23.7‰	25.8‰
60	26.1‰	27.6‰
50	28.5‰	29.5‰
40	31.0‰	31.6‰

Table 5.1: The differences in $\delta^{18}O$ between quartz and water having reached isotopic equilibrium at the given temperatures. Column **1** is for low temperatures and is calculated according to the equation $\Delta_{quartz\text{-}water} = ((169 - T(°C)) \cdot 4.1) - 0.5$ (Labeyrie, 1974). Column **2** is really for 200-500°C, but has been extrapolated to lower temperatures; the values were calculated from the equation $\Delta_{quartz\text{-}water} = 3.38 \cdot 10^6(T(°C)) - 2.9$ (Clayton, O'Neil & Mayeda, 1972).

5.4.2.1 BRANDVLEI

With a discharge temperature of 64°C, it can be assumed that the groundwater supplying

Brandvlei must reach about 70°C. Using either column of data in *Table 5.1*, and average values for the Table Mountain Group (10.7‰) or the Bokkeveld (11.1‰) and Witteberg (10.9‰) Groups, the discharging water, assuming it reached equilibrium with the host rocks at 70°C, would have a maximum $\delta^{18}O$ of -13‰. Even at 80°C, the $\delta^{18}O$ would still only be -11‰. These values are 5.5‰ to 7.5‰ lower than the average value for Brandvlei water. Temperatures of at least 100°C would be required to start shifting the $\delta^{18}O$ of the meteoric water in a positive direction.

At present the spring water line is shifted to less negative $d^{18}O$ values relative to the meteoric water line, yet exchange at the temperatures that could be anticipated in this study, would shift the groundwater to even more negative $d^{18}O$ values. Thus, it appears that no isotope exchange occurs between the circulating groundwater and its host rocks.

5.4.2.2 CITRUSDAL AND CALITZDORP

Calculations similar to those made above for Brandvlei can be made for the springs at Citrusdal and Calitzdorp. The lower temperatures of these springs means that the isotope values expected for the discharging water would be even more negative. It is therefore concluded that in both cases, no isotope exchange with the rock has occurred.

5.4.2.3 MALMESBURY

The Malmesbury spring discharges from a fault in the Malmesbury Pluton of the Cape Granite Suite. It is also possible that the groundwater supplying the Malmesbury spring circulates through Malmesbury Group metasediments. A similar calculation to that above for Brandvlei, indicates that no detectable oxygen isotope exchange occurs underground. The granite and the metasedimentary rocks both contain micas, which are hydrous and can potentially exchange hydrogen isotopes with groundwater. Hydrogen is considerably less abundant in the rock mass that oxygen and so it is even less likely to exchange with the passing groundwater.

5.4.2.4 SUMMARY

Isotope exchange in recent meteoric waters generally requires higher temperatures than can be found in non-volcanic terrains. Temperatures such as 200°C are required to produce changes in discharge isotope values and even then, the discharge waters are only perceptibly shifted at low flow rates when the water to rock ratio is lower, in the dry season (eg. Governa et al, 1989).

Quartz, which is the main mineral in the aquifers of this study, is a very unreactive mineral and does not exchange isotopes as easily as some other minerals. Furthermore, the nature of the porosity in the Table Mountain Group, being secondary, does not expose a large surface area to interaction and will not encourage isotope exchange.

Isotope exchange is temperature related, yet there is no observable temperature dependence in the shift in isotopes between present rain recharge and spring discharge. The conclusion must therefore be that no isotope exchange is occurring between the aquifer rocks and groundwater.

5.4.3 SIGNIFICANCE OF ISOTOPICALLY LIGHT SPRING WATERS

The isotope values of all the springs that were measured are lower than those that would be expected to be measured in ambient rain falling in the area of the spring. This observation is not totally conclusive for all the springs, as some of them are far removed from sites of rainfall collection, and in the case of Witzenberg and Toowerwater, are at quite high altitudes (800m), and also, most of the springs were sampled only once. For the four springs sampled monthly, however, a reliable average was determined and by comparison with the integrated recharge values from the nearest rainfall collection station, it is clear that the isotope values of the spring discharge is more negative than that of the rain that would fall at the spring itself (see *Figure 5.1*).

In order to discharge lighter isotopes, the springs could be recharged further inland or at higher altitude, to allow the continental or the altitude effects, respectively, to take effect. Considering the mountainous terrain which has created discontinuities and regional scale folds in the Table Mountain Group aquifers, and the presence of impermeable basement, the inland hypothesis can be discarded.

5.4.3.1 BRANDVLEI

At Brandvlei, the discharged isotopes are 0.5‰ for $\delta^{18}O$ and 10‰ for δD, lighter than the integrated recharge values at Tulbagh. Tulbagh is at a similar altitude to the spring, but is 55km away (to the NNW) from Brandvlei and has remarkably negative isotope values (see 5.2 above). However, the topography around Brandvlei is similarly mountainous, with peaks around 1600m to the north-west and 2000m to the west, such that, if this is the cause of the light values at Tulbagh, similar isotopically light rain water could be falling around Brandvlei. Assuming that the Tulbagh integrated recharge values are appropriate to use at Brandvlei, then somehow, the recharge area for the Brandvlei Spring must be located at higher altitude than the spring itself.

The altitude hypothesis is investigated in *Figure 5.3* where an accurate cross section has been attempted. The Table Mountain Group exists in such a geometry that allows the input of relatively light isotopes on the NE slopes of the Stettynsberge at about 1000m and subsequent groundwater flow to depths sufficient to heat the water to well over 60°C (see 5.3.3). A fault is present at the spring, which could provide the break through the Cedarberg Formation, for the

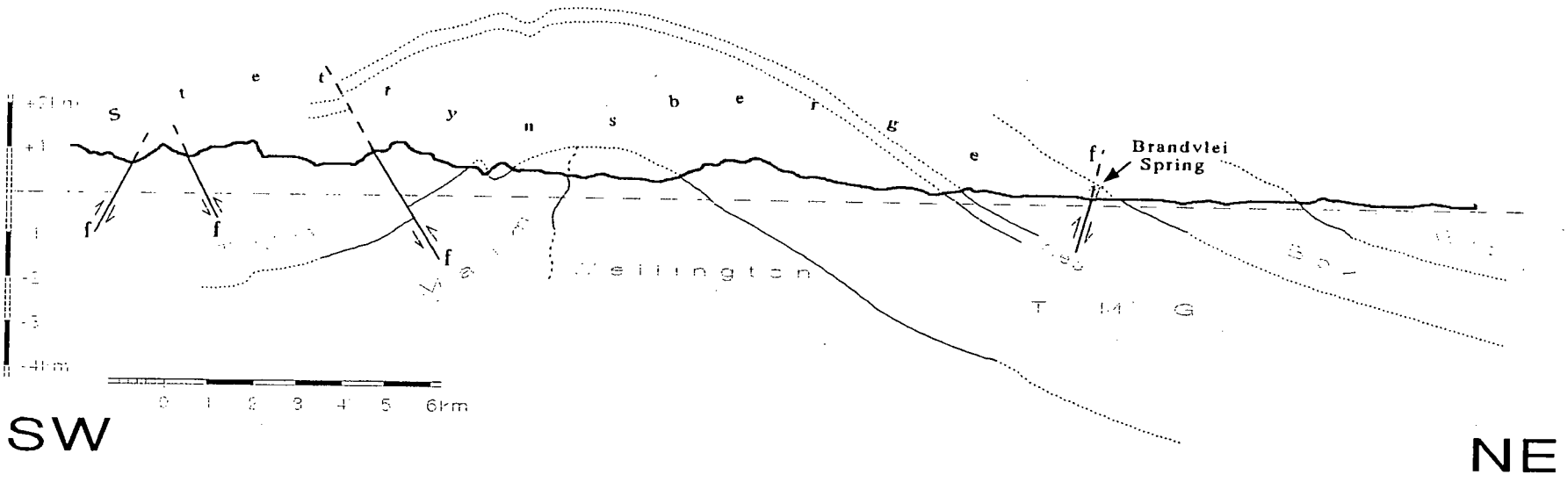

Figure 5.3: A cross section from the Stettynsberge in the south-west, to the southern part of the Worcester Valley in the north-east, with the Brandvlei Spring indicated. Recharge of the spring could easily occur on the north-eastern flanks of the Stettynsberge, in the vicinity of the 1300m high Victoria Peak, which is just north of the line of section. From here the groundwater can travel north-eastwards and can find itself at a depth of 3 to 4km at the base of the Table Mountain Group, when it is vertically below the position of the Brandvlei Spring. A fault exposed at the surface near the spring pools, which is traced for about 20km, could, at depth, provide the break in the otherwise impermeable siltstones and shales of the Cedarberg Formation, through which the heated water would have to flow. Malm = Malmesbury Group, Wellington = that pluton of the Cape Granite Suite, TMG = Table Mountain Group, Ced = Cedarberg Formation, Bok = Bokkeveld Group and Wit = Witteberg Group. Cross section drawn from map 3319C Worcester, 1:125000, Geological Survey, 1986.

heated water to pass upwards and be discharged at the spring.

Assuming a minimum geothermal gradient of -0.2‰.100m^{-1}, the difference in isotopes observed between the rainfall and the spring discharge at Brandvlei is easily achieved by recharge on the Stettynsberge, as described above. On the one hand, the isotope values of Tulbagh are particularly negative and so the possibility exists that recharge in the Worcester Valley is less negative and hence a higher altitude of recharge would be required, but on the other hand, an altitude effect of -0.2‰.100m^{-1} is a minimum value for what may well be -0.3‰.100m^{-1} or over.

A reason that the Brandvlei spring does not discharge water with isotope ratios that are more negative is possibly because of the high volume of discharge: 12l.s^{-1}. At an annual rainfall of 300mm, the recharge area required is 3.6km^2 and so it may be difficult for all of this area to be at high altitude. Mixing with lower altitude rain may well make the isotope ratios less negative.

5.4.3.2 CITRUSDAL

At The Baths, the discharge is more negative than the assumed recharge values by 0.5‰ for $\delta^{18}O$ and 9‰ for δD. These differences are almost identical to those at Brandvlei. The integrated recharge values calculated for Citrusdal are less robust than those for Tulbagh, but are in general agreement with all the other isotopes of H and O measured in rain. In favour of comparing the rain and spring values at Citrusdal are the facts that the rain station is only 15km away from the spring and at about same altitude. From *Figure 5.4*, a flow path can be pictured, from the Kouebokkeveldberge, the water sinking down, flowing westwards under the Citrusdal Valley and rising up below Warwbadberg to yield a discharge at the Baths that is heated and isotopically lighter than the ambient rainfall.

Rain that falls on the western portion of the Kouebokkeveldberge can percolate into the Peninsula Formation and reach depths of about 2km, which is adequate to heat the water to around 50°C. Thereafter, the groundwater is likely to use the local fault as a means of flowing through the Cedarberg Formation so that it can discharge out of the Nardouw Subgroup.

5.4.3.3 CALITZDORP

Of the four springs analyzed over a period of months, Calitzdorp discharges the most isotopically light water. The recharge values recorded at Oudtshoorn might seem not very applicable to high mountain recharge. In addition they are not representative of a full year's rainfall and Oudtshoorn is also 40km east of the Calitzdorp Spa. They are however, fairly similar to values recorded at Citrusdal and do plot on the Cape meteoric water line and so extrapolation down the line to more negative isotopes expected at higher altitudes, is possible.

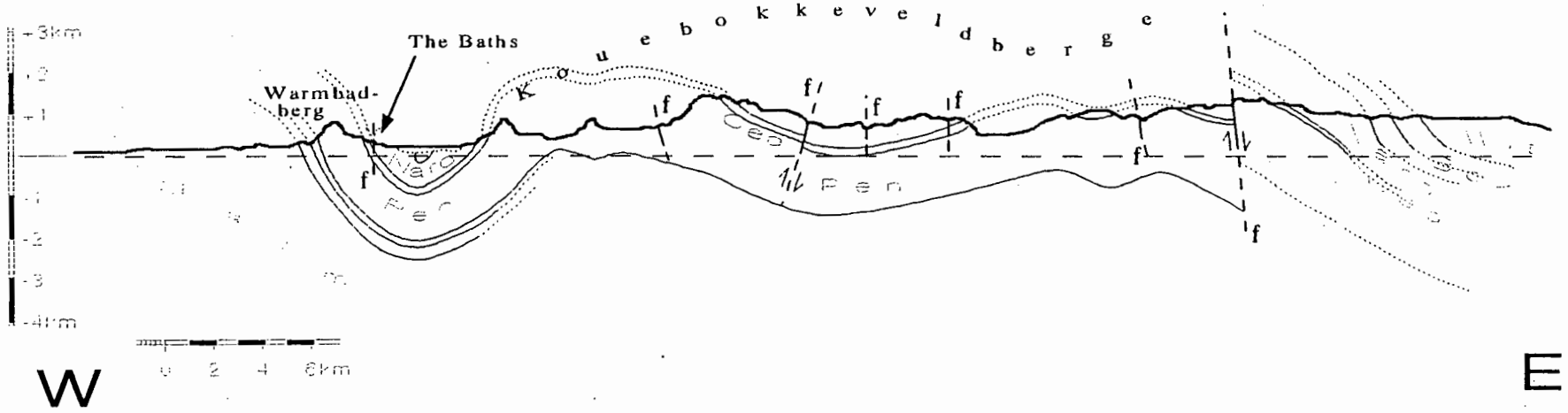

Figure 5.4: A cross section from the Kouebokkeveld in the east, through the Kouebokkeveldberge and the Olifants River Valley where 'The Baths' (Citrusdal Hot Spring) are situated, to the Swartland in the west. Possible recharge of the spring could be in the western portion of the Kouebokkeveldberge. The water could then flow westwards, through the Olifants River syncline where the water will heat up before emerging from a fault at the spring, on the western side of the syncline. Again, this fault is probably pivotal in allowing the water to move upwards through the otherwise impermeable Cedarberg Formation. Note that the Warmbadberg (English meaning: Hot-pool-mountain) has been named after the spring. Malm = Malmesbury Group, Pen = Peninsula Formation, Ced = Cedarberg Formation, Nard = Nardouw Subgroup, Bok = Bokkeveld Group and Wit = Witteberg Group. Cross section drawn from map 3218 Clanwilliam, 1:250000, Geological Survey, 1973.

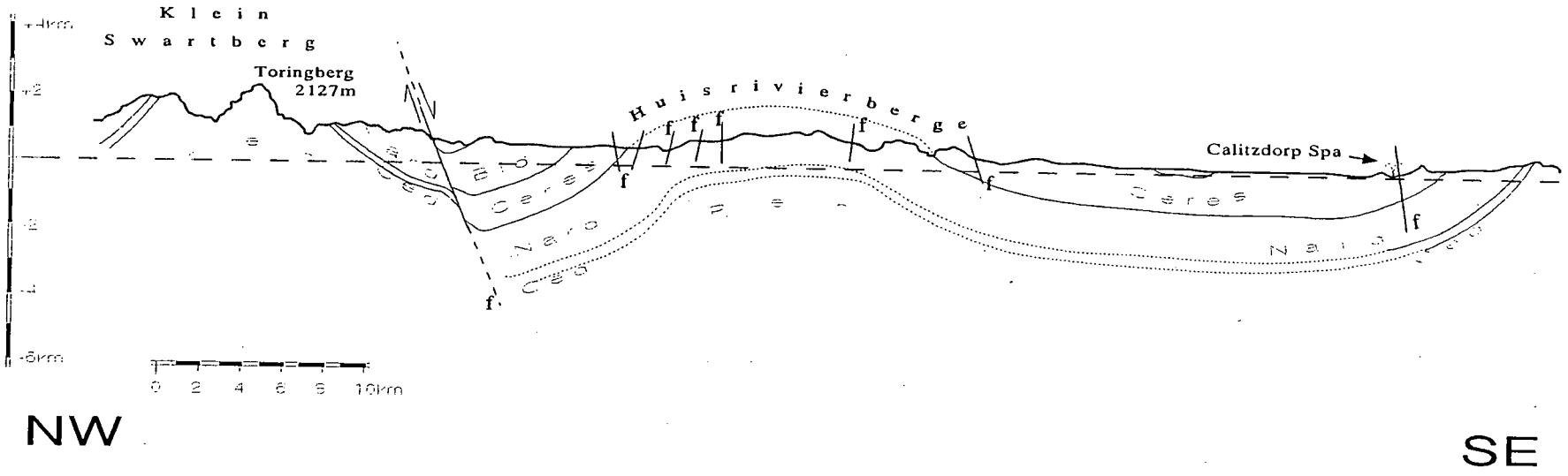

Figure 5.5: A cross section through the Klein Swartberg in the north, through and to the southern side of the Little Karoo, where the Calitzdorp Spa is located, a few metres onto the south bank of the valley of the Olifants River - a different Olifants River from that at Citrusdal. To generate isotopes as negative as those observed issuing from the spring, the Swartberg must be the recharge area. If rain fell in the vicinity of Toringberg in the Klein Swartberg, it is conceivable, although remarkable, that the groundwater could then flow down in the Peninsula Formation to a depth where it reaches either the Nardouw Subgroup, or the Peninsula Formation on the southern side of the regional fault, whereafter the now hot water could flow approximately horizontally before finding its way to the surface at the spring. Yet again it appears that a fault must provide a break through the Cedarberg Formation. Pen = Peninsula Formation, Ced = Cedarberg Formation, Nard = Nardouw Subgroup, Ceres = Ceres Subgroup and Bid = Bidouw Subgroup (the latter two both of the Bokkeveld Group). Cross section drawn from map 3320 Ladismith, 1:250000, Geological Survey, 1991.

By assuming a valley recharge of -4‰ and -11‰ for $\delta^{18}O$ and δD, with Calitzdorp discharge at -7.3‰ and -30‰, similarly, a difference of 3.3‰ and 30‰ needs to be accounted for by the altitude effect. From *Figure 5.5*, a potential flow path exists from the Huisrivierberge to the spring, but using an altitude effect of even $-0.3‰.100m^{-1}$, an average recharge altitude of about 1300m is required. The Huisrivierberge are only 1220m high at the highest peak.

The possibility exists that groundwater could flow from the Klein Swartberg to the Calitzdorp spring. Here, altitudes in excess of 2000m occur and so even with a reduced altitude effect of $-0.2‰.100m^{-1}$, the negative isotope ratios required could be generated. Again, a fault at the spring is responsible for the discrete discharge of the spring water.

5.4.3.4 MALMESBURY

At this spring the discharging isotopes are only slightly more negative than the integrated recharge value for Cape Town. The δD ratio is 8‰ more negative, yet the $\delta^{18}O$ value is only 0.2‰ more negative. This can be ascribed to evaporation prior to recharge, which is likely to be more marked in the Malmesbury area than at the other recharge areas, as the Malmesbury area is at low altitude, always below cloud level, in contrast to the mountain top environment of the other springs where limited evaporation of rain will occur.

The fact that the isotopes are shifted to more negative values has to partly be due to the inland nature of Malmesbury, where the continental effect will have taken place. Slight variations in topography in the area, of a few hundred metres, could also enhance this, but the altitude effect does not necessarily need to be invoked here. Hence, there can be limited speculation as to the flow path of the groundwater recharging the Malmesbury spring.

5.4.4 CONTINENTAL EFFECT

In *Figures 5.6 & 5.7*, the isotope ratios of oxygen and hydrogen, respectively, have been plotted against the distance of the springs from the west coast. Although the dominant winds that blow in winter are north-westerly, during the storms which supply the Western Cape with most of its rain, the movement of these weather systems across the Cape is from west to east. The point which signals the beginning of the rainout of any one weather system is then the west coast.

Figures 5.6 & 5.7 show the negative correlation between isotope ratios and continentality (distance from the sea) that is known for rainfall from other parts of the world (eg. Sonntag et al, 1979, in Mazor, 1991). The correlation found in this project is an interesting one, in that it is not the rain that is being sampled directly, but rather the discharge from springs. As can be seen from the plots however, the fit is not excellent, but this may also be due to the random and analytical errors that exists in the data. Random errors come about from small natural

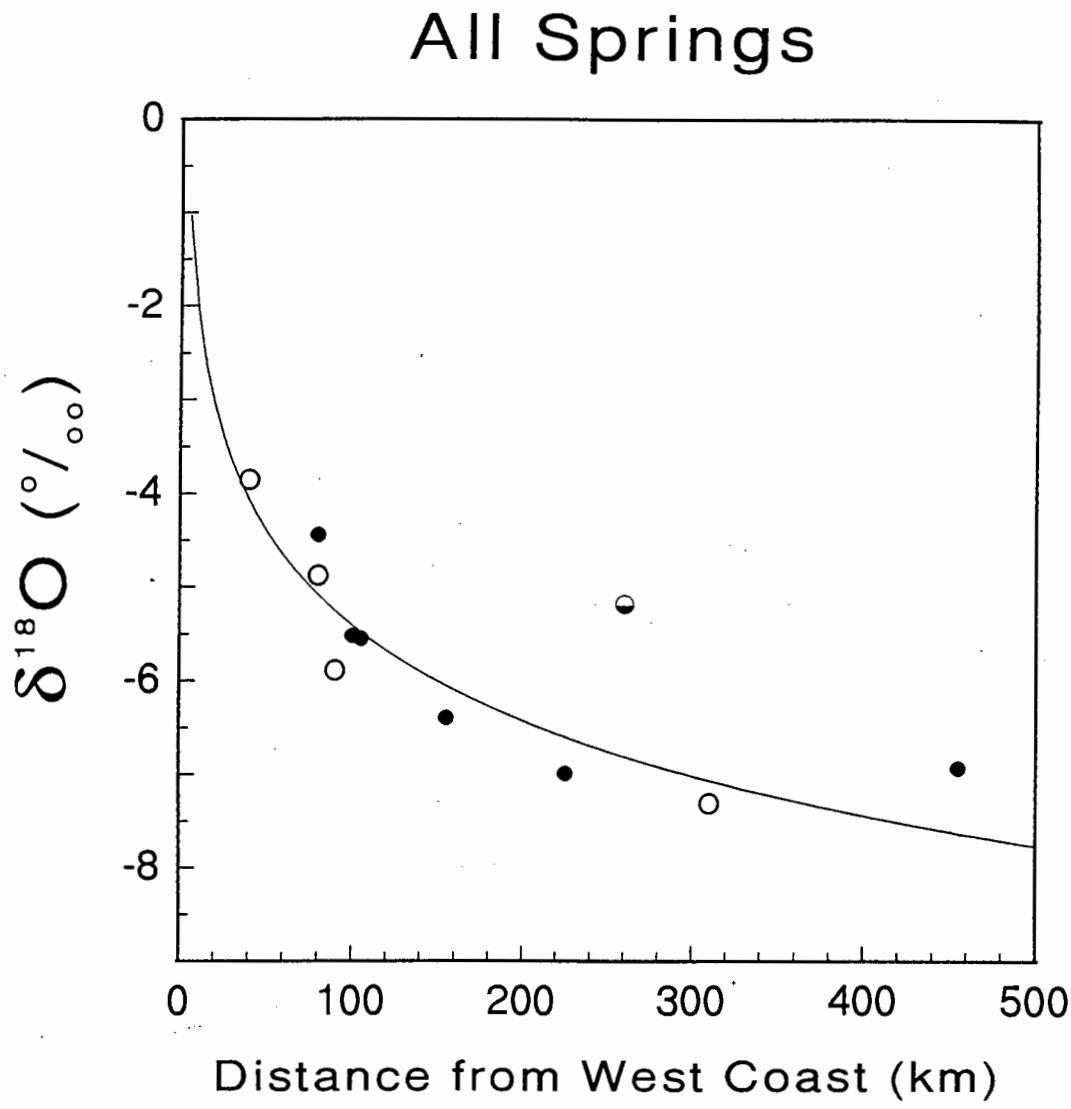

Figure 5.6: The $d^{18}O$ values of all the springs plotted against their distance from the Atlantic Ocean on the west coast. Average $d^{18}O$ values of the four springs sampled monthly are plotted as **O**, whereas the others are shown as ● and Rietfontein is shown as a half filled circle. The value for Rietfontein was not used to compute the curve plotted here. The curve $\delta^{18}O = -3.37\log(km) + 1.33$, where `km` is the distance from the west coast in kilometres, appears to describe the correlation well.

Important to realise is that some of the springs sampled only once (●) are sure to have random errors and so it is not critical if they do not lie on the curve. In contrast, the averaged points (**O**) can be thought of as very accurate values for those springs and therefore require that the curve should pass very close for the function to be of any value.

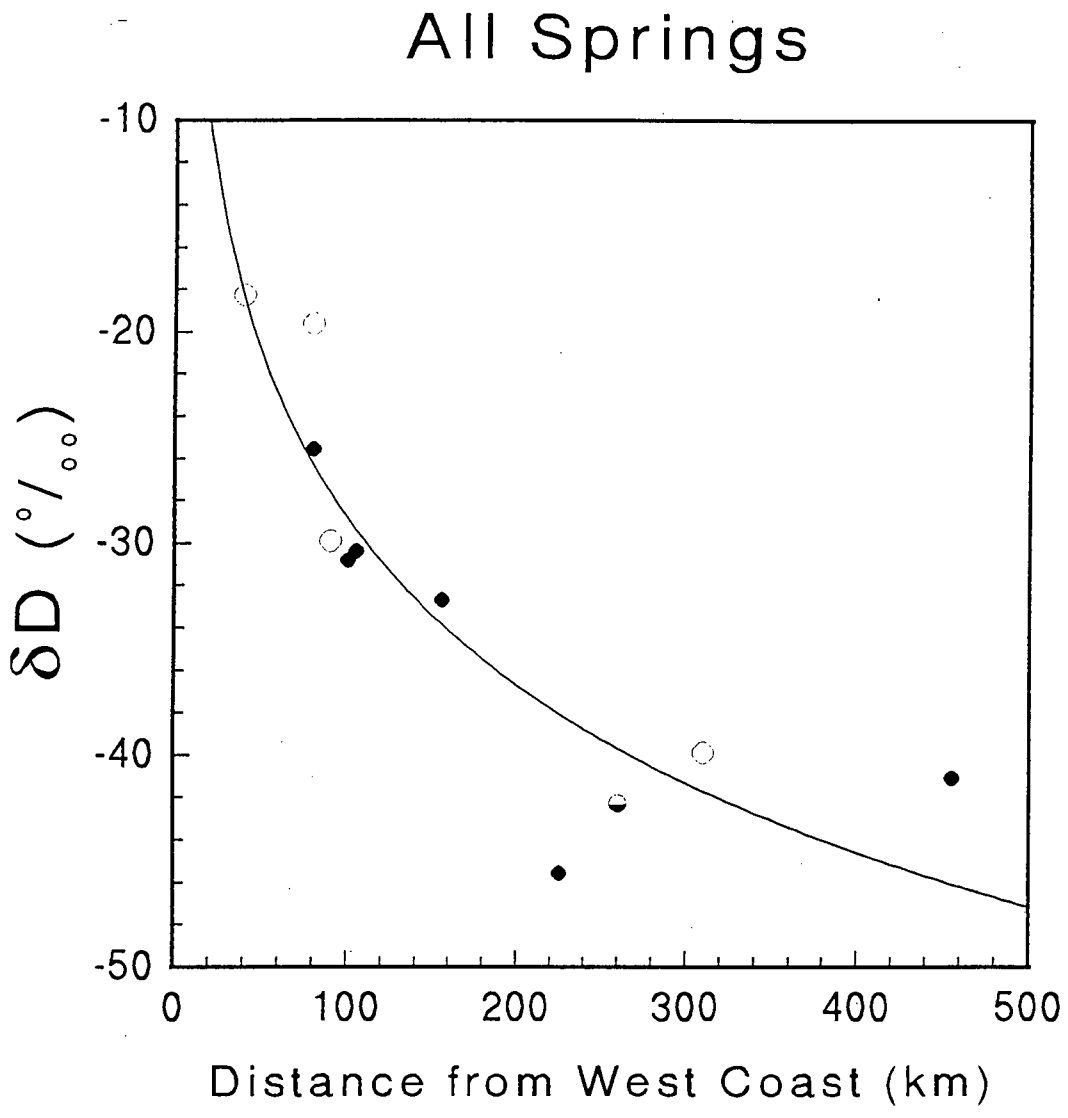

Figure 5.7: The δD values of all the springs versus their distance from the west coast. The four springs sampled monthly are plotted as o, whereas the others are shown as ● and Rietfontein is shown as a half filled circle. The value for Rietfontein was not used to compute the curve drawn here. The function $\delta^{18}O = -26.2\log(km) + 23.7$, where 'km' is the distance from the west coast, seems to describe the correlation well. The same points mentioned in the caption to *Figure 5.6* apply here too.

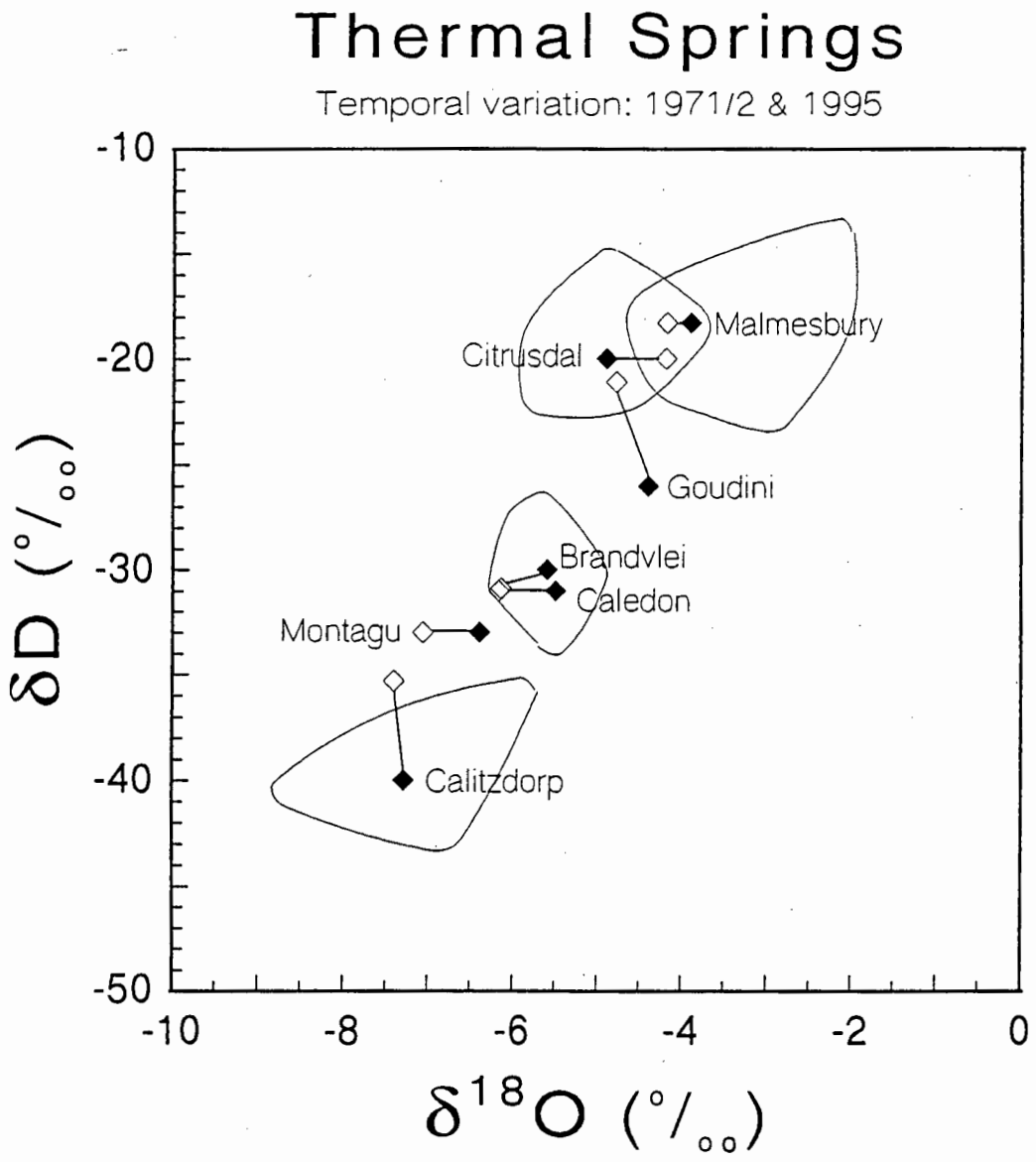

Figure 5.8: A δD versus δ^{18}O plot of the thermal springs that were studied in this project and also sampled and studied by Mazor & Verhagen (1983). The 1995 data is shown as solid diamonds (◆) and the 1971/2 data is shown as open diamonds (◇). Mazor and Verhagen (1983) sampled all of the plotted springs in December 1971 and some of them again in December 1972, but they do not say whether or not the reported values for those springs sampled twice are averages. The four data fields for Brandvlei, Calitzdorp, Citrusdal and Malmesbury (as drawn in *Figure 4.19*) have also been added, to show that, in most cases, the 1971/2 data point is within the random variation discovered in this study. This random variation can be due to any natural fluctuation such as underground mixing, recharge, evaporation and others.

fluctuations in evaporation, possible isotope exchange, recharge, underground flow, etc.

The equations used to describe the trend of this correlation should be applicable for almost all groundwater in the Cape, provided it has undergone only a limited degree of evaporation prior to recharge.

5.4.5 TEMPORAL CHANGE

Figure 5.8 is a plot which includes most of the spring isotope data collected for this project and compares this data to that collected by Mazor and Verhagen (1983) in 1971 and 1972. The differences between the data points are well above the analytical error. The random error though, can be gauged from the four fields that are drawn on the graph and in such a way, the samples taken 25 years prior to this study are isotopically indistinguishable from those taken in 1995. This confirms the evidence from constant discharge volumes and temperatures (5.3.1) that the underground spring reservoirs are well mixed and probably quite large.

There seems to be a subtle trend in *Figure 5.8* in that most of the points for this study are shifted to the right and sometimes downwards. Only at Citrusdal is the direction the opposite. This is a rather difficult trend to comment on, as it may just be because of the limited number of sites. It may, however, indicate that there could be a climatic effect. Climates are known to go through 20 to 30 year cycles (Preston-Whyte & Tyson, 1988); these could be reflected isotopically and so the groundwater reservoirs could have medium term inhomogeneities. Thus, the residence time of these deep groundwaters could be on the order of a few decades.

5.5 GAS COMPOUNDS AND ISOTOPES

The carbon isotopes from the three springs analyzed yielded $\delta^{13}C$ values between -21 and -24‰, which clearly labels the carbon as being of organic origin (Dai et al, 1996). This carbon came from CO_2 and CH_4 at all three springs.

5.5.1 ORGANIC CARBON FROM ROCKS

The most important feature of the $\delta^{13}C$ values is that they are approximately the same. This is important, considering that Malmesbury has a very different recharge environment to the other two springs. At Malmesbury, H_2S is given off in small yet distinctively odorous quantities. The presence of sulphur suggests that this spring does in fact have groundwater circulating through the Malmesbury Group metasediments, which can contain sulphur. This implies that groundwater can indeed circulate through the Malmesbury Group. Thus, the CO_2 and the CH_4 could also be rock derived.

The Malmesbury Group is not known to have any significantly carbonaceous rocks (eg Hartnady et al, 1974) and besides, it consists mainly of impermeable phyllitic or shaly material.

Discrete fractures that could exist are unlikely to be able to yield any appreciable surface area over which the groundwater could dissolve carbon. Important to remember here is that the quantity of gas being released at Malmesbury is around three orders of magnitude less than at Brandvlei. So although the Malmesbury spring may well be releasing CO_2 derived from the Malmesbury Group rocks, it seems an unlikely explanation for the vast quantities being released at Brandvlei and the considerable volumes released at Calitzdorp. Also the lack of H_2S at any of the other springs is good evidence for the lack of involvement of the Malmesbury Group at any of the other springs.

The last possibility for a rock source for the gases is in the thin Cedarberg Formation. It is apparent from earlier discussion (5.4.3.1 and 5.4.3.3) and from *Figures 5.3 & 5.5* that the water discharging at Brandvlei and Calitzdorp passes through the Cedarberg Formation on it's way up to the surface. If the carbon does indeed originate here and the Cedarberg Formation does not contain any sulphur, this could explain be why there is no H_2S emitted at these springs. This scenario does require that there is sufficient circulation within the thin Cedarberg Formation (typical thicknesses of around 50m), organic carbon in sufficient quantities and there must be no sulphur. Considering the minor size of this unit and the quantities of gas released at Brandvlei, and to an extent at Calitzdorp, this explanation is not very attractive.

5.5.2 ORGANIC CARBON FROM RECENT SURFACE ENVIRONMENTS

The sheer quantity of gas being discharged and the presence of CH_4 indicate that the environment prior to recharge must be able to supply considerable quantities of carbon and also be reducing. The Cape Mountains are known for their nutrient poor, structureless and nearly topsoil free soils. There are, however, flattish areas that become waterlogged in winter and have black organic rich soils and so would tend to be reducing as well as having a large supply of carbon. The fynbos (heath-like) vegetation that grows on the Cape Mountains is distinctive in producing fulvic and humic acids, which, if present in sufficient quantities, stain the water reddish brown. These organic compounds and possibly others could allow the water to contain appreciable dissolved organic carbon. Soil water is capable of holding over 30mg $C.l^{-1}$ and water in wetlands, such as the above mentioned bogs, can hold up to 60mg $C.l^{-1}$, however, by the time the water reaches the water table, most of the dissolved organic carbon is gone, having been left behind in the various soil horizons (Drever, 1988).

Bogs were also advocated above (5.4.1.3), as they might be the site allowing evaporation to occur prior to recharge into the groundwater system. Critical to the discussion here is how the CO_2 gets into the groundwater and stays there until it is discharged with the water at the springs. By the reaction

$$2C_{organic} + 2H_2O = CO_2 + CH_4$$

CO_2 and CH_4 can be produced. This reaction occurs by bacterial fermentation in the soil, after

which the water with the dissolved CO_2 and CH_4 would have to get into the groundwater system without losing these dissolved gases. This could be possible in the rather peculiar high altitude environments of these bogs. The bogs have very high organic matter concentrations within what are otherwise the typically poor sandy soils of the Table Mountain Group. There are no thick, well developed soils in which the organic carbon or the two gases may be lost. The only potential method of loss is thus through exsolution and emission to the atmosphere. Hence, if the above reaction takes place in the organic matter below the bog pond, or in some position where it is about to enter a recharge channel or zone, then it is conceivable that these gases could get into the groundwater system.

Once in the groundwater, the passage through the unreactive quartzites is unlikely to remove any constituents that are dissolved in the water and so the gases could remain dissolved until their final release at the springs. Thus, through a rather intricate set of circumstances, it is possible that the gases issuing at the springs are derived from decaying contemporary organic matter.

6 CONCLUSION

Rainfall collected during this work resulted in a meteoric water line for the Cape Mediterranean climate area with the equation $\delta D = 7.38\delta^{18}O + 18.6$, determined by using the general form of a structural regression (with $\lambda = 10$), using isotope values of integrated total monthly precipitation, weighted by rainfall amount. Other calculation techniques, such as reduced major axis regression or a classical regression, yielded meteoric water lines that were similar and quite applicable over the range of isotope ratios observed. Further study is warranted in order to calculate the altitude effect for the area of the Cape Fold Belt.

Stable isotopes from thermal springs of the area yield a water line with the equation $\delta D = 8.32\delta^{18}O + 16.5$. This line has a somewhat steeper gradient than the Cape meteoric water line which indicates that precipitation of the recharge water for the springs is occurring from a more fractionated water and vapour mass, under colder and possibly more humid conditions, such as at high altitude. Palaeorecharge is excluded on the basis of the similarity in deuterium intercept between the spring and the meteoric water lines. Similar deuterium intercepts indicate similar humidity conditions over the ocean when a vapour mass is forming.

Isotope ratios of water discharged at the springs are clearly isotopically lighter than recharge values estimated for rain that would fall at the spring. The springs have therefore been recharged at higher altitudes, for example, in a mountain setting. The position of the spring water line below the meteoric water line suggests evaporation prior to recharge.

The spring water $\delta^{18}O$ values have been shifted to less negative values than those for the rain; this is the opposite direction to that which would be expected for exchange with quartz at less than 100°C. Temperatures of about 200°C or more would be required before isotope exchange with rocks would shift the $\delta^{18}O$ values to higher values.

Groundwater must flow through discrete fractures in the Table Mountain Group, the Cape Granites and in places may flow through the Malmesbury Group. Temperatures of hot springs suggest that groundwater circulates to depths of up to three kilometres below sea level, to reservoirs that are large relative to the outflow at the springs. From this environment where heating occurs because of the geothermal gradient ($\pm 20°C.km^{-1}$), the water moves upwards via faults that provide breaks through the impermeable Cedarberg Formation.

Carbon dioxide and methane released at some springs may be sourced at depth geologically, but given the absence of a likely source, probably come from near surface bogs and areas of organic

matter accumulation in the mountains. Hydrogen sulphide released at Malmesbury indicates a geological source for that gas at least, from the Malmesbury Group.

A continental effect, that was not observable from only four rain collection stations, was found amongst the spring waters. This could be because the water discharging at the springs is more representative than the monthly values, which are subject to fluctuations. In southern Africa, which has an inland plateau, the continental effect will be coupled with the altitude effect. Rainout of heavy isotopes and decreasing temperatures must be the cause of this observed continental effect.

It is important to note here the fact that knowledge of the local climate dynamics is fundamental to any interpretation of hydrological isotope data; the example here is that the distance to the west coast (and not any coastline) is the parameter which reveals the continental effect.

A worthwhile study would be an isotopic comparison between the deep groundwater of this study versus shallow groundwater, as emerges from cold springs and boreholes. By calculating a water line for shallow groundwater, the opportunity could arise for a clearer picture to emerge on the matters of recharge area and time (ancient/present), evaporation, isotope exchange and a source for the gases released from some of these hot springs.

7 ACKNOWLEDGEMENTS

Thanks are primarily due to my supervisor, Dr Chris Harris, for suggesting and guiding me through this study. I acknowledge the support of: the FRD (Foundation for Research Development) for funding me with a Masters Bursary and a core grant to Dr Chris Harris; the FRD, the Goldfields Foundation and UCT for the recent purchase of fine new mass spectrometer. And for friendly help with the mass spectrometer, thanks to John Lanham of Archaeology, UCT.

Thanks also to those who supplied data or information: for isotope data: of water, Milo Simonic of DWAF (Department of Water Affairs and Forestry); of rocks, Susanne Egle; for unpublished reports: Alan Woodford of DWAF; Rowina Hay of Umvoto Africa; for meteorological data, the South African Weather Bureau.

Lastly, to all of those kind people without whom this project could never have happened - the water samplers: for spring water: Captain DC Taljaard of Brandvlei Prison, Worcester; Mr Hein van Huysteen of the Calitzdorp Spa; Mr Manie Gordon of The Baths, Citrusdal; my friends Alastair Sellick and Adrienne Adlington and my parents Elinor & José Milewski for sampling the Malmesbury spring; for rain water: Mr Brian Beylevelde of Citrusdal; Mrs Koen of Oudtshoorn and my grandmother, Mrs Vera Humphris of Tulbagh. Thanks also to NC Krone of Tweejongezellen and Mike Hunter of Tulbagh for alerting me as to the existence and whereabouts of the Witzenberg spring. Finally, thanks to all the personnel at the other hot springs for allowing us to take water samples.

8 REFERENCES

Borthwick J. & Harmon R.S. **1982** A note regarding ClF_3 as an alternative to BrF_5 for oxygen isotope analysis. *Geochimica et Cosmochimica Acta*, **46**, 1665-1668.

Broquet C.A.M. **1992** The sedimentary record of the Cape Supergroup: A review. In: De Wit M.J. & Ransome I.G.D. (editors), *Inversion Tectonics of the Cape Fold Belt, Karoo and Cretaceous Basins of Southern Africa*, 159-183, Balkema, Rotterdam, 269 pages.

Burchell W.J. **1822** Travels in the Interior of Southern Africa, Volume 1; reprinted from the original edition in 1953; The Batchworth Press, London, 381 pages.

Clayton R.N., O'Neil J.R. & Mayeda T.K. **1972** Oxygen isotope exchange between quartz and water. *Journal of Geophysical Research*, **77**, 3057-3067. In: Friedman I. & O'Neil J.R. **1976** Chapter KK: Compilation of Stable Isotope Fractionation Factors of Geochemical Interest. Geological Survey Professional Paper 440-KK; in: Fleischer M. (ed) Data of Geochemistry, Sixth Edition.

Coplen T.B. **1988** Normalization of oxygen and hydrogen isotope data. *Chemical Geology: Isotope Geoscience*, **72**, 293-297.

Craig H. **1961a** Isotopic variations in meteoric waters. *Science*, **133**, 1702-1703.

Craig H. **1961b** Standard for reporting concentrations of deuterium and oxygen-18 in natural waters. *Science*, **133**, 1833-1834.

Custodio E. **1989** Groundwater characteristics and problems in volcanic rock terrains. In: *Isotope Techniques in the Study of the Hydrology of Fractured and Fissured Rocks*, 87-137, International Atomic Energy Agency, Vienna, 306 pages.

Dai J-x., Song Y., Dai C-s. & Wang D-r. **1996** Geochemistry and accumulation of carbon dioxide gases in China. *AAPG Bulletin*, **80**, 1615-1626.

Dansgaard W. **1964** Stable isotopes in precipitation. *Tellus*, **16**, 436-468.

Diamond R.E. **1994** The Pan-African Malmesbury Group - Palaeozoic Cape Supergroup unconformity: Alteration and chloritoid forming metamorphism. Honours project, University of Cape Town, 73 pages, unpublished.

Diamond R.E. & Harris C. **1997** A meteoric water line for the Cape, South Africa. Submitted.

Donaldson I.G. **1982** Heat and mass circulation in geothermal systems. *Annual Review of Earth and Planetary Sciences*, **10**, 377-395.

Drever J.I. **1988** The Geochemistry of Natural Waters; Prentice Hall, Inc., New Jersey, USA; 437 pages.

Ehhalt D., Knott K., Nagel J.F. & Vogel J.C. **1963** Deuterium and oxygen 18 in rain water. *Journal of Geophysical Research*, **68**, 3775-3780.

Emiliani C. **1987** Dictionary of the Physical Sciences; Oxford University Press, New York; 365 pages.

Faure G. **1986** Principles of Isotope Geology, 2nd edition. John Wiley & Sons, New York, 589 pages.

Flora O. & Longinelli A. **1989** Stable isotope hydrology of a classical karst area, Trieste, Italy. In: *Isotope Techniques in the Study of the Hydrology of Fractured and Fissured Rocks*, 203-

213, International Atomic Energy Agency, Vienna, 306 pages.

Gat J. **1971** Comments on the stable isotope method in regional groundwater investigations. *Water Resources Research*, **7**, 980-993.

Governa M.E., Lombardi S., Masciocco L., Riba M. & Zuppi G.M. **1989** Karst and geothermal water circulation in the central Appenines (Italy). In: *Isotope Techniques in the Study of the Hydrology of Fractured and Fissured Rocks*, 173-202, International Atomic Energy Agency, Vienna, 306 pages.

Gray D.R., Gregory R.T. and Durney D.W. **1991** Rock-buffered fluid rock interaction in deformed quartz-rich turbidite sequences, eastern Australia. *Journal of Geophysical Research*, **96**, 19681-19704.

Gresse P.G. & Theron J.N. **1992** The geology of the Worcester area - explanation of sheet 3319. Geological Survey, Republic of South Africa, 79 pages.

Gresse P.G., Theron J.N., Fitch F.J. & Miller J.A. **1992** Tectonic inversion and radiometric resetting of the basement in the Cape Fold Belt. In: De Wit M.J. & Ransome I.G.D. (editors), *Inversion Tectonics of the Cape Fold Belt, Karoo and Cretaceous Basins of Southern Africa,* 217-228, Balkema, Rotterdam, 269 pages.

Hälbich I.W. **1992** The Cape Fold Belt Orogeny: State of the art 1970's - 1980's. In: De Wit M.J. & Ransome I.G.D. (editors), *Inversion Tectonics of the Cape Fold Belt, Karoo and Cretaceous Basins of Southern Africa*, 141-158, Balkema, Rotterdam, 269 pages.

Hammerbeck E.C. & Allcock R.J. **1985** Geological Map of Southern Africa, 1:4000000. Geological Survey of South Africa.

Harris C., Faure K., Diamond R. & Scheepers R. **1996** Oxygen and hydrogen isotope geochemistry of S- and I-type granitoids of the Cape Granite Suite, South Africa. Submitted.

Hartnady C.J., Newton A.R. & Theron J.N. **1974** Stratigraphy and structure of the Malmesbury Group in the southwestern Cape. In: Kröner, A. (ed) *Contributions to the Precambrian Geology of Southern Africa*, 193-213, Bulletin of the Precambrian Research Institute, University of Cape Town, **15**, 213 pages.

Hoal B.G. **1978** The pre-Cape Brewelskloof-Meiringsberg area north of Worcester: Structural analysis, petrography, geochemistry and application of white mica geothermometry and geobarometry. Honours project, University of Cape Town, 86 pages, unpublished.

Issar A. **1983** On the source of water from the thermomineral springs of Lake Kinneret (Israel). *Journal of Hydrology*, **60**, 175-183.

Jones M. **1992** Heat flow in South Africa. *Handbook of the Geological Survey*, **14**, 174 pages.

Kent L.E. **1949** The thermal waters of the Union of South Africa and South West Africa. *Transactions of the Geological Society of South Africa*, **52**, 231-264.

Kotze J.C. **1995** Little Karoo Rural Water Supply Scheme. Geohydrology Directorate, Department of Water Affairs and Forestry, Republic of South Africa, Technical Report Gh3858; unpublished report.

Labeyrie L. **1974** New approach to surface seawater palrotemperatures using $^{18}O/^{16}O$ ratios in silica of diatom frustules. *Nature*, **248**, 40-42.

Leontiadis I.L., Payne B.R., Letsios A., Papagianni N., Kakarelis D. & Chadjiagorakis D. **1983** isotope hydrology study of Kato Nevroko of Dramas. In: *Isotope Hydrology 1983*, 193-206, International Atomic Energy Agency, Vienna.

Maclear L.G. **1995** Cape Town Needs Groundwater: A note on the potential of the Cape Flats Aquifer Unit to supply groundwater for domestic use in the Cape Town Metropolitan Area. Geohydrology Directorate, Department of Water Affairs and Forestry, Technical Report Gh3868, 6 pages.

Mazor E. **1991** Applied Chemical and Isotopic Groundwater Hydrology. Open University Press, 274 pages.

Mazor E. & Verhagen B. **1983** Dissolved ions, stable and radioactive isotopes and noble gases in thermal waters of South Africa. *Journal of Hydrology*, **63**, 315-329.

Merlivat L. & Jouzel J. **1979** Global climatic interpretation of the deuterium-oxygen 18 relationship for precipitation. *Journal of Geophysical Research*, **84**, 5029-5033.

Midgley J.J. & Scott D.F. **1994** The use of stable isotopes of water (D and ^{18}O) in hydrological studies in the Jonkershoek Valley. *Water SA*, **20**, #2, 151-154.

Pollack H. **1982** The heat flow from continents. *Annual Review of Earth and Planetary Sciences*, **10**, 459-481.

Preston-Whyte R.A. & Tyson P.D. **1988** The Atmosphere and Weather of Southern Africa. Oxford University Press, Cape Town, 375 pages.

Rindl M.M. **1928** The medicinal springs of South Africa - Supplement II. *South African Journal of Science*, **XXV**, 116-126.

Rindl M.M. **1931** International standard measurements on hydrology and a provisional register of medicinal waters of South Africa based on these standards (second communication). *South African Journal of Science*, **XXVIII**, 124-130.

Rindl M.M. **1934** The medicinal springs of South Africa - Supplement V. *South African Journal of Science*, **XXXI**, 173-176.

Rock N.M.S. **1988** Lecture Notes in Earth Sciences, 18: Numerical Geology. Springer Verlag, Berlin, 427 pages.

Scheepers R. **1995** Geology, geochemistry and pertrogenesis of late Precambrian S-, I- and A-type granitoids in the Saldania Belt, western Cape Province. *Journal of African Earth Science*, **21**, 35-58.

Schoch A.E. **1976** The Darling Granite batholith. *Annals of the University of Stellenbosch*, **A1**, 1-104.

Schoch A.E. & Burger A.J. **1976** U-Pb zircon age of the Saldanha quartz porphyry, western Cape Province. *Transactions of the Geological Society of South Africa*, **79**, 239-241.

Sharma M.L. & Hughes M.W. **1985** Groundwater recharge estimation using chloride, deuterium and oxygen-18 profiles in the deep coastal sands of Western Australia. *Journal of Hydrology*, **81**, 93-109.

Siegenthaler U. & Oeschger H. **1980** Correlation of ^{18}O in precipitation with temperature and altitude. *Nature*, **285**, 314-317.

Socki R.A., Karlsson H.R. & Gibson Jnr. E.K. **1992** Extraction technique for the determination of oxygen-18 in water using preevacuated glass vials. *Analytical Chemistry*, **64**, #7, 829-831.

Taylor H.P. Jr. **1968** The oxygen isotope geochemistry of igneous rocks. *Contributions to Mineralogy and Petrology*, **19**, 1-71.

Theron J.N., Gresse P.G., Siegfried H.P. and Rogers J. **1991a** The geology of the Cape Town area - explanation of sheet 3318. Geological Survey, Republic of South Africa, 140 pages.

Theron J.N., Wickens H. de V. & Gresse P.G. **1991b** The geology of the Ladismith area - explanation of sheet 3320 (in Afrikaans). Geological Survey, Republic of South Africa, 99 pages.

Umvoto Africa c.c. **1995a** Hydrogeological Investigation and Borehole Siting on Thara Kamma Farm, Citrusdal District; unpublished report.

Umvoto Africa c.c. **1995b** Hydrogeological Investigation and Borehole Siting on Groot Brakfontein Farm in the Citrusdal District; unpublished report.

Urey H.C. **1947** The thermodynamic properties of isotopic substances. *Journal of the Chemical Society*, 562-581.

Valley J.W., Taylor H.P. Jr. and O'Neil J.R. (editors) **1986** Stable Isotopes in High Temperature Geological Processes. *Reviews in Mineralogy*, **16**, 570 pages.

Vennemann T.W. & O'Neil J.R. **1993** A simple and inexpensive method of hydrogen isotope and water analyses of minerals and rocks based on zinc reagent. *Chemical Geology: Isotope Geoscience*, **103**, 227-234.

Vennemann T.W. & Smith H.S. **1990** The rate and temperature of reaction of ClF_3 with silicate minerals, and their relevance to oxygen isotope analysis. *Chemical Geology: Isotope Geoscience*, **86**, 83-88.

Vitorello I. & Pollack H. **1980** Heat flow and thermal evolution of continents. *Journal of Geophysical Research*, **85**, 983-995.

Welhan **1987** Stable isotope hydrology. In: Kyser T.K. (ed) *Short Course in Stable Isotope Geochemistry of Low Temperature Fluids*, 129-161, Mineralogical Association of Canada, **13**, 452 pages.

Zojer H. & Stichler W. **1989** Groundwater characteristics and problems in carbonate rock aquifers. In: *Isotope Techniques in the Study of the Hydrology of Fractured and Fissured Rocks*, 159-171, International Atomic Energy Agency, Vienna, 306 pages.

A STATISTICAL METHODS

CALCULATION OF METEORIC WATER LINES BY STRUCTURAL REGRESSION

A.1 GENERAL FORM

Structural regressions are appropriate for bivariate data where both variables may be subject to error. The general form of the equation used to calculate the gradient of a straight line regression according to this technique has a term, λ, in it, which can be set to various values, depending on the nature of the data. For a full introduction to these statistical methods, see Rock (1988).

λ is the ratio of the random error variances of y over x, so for this project, λ was set at 10, which is approximately the ratio between the variation in δD and δ^{18}O. For a line of the form $y = mx + c$,

$$m = \frac{SS_y - \lambda SS_x + \sqrt{(SS_y - \lambda SS_x)^2 + 4\lambda SP_{xy}^2}}{2SP_{xy}}$$

and

$$c = \bar{y} - m(\bar{x}) \quad .$$

A.2 REDUCED MAJOR AXIS REGRESSION

This is a specific form of structural regression where $\lambda = s_y/s_x$, the total ratio of variances in y and x. For this line, the triangular areas between the points and the regression line are minimized. The simple calculation of an RMA is shown below.

For an RMA regression of the form $y = mx + c$,

$$m = \frac{\sigma_y}{\sigma_x}$$

where

$$\sigma_x = \sqrt{\frac{\Sigma (x - \bar{x})^2}{n-1}}$$

and

$$c = \bar{y} - m(\bar{x}) \quad .$$